Titre: Title:	Spinel bonded magnesia based refractory castables with hydratable alumina as binder
Auteur: Author:	Ning Wang
Date:	1996
Type:	Mémoire ou thèse / Dissertation or Thesis
Référence: Citation:	Wang, N. (1996). Spinel bonded magnesia based refractory castables with hydratable alumina as binder [Thèse de doctorat, École Polytechnique de Montréal]. PolyPublie. https://publications.polymtl.ca/8942/

URL de PolyPublie: PolyPublie URL:	https://publications.polymtl.ca/8942/
Directeurs de recherche: Advisors:	Michel Rigaud
Programme: Program:	Non spécifié

UNIVERSITÉ DE MONTRÉAL

SPINEL BONDED MAGNESIA BASED REFRACTORY CASTABLES WITH HYDRATABLE ALUMINA AS BINDER

NING WANG

DÉPARTEMENT DE MÉTALLURGIE ET DE GÉNIE DES MATÉRIAUX

ÉCOLE POLYTECHNIQUE DE MONTRÉAL

THÈSE PRÉSENTÉE EN VUE DE L'OBTENTION

DU DIPLÔME DE PHILOSOPHIAE DOCTOR (Ph.D.)

(GÉNIE MÉTALLURGIQUE)

OCTOBRE 1996

UNIVERSITÉ DE MONTRÉAL

ÉCOLE POLYTECHNIQUE DE MONTRÉAL

Cette thèse intitulée:

SPINEL BONDED MAGNESIA BASED REFRACTORY CASTABLES

WITH HYDRATABLE ALUMINA AS BINBER

présentée par: WANG Ning

en vue de l'obtention du diplôme de: Philosophiae Doctor

a été dûment acceptée par le jury d'examen constitué de:

M. ALLAIRE, CLAUDE, Ph.D., président du jury

M. RIGAUD, Michel, D.Sc.A., directeur de recherche

M. MASSICOTTE, BRUNO, Ph.D., membre

M. PALCO, Stéfan, D.Sc.A., , membre

ABSTRACT

This thesis is divided into three sections: MgO-Al_2O_3 Spinel Formation and Characterization; Preparation of Cement-Free Castables and Their Properties; and Estimation of Corrosion Resistance against basic ferritic slags.

The first section is about spinel formation; several mixtures composed of different alumina and magnesia powders are prepared and fired at various temperatures. The physical properties of the mixes as a function of the amount of spinel formed at different firing temperatures are investigated.

The nature and size of raw materials determine strongly the formation of spinel and the properties of mixture. The degree of dispersion of MgO and Al_2O_3 control the amount of spinel produced. The sinterability of raw materials and the quantity of spinel produced determine the ultimate properties of fired mixtures. The rapid sinterability of raw materials, in particular the sinterability of ultrafine alumina, versus fine alumina, leads to dense compacts, whereas the larger amounts of spinel produced will give rise to a volume expansion which retards the densification of the same compacts.

The very strong sinterability of ultrafine alumina at temperature below 1200°C results in an early shrinkage which is compensated by the expansion resulting from spinel formation. Therefore, dense mixture can be obtained. The fine alumina reacts easily with MgO at 1200°C. With the production of spinel, a strong volume expansion occurs, and since this fine alumina has less sinterability below 1200°C, the densification of the mixtures containing fine

alumina is always poor. At temperature of 1600°C, these mixtures will be densified. The stoichiometric ratio of MgO/Al_2O_3 is more difficult to densify than a non-stoichiometric ratio.

The mixtures containing fine alumina show a homogeneous and porous micro-structure, but those containing ultrafine alumina show the presence of agglomerates. Some solid centre-agglomerate and hollow centre-agglomerate are formed. Gaps or cracks can also be observed among agglomerates.

The Mg^{2+} cation of big MgO grains can diffuse into the alumina matrix to form spinel and a thin dense spinel ring around MgO grains can be observed. The Mg^{2+} cation can also diffuse deeply into big alumina grains to form a thick spinel layer adhering tightly onto the unreacted alumina core.

Silica fume added to Al_2O_3-rich mixtures can accelerate the densification, but when it is added to MgO-rich mixtures, a porous product is obtained depending on the amount of silica added.

Calcium aluminate cement increases the porosity of Al_2O_3-rich mixtures. Whereas in MgO-rich mixtures, the CA cement slightly densifies the product.

In the second section on castables and their properties, the effect of granulometry is studied. Using Andreasen's equation, it has been shown that the optimized compactness is obtained with the exponent of $n=0.37$.

Fine alumina in castables leads to a large expansion at 1400°C and a rapid shrinkage at 1600°C, and this sudden change will decrease the structural stability. The ultrafine alumina produces a gradual change from expansion at 1200°C to shrinkage at 1600°C and this continuous change can decrease the internal stresses.

The amount of ultrafine alumina in castables has an effect on the modules of rupture; with increasing ultrafine alumina, MOR increases due to the formation of ceramic bond. A low strength ratio between 1200°C and 1600°C can be optimized in order to improve the thermal spalling resistance.

Due to the large difference in thermal expansion between MgO and spinel, some large cracks or gaps around big magnesia grains form, resulting in a decrease in mechanical strength. A suitable small D_{max} should be found to improve the mechanical strength.

Alumina has a strong influence on the corrosion resistance of basic castables. When increasing the alumina amount, the erosion increases. The castable containing fine alumina shows less corrosion resistance than those containing ultrafine alumina.

The basic castable shows a deep penetration depth due to the lack of dissolution reaction between the aggregates and the penetrated slag which results in the change of slag properties. The matrix of basic castable is not dense enough to prevent slag penetration, and the grains are hence easily wetted by slag.

The penetration of slag in basic castables can accelerate the formation and growth of spinel.

A partially prefired sample has a lower penetration depth than a totally prefired sample. The reason is probably due to the dissolution of unreacted fine MgO and Al_2O_3 particles into the slag which changes the slag properties (viscosity and melting point), and hence minimizes penetration.

Of the two basic slags tested, the one containing more CaO leads to a more severe erosion and penetration. The addition of silica fume increases the erosion due to the

dissolution of silica into slag and the added cement increases the penetration. The in-situ MgO-rich spinel matrix shows a better corrosion resistance than the added preformed spinel matrix.

In summary, in this thesis it is possible to demonstrate that it will be possible to manufacture castables containing more than 80 weight% magnesia, with an hydraulic binder and without any hydration problem, during drying and at first heat-up. Those are castables with hydraulic binders, without any cement. Their refractoriness are intrinsically higher than the commercially available castables nowadays. This is then a major technological improvement. The binder is an hydratable alumina, called "actibond".

Of cause, those castables are not 100% basic. They are designed with an alumina matrix, which on firing reacts with magnesia, to form in-situ spinel, above 1000°C. This mineral evolution of those castables is one of their main characteristics.

This experimental work has also shown that it was possible, through a careful selection of the sizes and hence of the reactivity-sinterability of the fine fraction of aluminas, to obtain structurally stable products.

As expected, the corrosion resistance of the new castables which have produced is higher than all the best commercial castables, even in basic slags with 30% iron oxides. However the resistance to penetration is still a weak point.

Several opportunities need to be explored to pursue this work, in order to achieve a new line of products, Those opportunities are mentioned in the last chapter of this thesis.

RÉSUMÉ

Cette thèse est divisée en trois parties portant sur l'étude de la formation du spinelle $MgAl_2O_4$, l'élaboration de bétons réfractaires magnésiens sans ciment et la détermination de leurs propriétés et finalement sur l'évaluation détaillée de la résistance à la corrosion des bétons les plus performants.

Pour la partie formation des spinelles, des mélanges d'alumine et de magnésie, de différentes tailles et en proportions variées, ont été produits. L'évaluation des propriétés des pastilles ainsi produites en fonction de différentes températures de cuisson, et en rapport avec la quantité de spinelle formée, a été systématiquement effectuée.

Les caractéristiques des matières premières influencent fortement les propriétés des mélanges et la formation de spinelle. La quantité de spinelle produite est principalement fonction de la sinterabilité et donc de la taille des particules utilisées, et de la dispersion, donc du nombre de contacts entre particules de MgO et Al_2O_3. Les conditions de frittage des produits et la quantité de spinelle produite déterminent les propriétés ultimes des pastilles obtenues. Les deux phénomènes à considérer sont la contraction dû au frittage plus ou moins prématuré de l'alumine et l'expansion volumique qui accompagne inéxorablement la formation du spinelle.

Selon le rapport volumique alumine/magnésie, le fort frittage à basse température (<1200°C) de l'alumine ultrafine (d_{50}=0.5µm) produit un retrait très tôt, qui peut masquer l'expansion due à la formation du spinelle, menant ainsi à un mélange dense. L'alumine fine

(d_{50}=3.6μm) (à 1200°C) a plus tendance à réagir avec la magnésie et cela conduit à une importante expansion volumique à 1200°C et ce même pour la même production de spinelle, ceci parce que, à cette température, l'alumine de 3.6μm se fritte plus difficilement que l'alumine de 0.5μm. Mais à haute température (1600°C), cette différence disparaît et toutes les pastilles obtenues sont alors fortement densifiées. Le mélange stoechiométrique, 28%MgO-72%Al_2O_3, présente un cas intéressant, illustré dans cette thèse.

La microstructure des pastilles est fonction de la quantité finale de spinelle obtenue. Dans tous les cas, des microfissures entre les grains de spinelle et les particules d'alumine et/ou de magnésie résiduelles, apparaissent.

Selon les rapports volumiques d'Al_2O_3/MgO la phase spinelle apparaît principalement sur les plus gros grains, soit de magnésie, soit d'alumine, selon le cas.

Des additions de fumée de silice aux mélanges riche en Al_2O_3 peuvent accélérer la densification, mais dans les mélanges riches en MgO, plus le taux de silice est important, plus la porosité est grande.

Les additions de ciment alumineux (80%Al_2O_3-20%CaO) ont pour effet d'augmenter la porosité des mélanges riche en Al_2O_3, mais d'augmenter la densification des mélanges riches en MgO.

Dans la seconde partie traitant de l'élaboration de bétons à base de magnésie, une attention particulière a été apportée à la distribution granulométrique des granulats. Pour optimaliser la compacité il a été démontré expérimentalement que l'exposant, dans la courbe cumulative selon l'équation d'Andreasen était de 0.37.

De nouveau dans les bétons, comme dans les compacts produits dans la première

partie avec des fines seulement, la taille de l'alumine utilisée est déterminante, La stabilité structurale, estimée d'après la variation maximale de volume mesurée entre 1200 et 1600°C ou 1400 et 1600°C, selon le cas, est supérieure lorsqu'on utilise de l'alumine ultrafine (0.5μm) plutôt que de l'alumine à 3.6μm.

Ceci se traduit aussi sur les valeurs mesurées de module de rupture (MDR). En augmentant le % d'alumine ultrafine, le MDR augmente. Un faible rapport de résistance entre 1200 et 1600°C peut être optimisé pour améliorer la résistance thermique à l'écaillage.

À cause de la grande différence d'expansion thermique entre la magnésie et le spinelle, d'importantes fissures autour des grains de MgO apparaissent et diminuent la résistance mécanique. Ainsi en partant avec un agrégat D_{max} plus petit, il a été démontré expérimentalement, que la résistance mécanique pouvait être améliorée.

Dans la dernière partie, il a été vérifié que l'alumine avait une influence néfaste sur la résistance à la corrosion des bétons basiques. En augmentant la teneur en alumine, l'érosion augmente.

Mais ce qui ressort en négatif c'est que les bétons basiques montrent une profondeur de pénétration importante. Deux phénomènes sont en cause, d'une part, la matrice des bétons élaborés n'est pas assez dense pour éviter la pénétration, d'autre part l'oxyde ferreux dans les laitiers basiques est très soluble dans la magnésie.

Il est indéniable que le degré de cuisson des bétons conditionne le comportement à la corrosion. Dans notre cadre particulier les échantillons partiellement cuits ont eu un comportement supérieur aux échantillons entièrement frittés, à 1600°C.

Des additions de fumée de silice augmentent comme prévu le phénomène de corrosion

- érosion; il en est de même pour des additions de ciment alumineux. Dernier fait intéressant, le spinelle riche en MgO formé in situ montre une meilleure résistance à la corrosion que le spinelle préformé ajouté.

Au total cette thèse a permis de démontrer qu'il était possible d'élaborer des bétons contenant plus de 80% de magnésie (en % poids), tout en évitant le problème de l'hydratation de la magnésie, au séchage. Ce sont des bétons, avec liaisons hydrauliques, sans ciment. Il sont donc intrinsèquement plus réfractaires que tous les bétons commercialement disponibles présentement. En soi, cela représente un progrès indéniable sur le plan technologique. Le liant est d'alumine pure, de type χ, plus hydratable que l'alumine réactive de type α.

Bien sûr, ces bétons ne sont pas des bétons 100% basique. Ce sont au départ des bétons à matrice d'alumine, qui lorsque mis en température sont transformés en bétons à matrice spinelle. Le spinelle est formé in situ, lorsque la température dépasse 1000°C. L'évolution minéralogique de ces bétons est une de leurs caractéristiques principales.

Ce travail expérimental a permis de démontrer qu'il était possible par un choix judicieux de la taille et de là, de la réactivité, de la fraction fine des alumines, de maîtriser leur stabilité structurale.

Comme prévu la résistance à la corrosion de ces bétons s'est avérée supérieure aux bétons commerciaux testés, même dans des scories basiques contenant jusqu'à 30% d'oxydes de fer. Toutefois, il faut signaler que la résistance à la pénétration de ces béton constituera un point faible.

Des pistes sont encore à explorer pour la poursuite de ce travail. Elles sont esquissées dans le dernier chapitre.

ACKNOWLEDGEMENTS

I sincerely thank Professor Michel Rigaud for his help and support during the course of this work.

I sincerely thank Professor Claude Allaire who has accepted to act as chairman of the jury, Professor Bruno Massicotte and Dr. Stefan Palco for accepting to be members of the jury.

I gratefully acknowledge the useful discussions with Dr.X.Li, Dr.V.Kovac, Dr.V.Pandolfelli, Dr.W.Zhong, Mr.F.Ye and Mr.C.Xing; and the help from M.Lagacé, M.Allahverdi, S.Afshar, A.Labib, K.Chérif, R.Pelletier, S.Quesnel, A.Ratle, L.Rebouillat.

I also thank Jean-Philippe Bouchard and Julie Chamberlain for their technical and secretarial help during the course of this work.

Lastly, I wish to express my sincere gratitude to my parents for their support and encouragement.

TABLE OF CONTENTS

LIST OF FIGURES

LIST OF TABLES

CHAPTER 1 INTRODUCTION

For the past 15 years, monolithic refractory producers have been developing castables for steelmaking applications. This was made possible through the development of low and ultra-low cement castables based on alumina composition, preferably corundum, sometimes sintered bauxite, or a mixture of the two, trying all the times to minimize the CaO content to increase the refractoriness to the system. This leads naturally to the development of no-cement castables, still in progress, because there is still not a perfect binder available to replace satisfactorily the new available CA cement (80% Al_2O_3 for the most demanding applications).

As defined by Li et al. [1], castables can now be classified into conventional castable, low cement castable, ultra-low cement castable and cement-free castable according to CaO contents of castable, CaO contents of different kinds of castables are as follows:

Conventional (Traditional) Castable	For CaO content > 2.5 %
Low Cement Castable (LCC)	For CaO content 1.0 - 2.5 %
Ultra-Low Cement Castable (ULCC)	For CaO content 0.2 - 1.0 %
Cement-Free Castable (NCC)	For CaO content < 0.2 %

Low cement, ultra-low cement and cement-free castables are similar to conventional castables in compounding, i.e., they all consist of aggregate, powder and binder. For the former three kinds of castables, ultrafine powders are used to replace partly or wholly calcium aluminate

cement in the matrices consisting of powder and binder. A slight amount of dispersing agent is added to distribute the ultrafine powder uniformly among the aggregate grains and to fill submicron voids, thus forming a well-distributed structure. The ultra fine particles are still either of silica (silica fume) or alumina (reactive alumina). Other additives have been used in commercial preparations: chromic oxide, zirconia, silicon carbide, metallic silicon, with calcium aluminate cement and/or sodium phosphate as binders.

As mentioned by Rigaud et al. [2], definitive substitution of refractory bricks by monolithic in steel-ladle linings is, at this point in time, only hindered by the lack of appropriate castables at the slag line. Indeed, high alumina based materials are not the best to resist corrosion by basic slags. They are acceptable for barrel and bottom zones in ladle lining only. This is a real drawback since basic bricks, magnesia-carbon or magnesia-chrome are to be used together with a monolithic lining. The definitive solution will be to develop a truly basic based castable, but the unresolved question yet is: how to produce a water added magnesia based castable with very fine magnesia particles without magnesia hydration?

The most common routes to overcome this challenge has been to add alumina to the magnesia based castables, to form in-situ spinel in the matrix; and /or to add spinel grains and magnesia. Along this route, the optimum selection of the proper binder, and the limitations imposed on the matrix definition, to obtain after firing, the proper bonding system, are the two directions which have been retained to launch the present work. This is implicit in the thesis title. The first originality of this work was then to try not to use CA cement, but to use a reactive alumina, which by colloidal peptizing reaction with water, would form a sol-gel, to replace as a binder the CA hydrates. The second originality of this work was to define the

optimum magnesia to alumina particle size distributions, and ratio of the two, to be able to form in-situ spinel bond (MA) without having to cope with the problem of too much cracking due to exaggerated linear expansion (3% or more).

Magnesium aluminate spinel, MA, is the only compound in the MgO-Al_2O_3 system, as shown in figure 1.1 [3]. MA spinel ($MgAl_2O_4$) is a synthetic raw material, which has been used to manufacture refractories and is today gaining more and more acceptance. It has been successfully used in bricks manufacturing for cement rotary kilns, in addition to magnesia, to compete or replace the chrome-magnesia bricks (as well as in non-ferrous metallurgical furnaces). In recent years, it has been increasingly used as such, or as a result of an in-situ reaction between MgO and Al_2O_3 in monolithic (see chapter 2), in alumina based castables.

Simple formation from oxide mixture of periclase and corundum is well known to be accompanied with a volume expansion on 8%, which is simply calculated from their theoretical density differences (MgO: 3.58 g/cm^3; Al_2O_3: 3.99 g/cm^3; $MgAl_2O_4$: 3.58 g/cm^3). If the volume expansion is 8%, the linear expansion should be 2.6%. In practice, however, it is known that this linear expansion value does not predict the real expansion value. First the densities of the powders used, MgO and Al_2O_3, do depend largely on their respective origin and pretreatment and on their respective reactivity also. Two mechanisms have to be considered: the expansion, above 900°C or 1000°C, due to spinel formation and the shrinkage due to sintering above 1200-1300°C. The expansion-shrinkage behaviour of powder compacts, as it will be shown in chapter 3, is influenced by the particle sizes and the particle size distribution, as well as the reactivity of the particles. It was already known that the spinel stoichiometric compositions show the largest linear expansion, and may reach under certain

circumstances a value of 5%. The theoretical expansion had been provided by G.Yagamuchi and co-workers [4,5], but was made known to us only very recently by Nakagawa [6]. This aspect and others concerning the spinel structure and the formation of spinel are detailed in the last section of chapter 2.

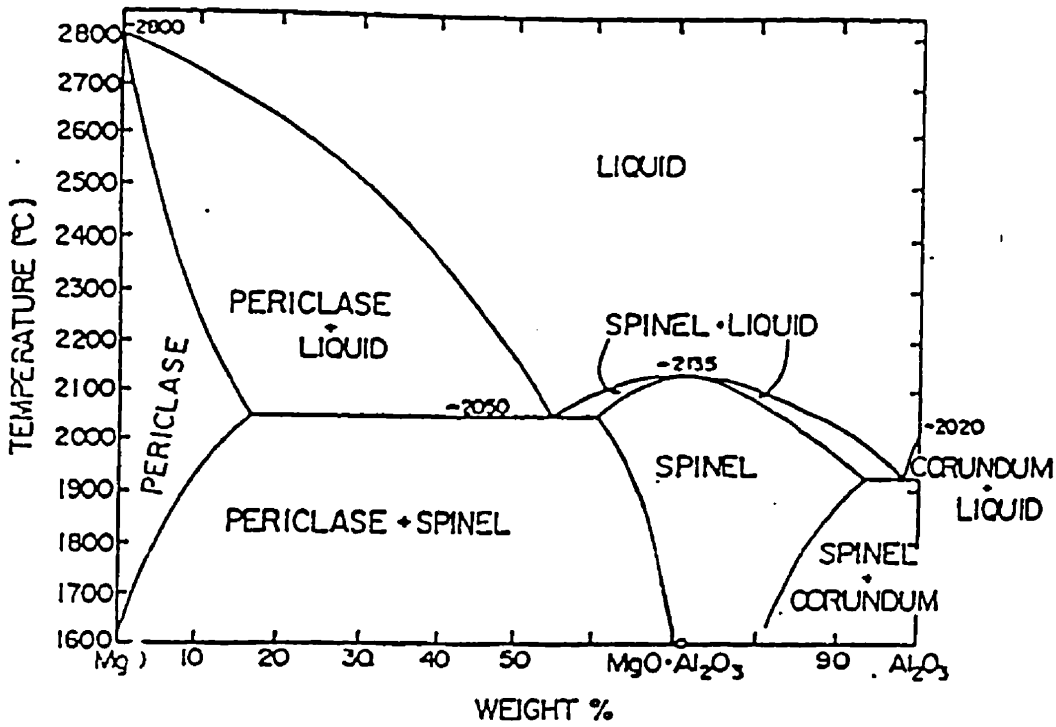

Figure 1.1 Phase Diagram of $MgO-Al_2O_3$ System [3]

The general objective of this work has been to contribute to the basic understanding of the $MgO-Al_2O_3$ system, in order to facilitate the manufacturing of magnesia based castables. Hence the first sub-objective was to document the in-situ spinel formation reaction

in order to clarify the role of the particle sizing, for specific magnesia and reactive alumina, industrially available grains, on the volume stability of the mixes. The second sub-objective was to define the acceptable ratios among an hydraulically bonded alumina, later named actibond alumina, two selected reactive fine and ultrafine alumina and a high purity sea-water magnesia grains. The third sub-objective was to prepare mixes, suitable for castable compositions, without the preoccupation to meet strict rheological criteria. Fluidity of the mixes was decided upon having to meet pre-set values of strength, porosity at room temperature and after firing as well as permanent linear changes after firing at 1000, 1200, 1400 and 1600°C. The fourth and last sub-objective was to compare the corrosion resistance of the mixes to basic slag (CaO/SiO_2>2, FeO>10%) with the corrosion resistance of commercial products based on alumina and alumina-magnesia compositions.

In total, about 50 mixtures with different compositions were made and fired at 1000°C, 1200°C and 1600°C respectively to study the spinel formation and the properties of compacts. All these samples were measured with the apparent porosity, bulk density and volume change. Eleven selected samples were identified by X-ray diffraction and EDS analysis were done for 3 samples. About 30 microstructural photographs were taken for these compacts.

More than 100 bars (230x64x54 mm) were casted to investigate the compaction, physical and mechanical properties of real castables. Apparent porosity, bulk density and MOR had been measured for all these bars, and 5 HMOR was tested for selected samples until 1500°C.

In corrosion testing, about 40 castable bars were tested, and some were corroded for

one time and others were repeatedly corroded for three times (cycle testing). Forty-six chemical analysis and 22 X-ray diffraction for the corroded samples were completed. More than 20 photographs of microstructure were interpreted.

The thesis is divided into four main chapters. In chapter 2, literature review is being made covering the main aspects of the developments of castables for steelmaking applications, starting with a short review on the compaction of particles with an extended size distribution; and then concentrating on the main results obtained with alumina-magnesia and magnesia-alumina based castables.

In chapter 3, several kinds of MgO and Al_2O_3 powders and some grains are chosen. These raw materials have been investigated in order to understand their characteristics and features, for example the size distribution, chemical composition, sinterability, etc. which are believed to influence the production of spinel and the properties of spinel. The spinel formation by mixing the MgO and Al_2O_3 powders is first studied. The alumina fineness and the ratio of MgO/Al_2O_3 decide essentially the physical properties of mixture. The productivity of spinel with different MgO/Al_2O_3 ratio is also investigated. Some big grains are mixed to observe the microstructural characteristics. Under the addition of silica fume and calcium aluminate cement, the sinterability and physical properties are differently affected and are a function of the added quantity, in the MgO-rich as well as Al_2O_3-rich proportion in the mixture.

Castable formation is dealt with in chapter 4. The size distribution is first discussed in order to form the densest castables. The mixture is produced following the Andreasen's equation for particle's distribution. To minimize open porosity in castables, the optimum

exponent (n) is determined. The effect of Al_2O_3 powders, including their nature, fineness, quantity, on the castable properties at different firing temperature has been investigated in order to understand the formation of ceramic bonding (spinel) and its characteristics, since it is the ceramic bonding which influences directly the castables mechanical properties and corrosion resistance. The influence of the maximum size grain of magnesia clinker used has been given a special attention, in order to understand the effect on porosity, volume change and also mechanical properties.

The chapter 5 describes the first estimation of corrosion resistance of castables in steelmaking slag. The commercial Al_2O_3 based castables and developed MgO based castables are compared for their corrosion resistance in basic slag environment. In the MgO based castables, Al_2O_3 powder play a very important role in the corrosion resistance because it determines the ceramic bonding and matrix properties which is the most sensible in castable to corrosion resistance. Three kinds of Al_2O_3 powders: Fine, Ultrafine and Active Al_2O_3 are investigated for their effect on castable corrosion resistance capacity. The effect of quantity of Al_2O_3 in castables is also reported. The prefiring condition determines also the castable corrosion resistance, so the specimens with total prefiring, or partial prefiring are studied. The corrosion behaviour is relative to the testing methods. The one cycle corrosion testing and two or three cycles corrosion testing are compared. The nature of slag is also an important factor to the castable corrosion. Two kinds of steelmaking basic slag, one high by ferritic and one high in CaO have been used to investigate the corrosion behaviour. The effect of addition of silica fume and calcium aluminate cement in the castables, on their corrosion resistance has also been measured. Some basic castables containing preformed spinel have been produced

and the corrosion behaviour of these castables is prospected.

At the end of this work, it is cleared that $MgO-Al_2O_3$ system deserves to be further investigated in order to produce valid commercial castables mixes. This goal seems now closer to reach than it was when this study was started. Several contributions, for examples, the control of volume change and the effect of silica or CA cement; the improvement of physical and mechanical properties of magnesia based castables; the realization of cement-free basic castables and their excellent erosion resistance to basic slag. Increasing the penetration resistance of magnesia based castables will be an important progress to commercial application and it would be possible to realize this by adding the appropriate additives in castables; they will be zirconia, zircon or graphite.

This investigation has clarified the main aspects of the spinel formation and its influence on the production of in-situ spinel containing refractories. The effective method to control the volume change, especially the expansion during spinel formation in refractories has been mastered. The formulation, in the $MgO-Al_2O_3$ system relevant to industrial refractories, has been tackled for the MgO-rich, the stoichiometric and the Al_2O_3-rich ratio. Informations available in this thesis are directly useful for the commercial production of magnesia based cement-free castables. The differences between magnesia based castables and alumina based castables, in terms of their physical and mechanical properties have been documented.

CHAPTER 2 LITERATURE REVIEW ON CASTABLES FOR STEELMAKING

At the First International Conference on Refractories in Tokyo, Japan, in November 1983, B.Clavaud et al. [7] reviewed the 15 years of low cement castables in steelmaking. They reported: "Conventional castables containing 15 to 30% calcium aluminate cement have many service restrictions, especially in the presence of molten slag and metal. This was the reason for the development of castables with low cement contents generally ranging from 4 to 8%. The first experiments with low cement castables were made in France fifteen years ago. Research work was originally concentrated on the choice of particle size, superfine powder additions, deflocculants and aluminous cement quality". The influence of these constituents on the properties of low cement castables has been discussed by many authors with special reference to hot strength, corrosion resistance and rapid heating behaviour [8-17]. "Low cement castables are now used in large quantities by the steel industry to solve problems where service conditions are particularly difficult or exacting. The selected applications in steelmaking which are presented include porous plugs, injection and bubbling lances, sliding gate repairs, degassing units and tundish linings. In all these cases, low cement castables are giving results which are unequalled by any other type of refractory. There is still a large potential for research work in this field and recent developments include ultra low cement castables with 1-2% cement content. These castables have a higher hot strength than low cement castables of similar chemical composition" [7].

However, castables have a long history of over one century! In 1856, Sainte-Claire Deville [18] in France reported on a kind of heated mixture of alumina and lime, which when mixed with corundum aggregate and water, could be used to produce crucibles suitable for application at very high temperatures. In 1918, Lafarge Company in France offered commercially a calcium aluminate cement. According to D.Lankard [19], the first commercial production of bagged mixture of refractory aggregates and calcium aluminate cement for monolithic refractory concrete was started in 1928. In 1932, Plibrico Company started the manufacture of castable refractories in Chicago [20]. Since then, refractory castable developments follow the development and progress of calcium aluminate cement. By 1940, the monolithic refractories accounted for 2~3% of the total refractory market in U.S. From 1940 to 1960, the development of monolithic refractories depended upon the development of purer refractory aggregates, high-purity calcium aluminate cement, and the introduction of phosphate bonding. At that time, the castables were mostly used in kiln car tops, furnace roofs, doors, etc., then in some alumina melting furnace hearths and lower sidewalls.

In the last three-decades, several new technologies have been implemented. In the 1970s, following the introduction of ultrafine silica fume (0.03~0.3 μm), a part of CA cement was replaced that reduces the content of CaO in the castable, and the mechanical resistance and refractoriness increase greatly. The application of castables at high temperature (over 1500°C) became available. Since 1976, Low-Cement Castable, Ultralow-Cement Castable and Cement-Free Castable have been developed and applied in the iron and steel industry. More recently, alumina-spinel castables have been used in barrel and bottom of lining steelmaking vessels [21-36]. But these castables are not capable to resist corrosion by high

basic slag, and hence can not be used at the slag line area.

Basic castables when available will have the potential to resist high basicity slag attack. Some investigations [37-53] at laboratory scale have been reported and the main problems are the hydration of fine aggregate which often cause cracking during drying and then high penetration. The cracking or explosive spalling of castables during drying, especially the magnesia based castables, has been reported as well as on the means to improve the hydration resistance [45-47, 49, 53].

2.1 Alumina Based Castables

In recent years, high alumina based castables for steelmaking ladle have been investigated; they are now all composed of Al_2O_3 aggregates with MgO or spinel or both[21-36, 54, 55]. First, alumina based castables with MgO added into matrix were examined [22, 27,28], and due to the difficult control of volume change from the spinel formation, the interests gradually changed to the Al_2O_3-spinel castables, especially in recent several years, a large number of reports describes this kind of castable [21-26, 28-36, 54, 55].

High alumina impact blocks made of 80% Al_2O_3 and 10% MgO have been developed [27] to prevent cracks and opening of joints with bottom floor brick. The alumina cement and ultrafine powders are minimized and a dispersion agent is blended to a suitable amount to increase the thermal shock damage resistance factor, and prevent the propagation of cracks. The added MgO causes a gradual expansion by spinel formation.

T.Nishitani et al. [28] described their investigation of Al_2O_3-MgO castable with 10% MgO. Although this castable refractories showed longer service life and less refractory consumption than the conventional high-alumina brick lining, it was not cost effective. The main wear mechanism is related to the large volume change due to spinel formation, causing many cracks then slag penetration, skull wedging into these cracks and finally structural spalling.

H.Naaby et al. [29] reported that with a 8% MgO addition, the castable show the lowest wear, infiltration and pores size. Their laboratory trials showed that neither the complete alumina nor MA spinel based castable possesses the required infiltration resistance against calcia-rich slag. Only the combination of alumina with a MgO-addition, which forms

MA spinel in situ, laid the foundation for a successful endless lining. Slag infiltration could largely be suppressed making it possible to reline directly into the weakly infiltrated zone without first having to remove it. They think that the fine grained matrix is decisive for the wear resistance of the monolithic. The spinel formed in situ is microcrystalline and forms the dense fine-grained matrix in which the corundum is embedded. The matrix essentially retains its microporous matrix due to the spinel formation. The spinel remains largely stable against slag attack. Corundum can react with CaO from slag, and form CA_6. The micro-pores are filled by the formed CA_6 under volume expansion. This gives rise to the formation of a 10 mm deep, dense infiltration barrier at the hot face of the monolithic. As the wear resistance is determined by the stability of fine grained matrix, the use of prereacted MA spinel in the medium to coarse grain range does not noticeably improve the wear resistance.

B.Nagai et al. [23] developed a series of Al_2O_3-MgO castables which containing about 17% MgO particles (0.6 to 0.7 mm). They found a large thermal expansion due to the formation of spinel at 1600°C. Adding 7.5% SiO_2 powder moves the maximal expansion at 1400°C. SiO_2 was found to be one of the factors which has an effect on rate of spinel formation. Spinel formation is accelerated as the SiO_2 content increases. The probable reason is that the liquid phase is formed at a low temperature, and ion diffusion is facilitated by the formation of such a liquid phase. In the commercial application of this alumina-magnesia castable, the affected layer is formed to a depth of about 30 mm and most of the periclase in this layer transforms to spinel.

A.Yamamoto et al.[30] reported one kind of Al_2O_3-spinel-MgO castable used around impact bricks in the bottom of VOD ladle. This castable shows excellent corrosion and

penetration resistance, and meanwhile, has the ability to be easily cast around the impact area in VOD bottom. In this case, the life of VOD ladle has been prolonged by 50%, over ordinary life.

Since 1980s, Al_2O_3 based castables with spinel addition have been investigated. This castable shows better wear resistance, especially the penetration resistance. At present, Al_2O_3-spinel castables are increasingly used in ladle's barrel in Japan [23, 28, 30-35, 56-58]. It has been reported that Al_2O_3-spinel castable leads to ladle life of 310 [57] or 250 [58] heats, but repairs had to be done. J.Mori et al. [33] reported their development of alumina-spinel castable for steel ladle, with a shorter life of 150 heats. According to I.Ohishi et al.[56], with alumina-spinel castable into ladle wall, ladle life of 294 heats can be obtained.

Alumina-spinel castable applied in the teeming ladle wall and bottom was reported by T.Kanatani et al., with the ladle life up to 240 heats and refractory cost reduced by about 34%. This castable contained about 20% spinel fine grains to effectively prevent slag penetration [32].

After Ohishi [56], K.Adachi et al. [57] reported that alumina-spinel castable showed approximately twice the durability of zircon castable which was used before, but this material did not fully demonstrate its characteristic of high erosion resistance due to structural spalling (likely cracking and peeling). By the improvement of curing regime and reduction of temperature variations, an average ladle life of 310 heats has been achieved.

Y.Ochiai et al. [58] described the application of alumina-spinel castable for steel ladle at Kakogawa Works. In 1992, side walls were changed from the conventional high-alumina brick to alumina-spinel castable and then bottom were also changed to alumina-spinel

castable. The applied alumina-spinel castable contains 20% fine grain spinel material to prevent slag penetration. As a result, steel ladle's life was improved from 100 heats to 250 heats.

In order to analyse the role of spinel on the corrosion resistance , one has to analyse both the erosion and the penetration resistances of the materials used. According to J.Mori et al. [33], a basic slag CaO-FeO-SiO_2 first penetrates into the matrix. Then CaO in the slag reacts primarily with Al_2O_3 and forms CaO-Al_2O_3 compounds such as CA_6, while FeO forms a solid solution with the spinel. The slag composition moves to a SiO_2-rich or Al_2O_3-rich composition as penetration proceeds. This liquid phase becomes viscous and further slag penetration is suppressed. H.Sumimura et al.[17] recently set up a new mechanism to explain the slag penetration resistance of alumina-spinel castable: (1) spinel reacts with alumina to form solid solution having lattice defects of cation vacancy by the alumina-rich composition. (2) SiO_2 and CaO in the slag accelerate this reaction. (3) FeO in the slag is trapped in the cation vacancy of the alumina-rich spinel. (4) CaO reacts with alumina to form $CaO.6Al_2O_3$. (5) the crystal growth of $CaO.6Al_2O_3$ leads the densification of the castable texture. (6) these reactions restrain slag penetration.

The present literature review has revealed that the principal parameters to consider are:

- total amount of spinel
- spinel composition and size
- amount of superfine silica and CA cement used
- grains size of the aggregates

The amount of added spinel in the Alumina-Spinel castable has a very important effect on the erosion and penetration resistance of castable. Some reports [28, 31-33, 54] show the erosion and penetration with the change of spinel amount in castable. Figure 2.1 indicates the erosion and penetration resistance with the spinel addition. The corrosion index tends to decrease with the increase of spinel addition. On the other hand, the depth of slag penetration considerably diminishes between the addition range of 10 to 30%. However, it turns to increase with addition over 30%.

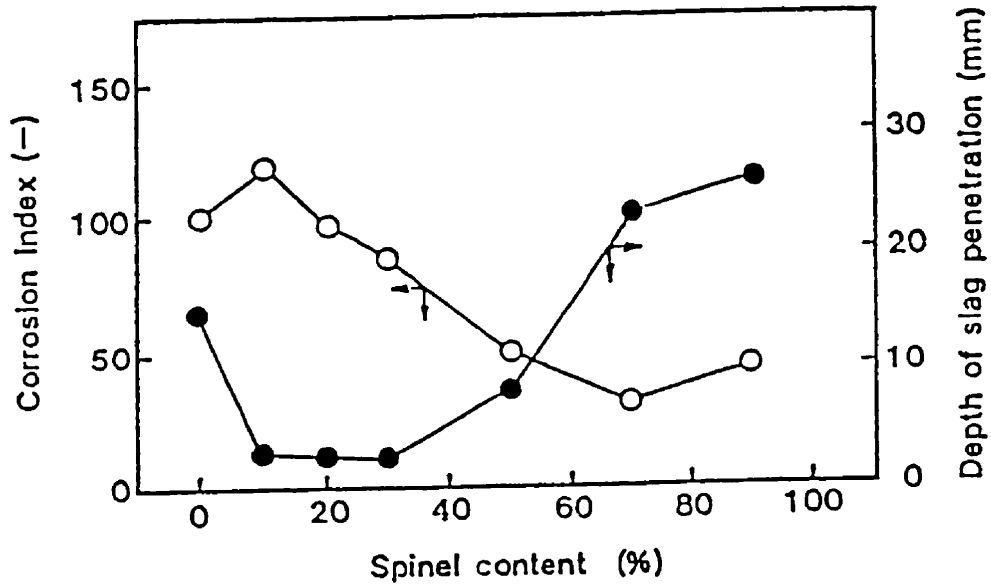

Figure 2.1 Relation Between Spinel Content and Corrosion Resistance [31]

T.Kanatani [32] compares the spinel contained castables with content of 20% and 60%. The spinel in the 20 % content is added in fine particles, and in 60 % castable, spinel is in agglomerate. After 50 heats in laboratory tests, 20% spinel contained castable has 60 mm residual thickness with 15 mm penetration layer and the 60% spinel contained castable has 80 mm residual thickness with 30 mm penetration layer. But in practical application, both castables show similar wear rate in initial 50-60 heats, and then, 60% spinel contained castable began to wear rapidly due to structural spalling caused by slag penetration, while 20% spinel contained castable shows a constant wear rate until the final heat. The life of 20% spinel contained castable is considerably longer than 60% spinel contained castable.

The composition of spinel clinker was found to influence the penetration resistance of castable. T.Yamamura et al. [34] compared the spinel clinker with Al_2O_3 content at 70%, 80%, 90% and 95%. Both 70% spinel content and 25% spinel content castables show a minimum slag penetration index with the spinel clinker of 90% Al_2O_3. The added 70% spinel of 90% Al_2O_3 castable shows a lower penetration than that of 25% spinel addition. The mechanism was believed that the spinel clinker with 90% alumina content is a lattice defective spinel solid solution in which the crystal structure of its spinel dissolved Al_2O_3. The lattice content is smaller than stoichiometric spinel, and the coefficient of thermal expansion is low. The coefficient of thermal expansion of castable using this spinel clinker is also lower than that of castable using the stoichiometric spinel clinker. The spinel with 90% Al_2O_3 has high performance of FeO trapping in the vacant cation position of lattice defective spinel that improves the penetration resistance.

Y. Sato et al. [35] investigated the effect of added spinel grain size on the corrosion

resistance. He added spinel with the coarse, small and fine size and test the castable in a rotary slag corrosion kiln. He finds that the addition of spinel in the small and fine grains can effectively suppress the penetration and the wear rate decreases to about 1/2.

T.Yamamura et al. [31] suggested that addition of 30% spinel with a particle size of over 0.3 mm is desirable to improve the thermal spalling resistance due to the occurrence of residual expansion. J.Mori et al. [24, 33] also reported that the addition of 20% spinel in fine or both fine and small shows the best slag penetration resistance.

T. Yamamura et al. [31] investigated the Alumina-Spinel castable with the addition of superfine silica powder or alumina cement. The superfine silica powder has a purity of 98.2% SiO_2 and size under 0.1 μm. The linear change after firing at 1600°C x 3 hr. shows shrinkage tendency with the increase in the addition amount of superfine silica powder, and even 0.5% addition can lead to a residual shrinkage. The addition of superfine silica powder was believed to heighten strength in the medium temperature range, but a risk of over-sintering at high temperature can decrease the thermal spalling resistance. The corrosion testing shows that the erosion increases with the increase of superfine silica powder, but the penetration almost keeps constant.

The addition of CA cement only causes a slight shrinkage, even the addition amount reaches to 16 %, the castable also shows residual expansion. The addition of CA cement increases the strength in the medium-temperature range, so this is believed to improve the thermal spalling resistance. The corrosion testing shows an increase of erosion and decrease of penetration with additive amounts of CA cement. They found that an addition of 12% CA cement is optimal to improve slag penetration, and structural spalling resistances.

T. Yamamura et al. [31] reported on some alumina-spinel castables with very coarse grain additions. Three kinds of very coarse grains: sintered spinel pellet, sintered alumina pellet and crushed fused alumina were compared. In samples containing very coarse grains of sintered spinel and sintered alumina pellet, cracks occurred between the very coarse grains and the matrix, and spalling resistance decreased compared with samples without very coarse grains. Moreover, corrosion depth decreases by the addition of very coarse grains, while the addition of very coarse grains of sintered spinel pellets accelerates slag penetration. By contrast, a sample containing very coarse grains of crushed fused alumina occurs no crack, and has improved spalling and corrosion resistance compared with those not containing very coarse grains.

It can be concluded that a suitable amount of spinel in alumina based castable is considered in the range of 10wt% to 30wt%. The less amount leads to poor corrosion (erosion) resistance, but more amount causes deep penetration and spalling. Alumina rich spinel improves the penetration resistance due to its crystalline structure. The fine or small size of spinel can more effectively limit the penetration than coarse grains. The addition of silica leads to a shrinkage and high strength at intermediate temperature, but an over-sintering may occur at high temperature; and silica also decreases the erosion resistance. The addition of CA cement increases the erosion, so it must be carefully dealt with the addition of silica and cement when they are used to control the volume change or improve the corrosion resistance. Very coarse grains in castables often lead to cracks between grains and matrix. The corrosion resistance depends on the nature of these big grains.

2.2 Magnesia Based Castables

Alumina is a typical ingredient of castables, but its resistance to corrosion by high basicity slag is not satisfactory. Therefore, basic castables have been studied and developed, mainly for ladle lining, which have higher resistance to slag attack and are more suitable for the refining of high grade steel. Most of the reports about magnesia based castables are still in the form of laboratory progress reports rather than results from practical applications [37-39, 59-61]. The main investigations of magnesia based castables are divided into magnesia-silica castables and magnesia-alumina castables. According to S.Kataoka [62], the magnesia-silica castables were intended to replace the zircon castables in Japan, because the zircon raw material had to be imported and the supply of these materials was unstable and unreliable. Magnesia-silica castables performed well under general conditions, but their use was limited due to the temperature drop of molten steel, buildup and peeling in operation [62]. The requirement of silica-free refractories which is needed to improve steel quality also limits the development of magnesia-silica castables. Descriptive reports about magnesia-alumina castables are less in number and they deal mainly with the expansion due to the spinel formation which often causes spalling [37-39].

The magnesia-silica castable studies started in the early 1980s; the basic idea is to add superfine silica to produce forsterite bond at high temperature. H.Kato et al. [59] reported the first development of such castables. The rotary slag corrosion test in Figure 2.2 shows that the depth of the slag penetration decreases as the content of silica increases. In practical application, this castable has the same level of corrosion resistance as some magnesia-carbon bricks. Nishi et al.[60] reported extensively on other magnesia-silica castables and found that

the optimum composition was 12 % SiO_2. In the early stage, small scale peeling was caused by structural spalling. But, a repair layer with slag-deposited layer grew thick on the hot face, and virtually no corrosion at the end of life (119 heats) was encountered. However, inside the refractories, there were large cracks parallel to the hot face. Slag penetration was slight (10 to 15 mm) and the effect of added SiO_2 densified and hardened the microstructure, so that crack generation was thought to be due to thermal spalling.

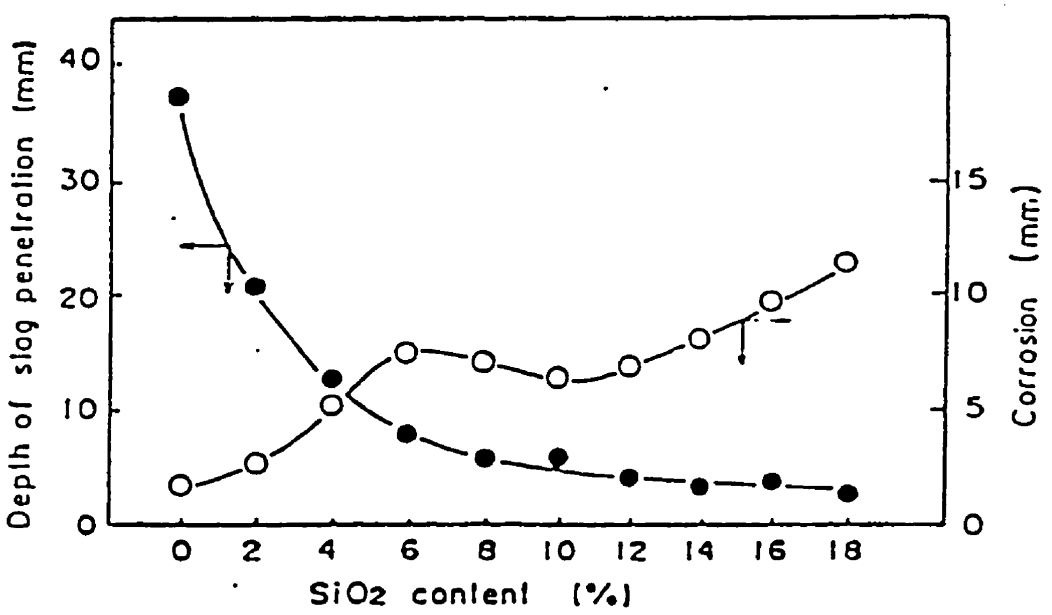

Figure 2.2 Results of Rotary Slag Corrosion test [59]

R. Ebizawa [37] described a magnesia-alumina castable which contained about 54% MgO, 29% Al_2O_3 and 6% carbon and carbonate components which were added to prevent slag penetration. This castable was designed to apply on ladle lining. The main wear in this application is peeling, due to the residual expansion caused by spinel formation in the castable. An improved castable containing 86% MgO, 4% SiO_2, 4% SiC and 4% C reduced greatly the porosity and residual expansion. So the wear mechanism is changed from peeling to corrosion that extended ladle life. Y. Watanabe et al. [38] develop a basic castable containing 80% MgO, 14% Al_2O_3, 4% superfine SiO_2 to be used as TD dams in order to produce clean steel. The penetration of CaO was about 5 mm from the working surface to form monticellite, inside of dam, $MgO.Al_2O_3$ (spinel) and $MgO.2SiO_2$ (forsterite) are also formed. The main failure was due to spalling which reduced the life. H.Kyoden et al., [61] reported their magnesia-alumina castables which showed similar or slightly better erosion resistance than the magnesia burned brick under the testing condition of 1700°C for 4 hr with basic slags (40-45% CaO and 16-34% SiO_2) and an excellent thermal spalling resistance; these castables could be used in EAF roof, upper wall parts, as bottom fill, and as permanent lining in ladles.

At present, magnesia based castables show an arduous progress. The main difficulties, in the development of magnesia based castables, are the hydration of fine magnesia, the suitable binder, the cracking during curing and drying, the formation of bonding, etc. Some fundamental work on improving magnesia hydration resistance is being done to overcome these difficulties [2, 6, 37-39, 43-48, 53]. According to Kataoka [62], magnesia-silica castable applications were limited due to the defects of temperature drop of molten steel, buildup, peeling in operation and silica-containing. The corrosion resistance of magnesia-alumina

castable to basic slag, due to its MgO content, is good and spinel is one of best binary oxide to resist basic slag attack. Both have high refractoriness and chemical stability. The combination between them will determine the performance of refractories. The crux is the formation of ceramic bond--spinel in matrix, which accompanies a volume expansion often causing the cracking and peeling. So it is necessary to understand the spinel formation and its corrosion resistance.

2.3 Corrosion Mechanism of Spinel in Basic Slag and Spinel Formation

Spinel will be the major matrix component in the magnesia-alumina castables, and the main advantage of spinel in castables is to enhance the corrosion resistance of castables by improving the matrix. Spinel can form solid solution with alumina or magnesia, meanwhile, the co-clinker of spinel-magnesia or spinel-alumina often exists in practice. The corrosion resistance of spinel depends mainly on the spinel structure and composition. Therefore, it is necessary to review some basic knowledge about the spinel structure and formation. In this section, the corrosion resistance, structure and characteristics of spinel will be discussed.

Spinel has greatly contributed to the success of alumina-spinel castables, due to its relatively high corrosion resistance in basic slag. The investigation about the corrosion resistance of spinel with different MgO/Al_2O_3 ratio has been reported by A.Nagasoe et al. [63]; they compared the corrosion resistance of different spinels in basic slag (52%CaO, 27%SiO_2, 10%Al_2O_3) . After corrosion at 1500°C, in the sample containing 50wt% Al_2O_3 and 47wt% MgO spinel clinker, strong peaks of spinel and periclase phases and weak peaks of C_2S and C_3S from slag are detected by X-ray. The sample with 70wt% Al_2O_3 spinel clinker has strong spinel and weak C_2S and C_3S peaks. The mixture containing pure sintered 80% Al_2O_3 spinel clinker has strong spinel and C_2AS, and weak CA_2 peaks. The mixture of 90% Al_2O_3 spinel clinker has strong X-ray peaks of spinel, C_2AS and CA_2. Finally, the pure sintered Al_2O_3 has only C_2AS, CA_2, CA_6 X-ray peaks. This proves that MgO-rich spinel clinker is more chemically stable than Al_2O_3-rich spinel clinker in basic slag, and Al_2O_3-rich spinel is more chemically stable than pure alumina.

Due to its importance in spinel contained castables, it is necessary to review the spinel

structure and some fundamental knowledge concerning this mixed oxide.

In 1927, Jander [64] published a model for the kinetic study of solid state reactions. Since then a number of workers [65-73] have proposed various kinetic equations based on Jander's model. Further experimental evidences have been presented in [74-81]. Wagner [82] and Schmalzried [83] have derived equations giving the rate constant for the counter-diffusion system in which the reaction proceeds by the counter-diffusion of two components and succeeded to calculate the rate constant from some fundamental quantities; conductivity, transference number, diffusion constants and so on. The resulting rate constants were found to be in fair agreement with the observed one. After that, many reactions also have been shown experimentally to proceed by the counter-diffusion of two components in the product layer [74, 76, 83-85]. The spinel formation is believed to follow the Wagner's model.

Koch and Wagner [86] gave a cations diffusion model after they investigated the formation of Ag_2HgI_4 from AgI and HgI_2 by solid reaction and they indicated that the formation of spinel($MgAl_2O_4$) follows this model in Figure 2.3. With the formation of spinel and the growth of spinel layer between MgO and Al_2O_3, the ions diffusion through the product layer must be followed to maintain the continuous production of spinel.

O^{2-} anions in spinel is in the structure of face-centred cubic closest packing and the Mg^{2+} and Al^{3+} cations distribute in the O^{2-} anions [87-89]. This closest packing of O^{2-} anions decreases significantly the diffusion of O^{2-}. In Wagner's model, the O^{2-} anions is rigid and only the Mg^{2+} and Al^{3+} cations move through the O^{2-} lattice. Three Mg^{2+} and two Al^{3+} counter-diffuse through the spinel layer and form one spinel at the MgO-spinel interface and three spinels at the Al_2O_3-spinel interface.

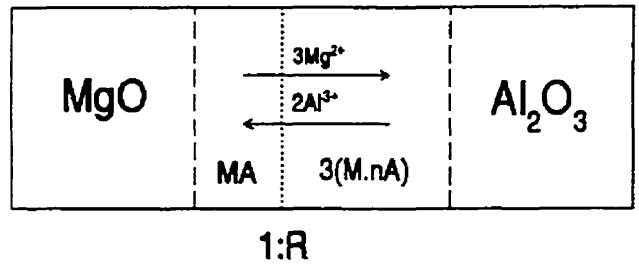

Figure 2.3 Spinel Formation and Ratio of Growth Thickness [74,86]

Carter [74] has confirmed the Wagner's model for the formation of spinel with a very beautiful marker experiment. He put a dense single crystal Al_2O_3 disk with 1 by 0.10 in. thick, marked by molybdenum wire ϕ0.002 in. on the surface, in a closed molybdenum boat, containing an excess of MgO not in contact with the Al_2O_3 and fired at 1900°C for 18 hrs. in H_2 atmosphere. The MgO is transferred as gaseous elements to the solid Al_2O_3 surface (or spinel surface after producing spinel) and then converts to spinel by a solid state reaction. The results showed that the Mg^{2+} and Al^{3+} ions counter-diffuse and produce spinel above and below the marker with a ratio of 1:3.

Navias [90] also studied the solid reaction for the formation of spinel from MgO and Al_2O_3 in the range of 1500°C to 1900°C and found that spinel can be formed by reaction between MgO vapour products and solid Al_2O_3 in an hydrogen atmosphere, but only by solid

state reaction in an oxidizing atmosphere.

Generally, the mixture of MgO and Al_2O_3 powders begins to produce spinel at about 1200°C, but the spinel can be found at lower temperature if one uses more active MgO and Al_2O_3 fine powders or hydroxides. J.T.Bailey and R.Russell,Jr. [91] found that the formation of spinel begins between 925°C and 950°C, using highly reactive grades of alumina and magnesia with an average particle sizes of 1.6 and 2.5μ, respectively, and corresponding purities of 99.75 and 99.70%. At 1300°C for three hours, 88.8% spinel completion can be obtained. Bratton [92] found the spinel at 400°C and above starting with magnesium-aluminum hydroxides coprecipitates.

The growth of spinel crystal by the solid reaction is interesting because it involves not only a counter-diffusion of cations but also a rearrangement of the cations and a transformation of the O^{2-} sublattice from hexagonal closest-packing to face-centred cubic at the phase boundary of Al_2O_3-spinel. Rossi and Fulrath [93] found the epitaxial growth of spinel on the sapphire because the (111) plane of spinel phase is closely parallel to the (001) Al_2O_3 plane. They also calculated a misfit, in sample fired at 1560°C, for the (001)/(111) relation, of 3.1% along the direction of closest packing using the room-temperature oxygen-oxygen distances of 0.275nm for sapphire and 0.286nm for spinel. The epitaxy that was determined by the orientation of the sapphire can be observed in both sapphire-grown or periclase-grown spinel and was never observed to depend on the periclase orientation.

The stoichiometric spinel is known as $MgO{\cdot}Al_2O_3$, however, in practice, spinel contains some excess MgO or Al_2O_3 to form solid solution as indicated in figure 1.1 [3]. The amount of dissolved MgO or Al_2O_3 increases with the increasing temperature, and the

maximum amount of MgO soluble in spinel is 6wt% Mg ions or 10wt% MgO (39% MgO and 61% Al_2O_3) at about 1995°C and a composition of solid solution with 35% MgO and 65% Al_2O_3 was found at 1680°C [94]. The MgO-spinel solid solution can be stably formed at above 1500°C. Alumina has a wide solid solubility in magnesia-aluminate spinel ($MgO{\cdot}nAl_2O_3$). Single phase spinel can form in the range from $MgO.Al_2O_3$ to $MgO.5Al_2O_3$ [95]. When $n<1.7$, α-alumina could not be precipitated in single crystals even after long-term annealing at temperature up to 1673K [96-97].

Due to the Mg^{2+} and Al^{3+} cations counter-diffusion, the spinel grows on both sides of the initial interface between MgO and Al_2O_3. The growth ratio of the thickness at the MgO-spinel and Al_2O_3-spinel is different, because the number of cations diffusing is different ($3Mg^{+2}$ ions enter Al_2O_3 and only $2Al^{+3}$ ions enter MgO), that produce one spinel at the MgO-spinel boundary and three spinel at the Al_2O_3-spinel boundary. Al_2O_3 and spinel can also form wide solid solution and the composition with maximal soluble Al_2O_3 is $MgO{\cdot}1.7Al_2O_3$ at room temperature. The growth rate at Al_2O_3-spinel boundary is much greater than that at the MgO-spinel boundary. The ratio is shown in Figure 2.3, where R is the following value:

$$R=\frac{3(7n+1)}{3n+5}$$

If $n=1.7$, $R=3.83$. Carter [74] observed the ratio of 1:3 and Rossi et al [93] measured the ratio of 1:4.83. G.Yamaguchi et al. [98] found that the ratio of the thickness of the MgO side texture to that of the Al_2O_3 side texture is about 1 to 4.5, and the composition of the spinel is almost $MgO{\cdot}Al_2O_3$ at a contact face with MgO, while it is nearly $MgO{\cdot}1.5Al_2O_3$ at a contact face with Al_2O_3.

Y.Chiang and W.D.Kingery [99] investigated the grain-boundary mobility in magnesium aluminate spinel ($MgO.nAl_2O_3$) of magnesia-rich ($n<1$) and alumina-rich ($n>1$) compositions by the measurement of normal grain growth in dense, hot-pressed samples. Over the temperature range 1200°C to 1800°C, the magnesia excess spinel has a much more rapid grain growth rate than the stoichiometric spinel. The mobility in magnesia-rich composition is found to be greater by a factor of 10^2 to 10^3 than that in stoichiometric and alumina excess solid solutions.

Pure spinel mineral is rare in the nature, so the industrial spinels are often produced by synthesis. For the commercial grade spinel, we usually find the Al-rich or Mg-rich spinel [100, 101], and less stoichiometric spinel, this is probably due to the more difficult sintering of stoichiometric spinel.

2.4 Conclusion

Spinel structure and its formation mechanism have been reviewed to understand and master the spinel formation and its properties as a refractory matrix constituent.

From literature's review, alumina based castables with fine spinel contained matrix have successfully been used in steel ladle, for example at the bottom and metal barrel. This castable shows a relatively high corrosion resistance. But few successful reports described the application of castable at slag line. The reason probably is due to the very severe corrosion at slag line zone and long contact time between liquid slag and refractories, so alumina based castables cannot be accepted.

Reported magnesia based castables [59-61] show some improvement of the corrosion resistance, but some defects still exist, for example, MgO-SiO_2 castables show a deep penetration with less SiO_2 addition, however, a high erosion and thermal spalling occur with higher content of SiO_2. For steelmaking, a free-silica refractory is required. Magnesia-alumina castables [37-39] lives are limited due to the spalling or peeling. The main reason is believed to be related to the expansion-shrinkage behaviors during the spinel's formation.

Magnesia based castables with spinel bonding are potentially good refractories to develop for corrosion resistance. But the volume expansion during spinel formation greatly influences the properties of castables. In this thesis, spinel formation is being investigated first, as it is relevant to refractory matrix, then the physical and mechanical properties are estimated, and lastly the corrosion resistance is determined.

CHAPTER 3 STUDY ON SPINEL FORMATION IN COMPACTS

As reviewed in chapter 2, the formation of spinel is the source of a volume expansion which influences effectively the properties of refractory castables. Some unexpected expansions causing extreme damages have been reported [37-39].

Many reports described the application of spinel in refractory castables, but few are available on the formation of spinel relevant to refractory matrix level and on the effect of the net expansion-shrinkage phenomena on refractory properties.

The refractory raw materials chosen in this investigation are described hereafter. They have a strong effect on the formation of spinel and properties of compacts.

Because the CA cement or silica fume is often the binder or additives in castables, the effect of these two additives in mixtures on the properties and microstructure of compacts is also reported.

3.1 Raw Materials

The main raw materials are high purity seawater magnesia powder from the crushed sintered magnesia (periclase) clinker and high purity very fine alumina powder. Some big grain of sintered magnesia clinker and fused alumina are also used.

3.1.1 Magnesia

Magnesia raw material is high purity periclase. This high purity periclase is produced

from seawater. According to the A.N.Copp [102], the production method is by the thermal decomposition from magnesium hydroxide ($Mg(OH)_2$) obtained from seawater. If MgO is produced at temperature over 1400°C, it is called dead-burned MgO [102]. Dead-burned MgO is characterized by its low chemical reactivity and high resistance to basic slag, so the dead-burned MgO is consumed almost exclusively in refractory applications in the form of brick and granular refractories used in the cement, glass, steel, and non-ferrous metals industries [102].

The chosen periclase (sintered MgO) has a specific gravity of 3.58 g/cm3 and its detected chemical composition is indicated in Table 3.1. Two kinds of fine magnesia powders have been used: one under 45 microns and the other under 100 microns. These magnesia powders have beeen obtained by sieving laboratory made ball milled periclase. The size distribution, which is measured with a Sedigraph, is shown in Figure 3.1. The median diameter (D_{50}) for -0.045mm powder is about 12 micron and for -0.1mm powder is about 27 micron. Only one other fraction of magnesia, with size of 0.125 to 1.41 mm (D_{50}=130μ) has been used.

3.1.2 Alumina

Several kinds of alumina powders and aggregates have been used. They are fine alumina--Alcan's C71-FG; ultrafine alumina--Alcan's XA45B; active alumina binder--Alcan's Actibond101; fused alumina powder and aggregate--Washington Mills' Brown, fused alumina grains.

Table 3.1 Chemical Composition of Raw Materials

Chemical Composition of Alumina [103-106]					
Chemical Composition and Properties	Fine Alumina		Ultrafine Alumina	Active Alumina	Fused Alumina
	Typical	Max.			
Na_2O (%)	0.18	0.30	0.05	0.4	
SiO_2 (%)	0.03	0.05	0.002	0.02	0.67
Fe_2O_3 (%)	0.03	0.05	0.03	0.02	0.11
Al_2O_3 (%)	99.8		>99.8	95.5	96.12
TiO_2 (%)					2.70

Chemical Composition of Magnesia						
MgO	Al_2O_3	SiO_2	Fe_2O_3	CaO	Na_2O	Others*
99.00	<0.02	0.10	0.22	0.50	0.16	<0.01

*Others: K_2O, TiO_2, MnO.

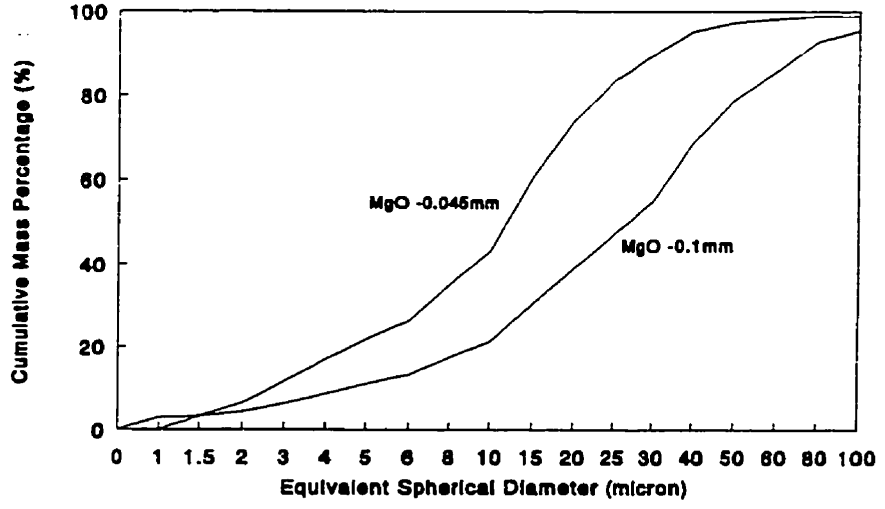

Figure 3.1 Size Distribution of Fine Magnesia Powders

3.1.2.1 Fine alumina

Fine alumina is produced by calcining Bayer process alumina trihydrate (more correctly aluminum trihydroxide) in rotary kilns. During calcination, the combined water is driven off and the oxide formed passes through several intermediate phases until the stable alpha-alumina structure is reached. Grain size of the alumina is determined during the hydrate precipitation stage of the Bayer process, but crystal size of α-Al_2O_3 is developed during the calcination process. Although the alumina trihydrate precursor is a non-porous grain of specific gravity 2.42 g/cm^3 and bulk density of about 1.3 g/cm^3, the resulting α-Al_2O_3 is a porous aggregation of monocrystal platelets whose specific gravity is 3.98 g/cm^3, but whose bulk density is only about 1.1 g/cm^3 [103]. The open structure of crystallites within the aggregate makes the alumina easily ground into its component crystals. Figure 3.2 shows the evolution from one alumina trihydrate grain to one porous aggregate of α-alumina platelets. Final alumina powder product is produced by grinding these porous aggregates in ball mill. Due to the porous structure, the aggregate is easily crushed to release the unit crystals. Figure 3.3 is the typical particles of final product.

3.1.2.2 Ultrafine alumina

Ultrafine alumina is a highly reactive alumina in the Alcan family of reactive alumina. This ultrafine alumina exhibits very high fired densities in the supplied state, making it as an ideal alumina for very high alumina bodies, where high density is required. It also shows very low levels of silica contamination [104].

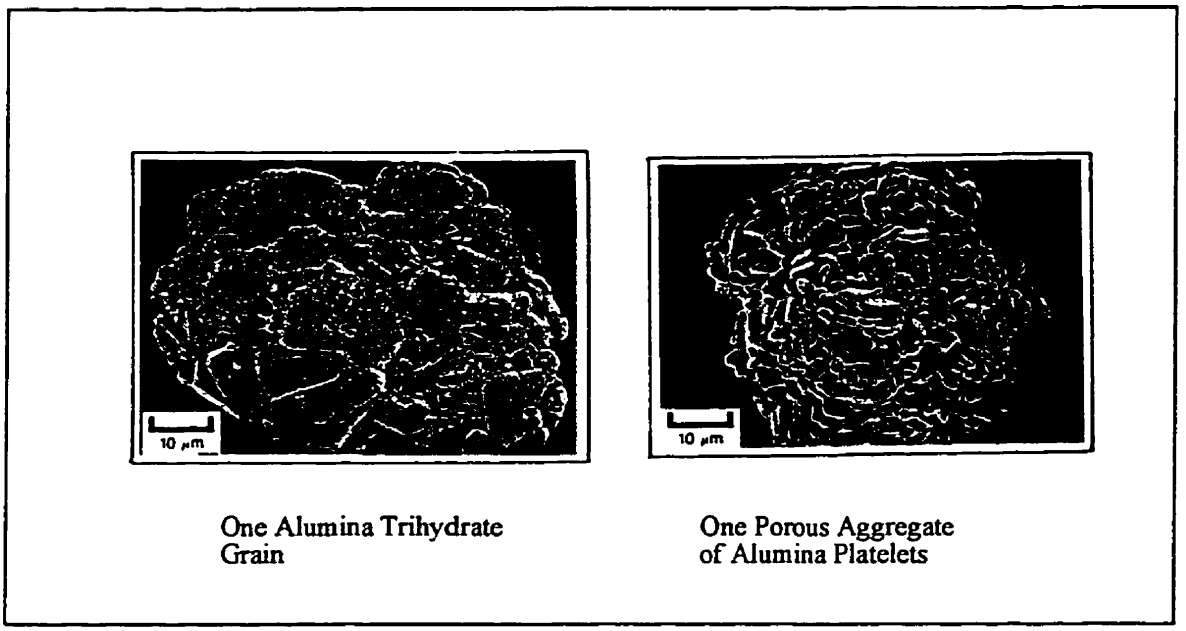

Figure 3.2 The Evaluation from Alumina Trihydrate to Porous Aggregate of Alumina Platelets

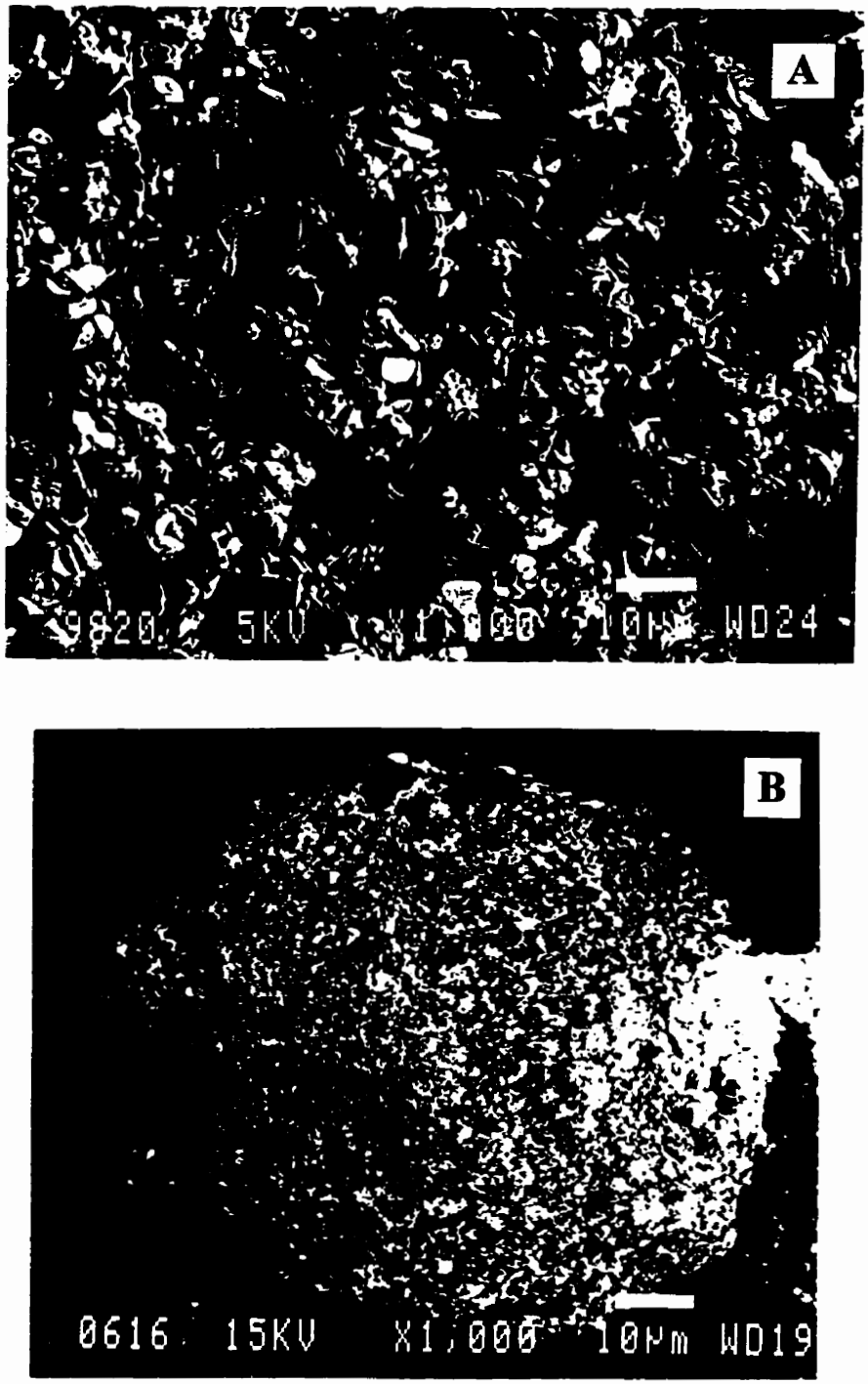

Figure 3.3 Pattern of Alumina Powder

a: fine alumina, b: ultrafine alumina

3.1.2.3 Active alumina binder

Active alumina binder is a white, transition alumina powder. It has a crystal structure which is predominately chi phase but small amounts of other forms can be present. In a refractory mix, the active alumina reacts with water to form a hydraulic bond. This hydraulic bond imparts green strength to the refractory object being made, allowing further processing and handling. Active alumina is greater than 95% alumina with a calcium level of less than 0.05% [105]. Consequently, very low quantities of low temperature phases are formed, as compared to traditional calcium aluminate cements. On firing, active alumina reacts with other finely divided powder to produce ceramic bond.

3.1.2.4 Fused alumina

Fused alumina are produced in an electric arc furnace, from selected grades of bauxite. Chemical composition and crystalline size are carefully controlled to ensure maximum product uniformity. Fused alumina is mainly alpha alumina (corundum) in the hexagonal crystal system and has 60% monocrystalline grains of 650 microns in size [106]. The fine fused alumina powders are produced by crushing the big grains. In this study, the small grains with size between 0.125 and 1.41 mm are used.

Fine and ultrafine alumina are the major raw materials in the mixtures comparing with other kinds of alumina. Fine alumina is in fine grind form. Ultrafine alumina is available in dry ball milled to ultimate crystals. Their size distribution is measured by Sedigraph and shown in figure 3.4.

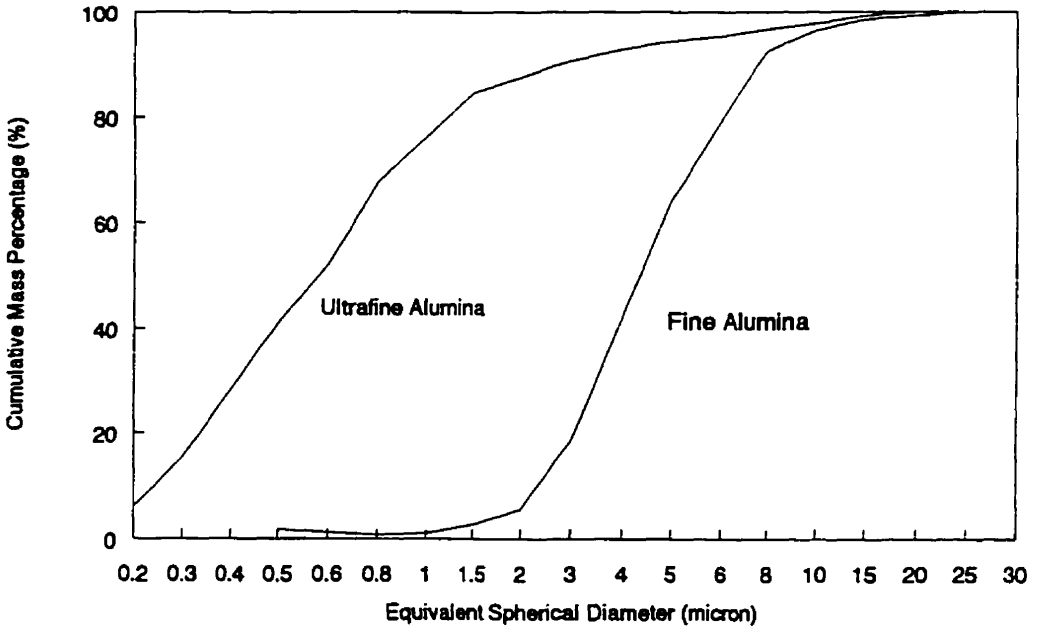

Figure 3.4 Size Distribution of Fine and Ultrafine Alumina Powders

Chemical composition and properties of the four kind of aluminas are indicated in Tables 3.1 and 3.2, respectively. Fine alumina powder is an intermediate soda α-alumina developed specifically to satisfy the requirements of the refractory. Ultrafine alumina shows a lower Na_2O and SiO_2 content which will influence the chemical activity to some extent. Active alumina binder is mainly a chi-alumina has a relatively low Al_2O_3 purity and very high specific surface area; a high Fe_2O_3 and SiO_2 contents appear in this alumina. The specific surface area is determined by the BET method, ultimate crystal size is determined by optical microscope and median particle size is determined by Sedigraph.

Table 3.2 Properties of Alumina [103-106]

Chemical Composition and Properties	Fine Alumina		Ultrafine Alumina	Active Alumina	Fused Alumina
	Typical	Max.			
Specific Surface Area (m^2/g)	0.6		8.0	260	
Ultimate Crystal Size (μm)	3-4				
Median Particle Size D_{50} (μm)	3.65		0.46	10	130
Specific Gravity (g/cm^3)	3.89		3.89	3.03	3.92

3.2 Expansion-Shrinkage Behaviour of MgO-Al_2O_3 Compacts

The mixtures made of MgO-Al_2O_3 are first investigated. Ultrafine alumina and fine alumina are denoted by UA and FA, respectively in the mixtures. The magnesia of under 0.1 mm is denoted by M and one of under 0.045 mm is denoted by FM.

3.2.1 Experimental Procedure

The magnesia and alumina powders are first dried at 800°C. Powders are then mixed for 40 minutes in a plastic bottle with a charge of about 20g alumina balls using a Turbula mixer. The dry mixtures are then introduced in a rubber bag and compress in an isostatic press at 200 MPa, to form compact samples. All samples are fired at 1000°C to measure the apparent porosity and bulk density, and then refired to 1200°C and 1600°C, respectively. The program of firing is done in 3 steps, heating at 200°C/hour, then holding 6 hours, finally cooling at 200°C/hour. Samples for dilatometry were prepared by uniaxial pressure at 100 MPa.

The composition of mixtures is indicated in Table 3.3. MFA series are the mixtures of under 0.1 mm MgO powder and fine alumina, and MUA series are the mixtures of under 0.1 mm MgO powder and ultrafine alumina. Some mixtures with the stoichiometric ratio between MgO and Al_2O_3 are also indicated in order to compare their characteristics.

Apparent porosity and bulk density are measured following the method of liquid immersion in vacuum pressure which is referred to ASTM Standard C830-88. The bulk density (D) and apparent porosity (P) are calculated by following equations:

$$D = \frac{m_{dry}}{m_{sat.} - m_{imm.}} \rho_l$$

$$P = \frac{m_{sat.} - m_{dry}}{m_{sat.} - m_{imm.}} \frac{\rho_l}{\rho_L}$$

Table 3.3 Composition of Mixtures Made of MgO-Al_2O_3 Powders

	<0.1mm MgO (%)	<0.045mm MgO (%)	Fine Alumina (%)	Ultrafine Alumina (%)
M	100			
MFA90/10	90		10	
MFA80/20	80		20	
MFA70/30	70		30	
MFA60/40	60		40	
MFA50/50	50		50	
MFA28/72	28		72	
FA			100	
MUA50/50	50			50
MUA28/72	28			72
MUA20/80	20			80
UA				100
FMFA28/72		28	72	
FMUA28/72		28		72

where m_{dry} is the weight of the dry specimen (g), $m_{sat.}$ is the weight of the specimen saturated with a liquid, determined by weighing in air (g), $m_{imm.}$ is the weight of the specimen saturated with a liquid, determined by weighing the specimen immersed in the liquid (g), ρ_l is the density of liquid used for the saturation of the specimen (g/cm^3) and ρ_L is the density of the liquid for the weighing of the immersed specimen (g/cm^3). Kerosene is chosen as the liquid for the saturation and for immersion in this test, so the ρ_l and ρ_L is 0.788 g/cm^3.

The volume changes are calculated from the bulk density by the equation

$$\Delta V = \frac{\frac{1}{D_1} - \frac{1}{D_0}}{\frac{1}{D}}$$

where D_0 is the bulk density fired at 1000°C and D_1 is that fired at 1200°C or 1600°C. The quantity of spinel are evaluated by the calculation of the change of true density.

The relative portions of magnesia, alumina and spinel in the fired samples are estimated by the following equations:

$$\rho = \frac{1}{\frac{X_M}{\rho_M} + \frac{X_A}{\rho_A} + \frac{X_S}{\rho_S}} \qquad \text{(A)}$$

$$X_M + X_A + X_S = 1 \qquad \text{(B)}$$

$$\frac{X_{Mo}-X_M}{X_{Ao}-X_A} = \frac{0.28}{0.72} \qquad (C)$$

where ρ is the true density (or specific gravity) of the fired mixtures which can be calculated by the $\rho=D/(1-P_{total})$. The bulk density (D) is measured and the total porosity (P_{total}) is approximately equal the apparent porosity (P) in these samples because the closed porosity is relatively low for these samples. ρ_M, ρ_A and ρ_S are the specific gravity of magnesia, alumina and spinel, respectively. X_M, X_A and X_S are the portion (%) of magnesia, alumina and spinel in the fired mixtures. X_{mo} and X_{Ao} are the initial portion between magnesia and alumina. The formed spinel is supposed to correspond to the stoichiometric ratio (28/72). Because the formation of spinel, especially in the alumina rich mixture, will not lead to composition having exactly the stoichiometric ratio, some errors will be attached to the calculation. Those results will then give only a trend.

Some selected samples have been analyzed by X-ray diffraction. Microstructural observations have been performed. The sintering curves of fine and ultrafine alumina have been measured by the dilatometer with 2°C/min., up to 1600°C.

Sinterability of fine oxides are tested by firing the compact samples isostatically pressed at 200 MPa, and then measuring the bulk density and apparent porosity. Results are indicated in Table 3.4.

The sintering behaviour of fine and ultrafine alumina have also been measured by dilatometry, fired at 2°C/minute up to 1600°C. The samples are prepared by uniaxial pressing at 100 MPa. The sintering curves are shown in Figure 3.5.

Table 3.4 Sinterability of Oxides Powders

	Prefired at 1000°C		Fired at 1600°C		From 1000°C to 1600°C
	Bulk Density (±0.5g/cm³)	Apparent Porosity (±1%)	Bulk Density (±0.5g/cm³)	Apparent Porosity (±1%)	Volume Change (±1%)
Fine Alumina	2.3	42	3.2	18	-29
Ultrafine Alumina	2.3	42	3.9	1	-41
Magnesia (-100μm)	2.7	23	2.8	20	-4
Magnesia (-45μm)	2.6	27	2.8	20	-9

The fine alumina begins shrinkage at about 1100°C and the shrinkage is very slow up to 1400°C. After 1400°C, the shrinkage accelerates and the total shrinkage at 1600°C is about 7.6%. For ultrafine alumina, the shrinkage starts at about 1000°C and then goes on rapidly after 1200°C. The total shrinkage at 1600°C is about 17.7%. The ultrafine alumina is made of very fine broken crystals with high surface energy [104], so this alumina is very reactive. From the results of isostatic pressed samples in Table 3.4, the bulk density of ultrafine alumina can reach 3.9 g/cm^3 at 1600°C, but the fine alumina is only 3.2 g/cm ^{3} at this temperature. Consequently, the volume shrinkage is very strong for ultrafine alumina.

The magnesia powders show a small volume shrinkage because the size of this two powders is relatively larger than the alumina powders. But between the two magnesia powders, the finer powder (D_{50}=12 μm) also shows a stronger shrinkage than the coarser powder (D_{50}=27 μm). These results show the importance of particle size in relation with sinterability.

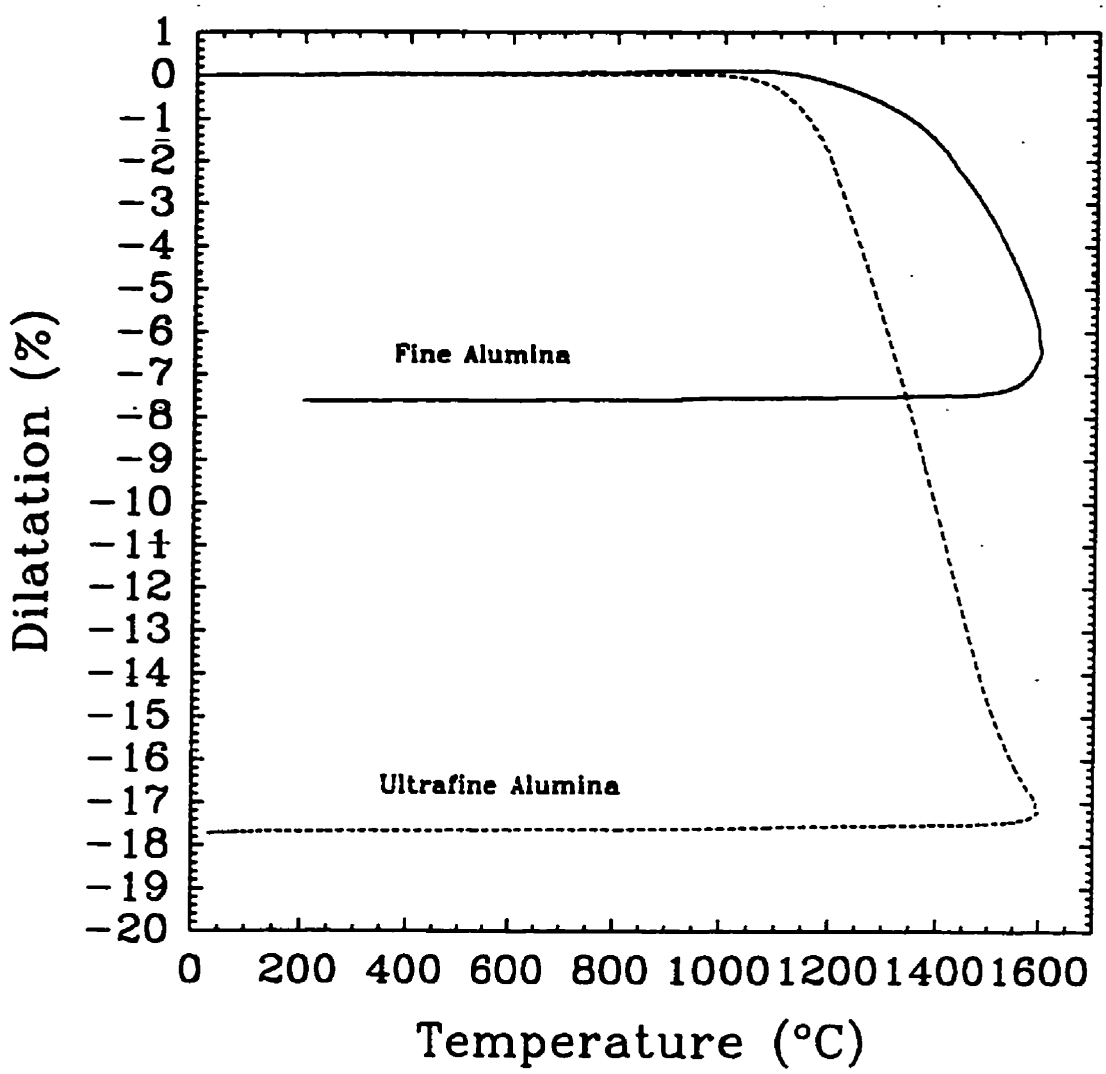

Figure 3.5 Sintering Curves of Alumina Powders

3.2.2 Results and Discussion

The compacts made of Al_2O_3-MgO oxides are produced by firing at different temperature and the main properties, such as, bulk density, apparent porosity and volume change are measured. The spinel quantity in mixture are calculated. These results are indicated in Tables 3.5 and 3.6, and their composition is shown in Table 3.4. The properties of mixtures made of fine oxides are first discussed. The effect of fineness of alumina and alumina/magnesia ratio in mixtures on the porosity and expansion-shrinkage behaviour is studied. The features of stoichiometric compacts are described. And then, some mixtures containing coarse magnesia or alumina grains are researched by microstructural observations in order to discover the performance of big grains in the formation of refractory bonding.

3.2.2.1 Effect of Ratio of Alumina/Magnesia on Expansion-Shrinkage Behaviour of Mixtures

The sintering shrinkage of pure magnesia and pure alumina has been discussed in previous section. Magnesia powders (<0.045 mm and <0.1 mm) show much less sinterability than the fine or ultrafine alumina at 1600°C (Table 3.4). Figure 3.6 also indicates the sinterability of under 0.1 mm magnesia and fine, ultrafine alumina at 100% magnesia or alumina ratio. Pure MgO (-0.1 mm) sample has only a slight densification from 1000°C to 1600°C with a very small volume shrinkage. Pure fine alumina powder densification begins at 1200°C, but greater shrinkage and densification occur at 1600°C. Pure ultrafine alumina exhibits greater densification and shrinkage than fine alumina at 1200°C. The ultimate bulk density at 1600°C is near the theoretical value, so the shrinkage is extremely strong. The

different sinterability of MgO, Fine and Ultrafine Al_2O_3 powders will influence directly the sintering shrinkage of their mixtures.

Table 3.5 Physical Properties and Spinel Synthetical Amount in Mixtures of Fine Oxides

	Firing at 1000°C		Firing at 1200°C				Firing at 1600°C			
	D (±0.05)	P (±1)	D (±0.05)	P (±1)	ΔV (±1)	X_s (±5)	D (±0.05)	P (±1)	ΔV (±1)	X_s (±5)
M	2.73	23	2.76	22	-1		2.84	20	-4	
MFA90/10	2.67	25	2.58	28	4	9	3.06	14	-12	14
MFA80/20	2.61	28	2.36	34	10	28	3.13	12	-16	28
MFA70/30	2.54	31	2.21	38	15	39	3.13	12	-19	42
MFA60/40	2.48	33	2.10	42	18	42	3.22	9	-23	56
MFA50/50	2.43	35	2.09	43	16	37	3.21	9	-24	70
MFA28/72	2.33	39	2.11	43	10	28	2.62	27	-11	100
FA	2.27	42	2.30	41	-2		3.20	18	-29	
MUA50/50	2.46	34	2.44	34	0		2.98	15	-17	
MUA28/72	2.39	37	2.46	35	-4	0	3.03	13	-21	100
MUA20/80	2.35	39	2.41	37	-3		3.18	8	-26	
UA	2.30	42	2.73	30	-16		3.89	1	-41	
FMFA28/72	2.26	41	1.97	47	15	39	2.52	30	-10	100
FMUA28/72	2.46	36	2.48	34	-1	10	3.05	13	-19	100

Note: D is bulk density (g/cm^3), P is apparent porosity (%), ΔV is volume change (%) and X_s is produced spinel portion (%).

Table 3.6 Physical Properties of Mixtures Containing Big Grains

No.	Composition	1000°C		1200°C			1600°C		
		D (±0.05)	P (±1)	D (±0.05)	P (±1)	ΔV (±1)	D (±0.05)	P (±1)	ΔV (±1)
CM-FA	28%CM and 72%FA	2.39	37	2.39	37	0	2.67	28	-11
CM-UA	28%CM and 72%UA	2.53	33	2.67	30	-5	2.89	21	-13
FM-CA	28%FM and 72%CA	2.90	24	2.87	25	1	2.18	40	33

Note: CM: MgO grain with 0.125-1.41 mm, FM: fine MgO powder of under 0.045 mm, FA: fine alumina, UA: ultrafine alumina, CA: fused alumina with 0.125-1.41 mm; D: bulk density (g/cm³), P: apparent porosity (%), ΔV: volume change.

At 1000°C, for all mixtures, nearly no sintering occurs, only the start of spinel formation is occuring. As shown in Figure 3.7, the initial apparent porosity follows an increasing trend with the decrease of MgO/Al_2O_3 ratio. At pure alumina composition, the porosity is maximum and at pure magnesia composition, the porosity is minimum. The reason mainly is due to the size distribution of the green body because the sintering procedure is very less at 1000°C. The magnesia powder has a relatively great $D_{max.}$ which leads to the wide particles distribution range and a larger mean particle size, for this reason, the structure will be denser, but the pure alumina powders have a very small $D_{max.}$ which limits the size range that causes the diminution of mean particle size. The relationship of porosity and particle size has been discussed in detail in R.M.German's book [107]. So, at 1000°C, the compacts do not show the spinel formation expansion and mixture sintering shrinkage.

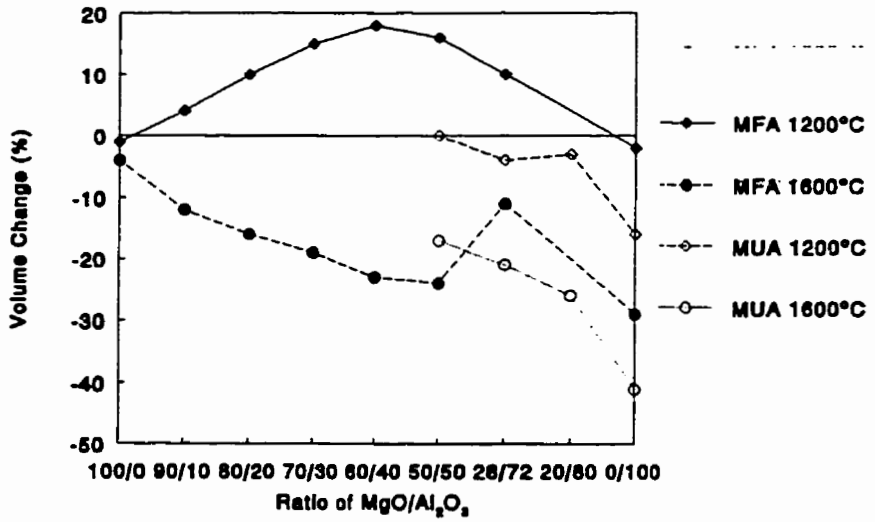

Figure 3.6 Effect of Fineness of Alumina and Ratio of MgO/Al_2O_3 on Volume Change

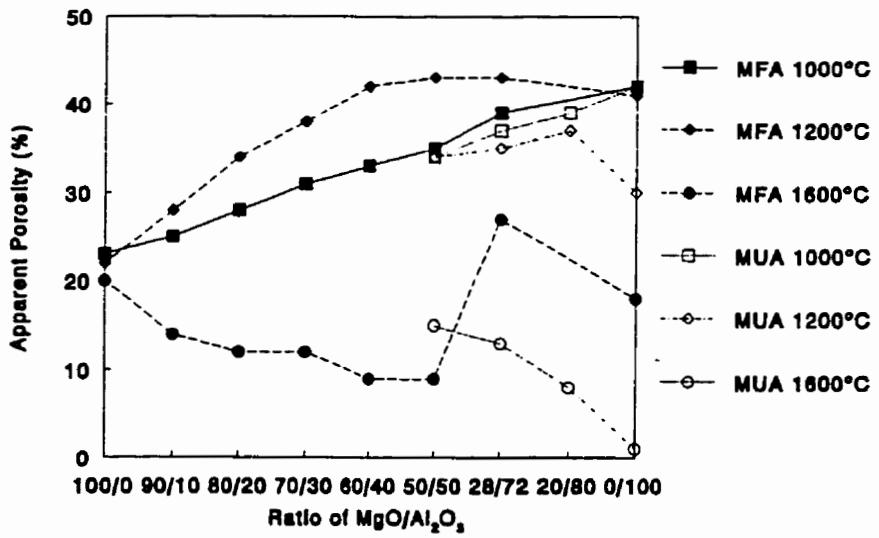

Figure 3.7 Effect of Fineness of Alumina and Ratio of MgO/Al_2O_3 on Apparent Porosity

At 1200°C, for the mixtures (MFA series) composed of magnesia (-0.1 mm) and fine alumina, the bulk density decreases with the increasing content of Al_2O_3, while, apparent porosity and volume expansion increase relative to 1000°C. This is due to the rearrangement of particles caused by the different thermal expansion between the MgO and Al_2O_3 and the formation of spinel at the contact point or surface between MgO and Al_2O_3 particles which always accompanies an expansion. The maximal value of volume expansion is found at the proportion of MgO/Al_2O_3=60/40. This is attributed to the maximum contact surface between the MgO and Al_2O_3 particles that leads to the maximum quantity of spinel formed.

Following the procedure of sintering or calcination for these compacts, generally, there are three factors which determine the ultimate volume change and porosity. They are sintering shrinkage of raw oxides (unreacted MgO and Al_2O_3 powders); expansion produced by the spinel formation; and sintering shrinkage of products (spinel). The three factors may happen simultaneously and the volume change is determined by the predominant factor(s). The results of MFA series at 1200°C indicate that the volume expansion is produced by the spinel formation; this has been confirmed by X-ray diffraction in Table 3.7.

Table 3.7 X-ray diffraction results for some selected samples

	Firing Temperature	Major phases	Minor phases
MFA28/72	1200°C for 6 hr.	periclase corundum	spinel
MFA28/72	1600°C for 6 hr.	spinel	periclase corundum
MUA28/72	1200°C for 6 hr.	periclase corundum	spinel

Due to the weak sinterability of raw materials (MgO and Fine Al_2O_3) and produced spinel at 1200°C, the spinel formation is the major factor to determine the ultimate properties of compacts. And the amount of spinel produced in compacts strongly influence the expansion and porosity. The proportion of formed spinel is calculated with equation-A, -B and -C in previous section by the change of specific gravity before and after firing, and the results are shown in Figure 3.8. The maximum amount of formed spinel at 1200°C is at the ratio of 60/40, the contact surface between the magnesia and alumina reaching a maximum. But the relative amount of spinel at 1200°C, relative to the total amount of spinel at 1600°C (where all the Al_2O_3 is assumed to transform to spinel), decreases when the proportion of MgO/Al_2O_3 approaches the stoichiometric ratio. This is due to a decrease in the amount of MgO which leads to a reduction of contact between individual Al_2O_3 and with MgO particles; consequently, the distance of diffusion increases and the spinel formation decreases. At 1600°C, most Al_2O_3 seems to transform to alumina-rich spinel. From Figure 3.6, 3.7 and 3.8, we can find a relation between the formed spinel amount and the amount of expansion.

At 1600°C, the bulk density and volume shrinkage increase (Figure 3.6), and apparent porosity in Figure 3.7 decreases with the increasing addition of alumina until 50%, however, at stoichiometric ratio (MgO/Al_2O_3=28/72), the reversion occurs. This proves that the stoichiometric spinel is much more difficult to densify than non-stoichiometric proportion. This probably is due to the great deal of formation of spinel with a large expansion which causes sintering difficulty. This result agrees with Chiang and Kingery's [99] investigation where they found that MgO rich spinel has a much more rapid grain growth rate than stoichiometric or Al_2O_3-rich spinel.

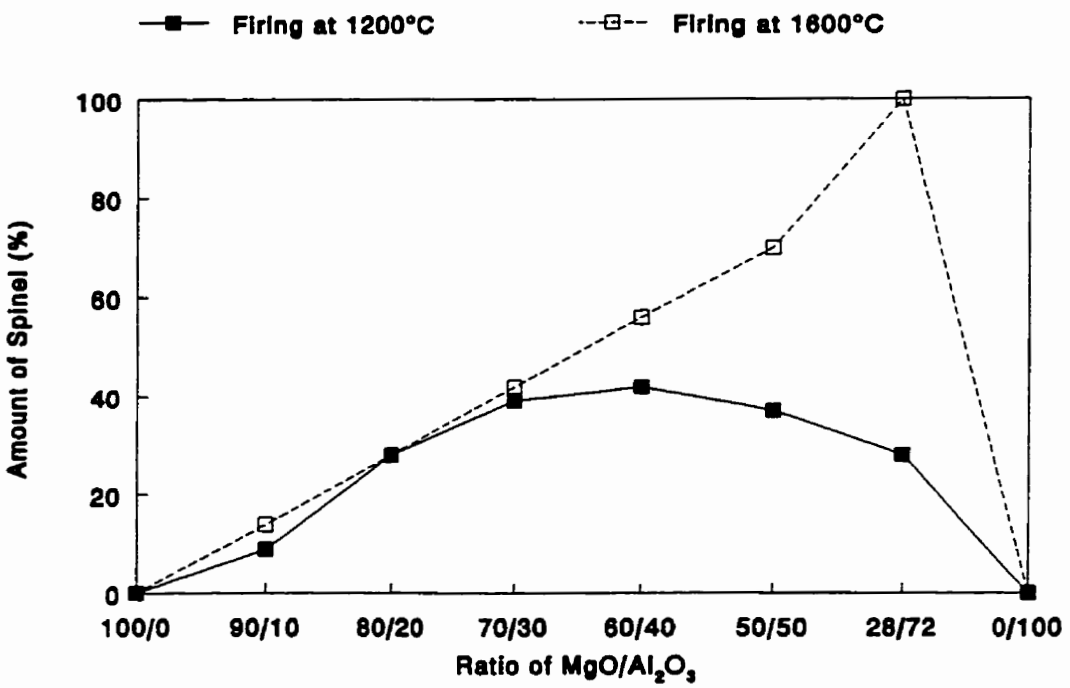

Figure 3.8 Quantity of Formed Spinel vs Proportion of Magnesia and Alumina in MFA Series Mixtures

Kanai [107] and Nakagawa[6] also studied the expansion behaviour of MgO-Al_2O_3 mixtures and showed a series of linear thermal shrinkage curves for powder compacts having various MgO/Al_2O_3 compositions. The specimens were composed of fine powder (-0.5 μm) of corundum and periclase. Every specimen had an expansion trend before 1300°C and begins to shrink after 1300°C. The spinel stoichiometric composition shows the largest linear expansion. Their results also prove that the largest expansion is produced with the stoichiometric ratio which agrees with our investigation.

Stoichiometric spinel shows a special expansion behaviour between the different MgO/Al_2O_3 ratio. It is necessary to investigate further the performance of stoichiometric spinel made of different raw materials.

3.2.2.2 Effect of Alumina Fineness on the Expansion-Shrinkage Behaviour of Mixtures

Mixtures (MUA series) made of ultrafine alumina have also been prepared. At 1200°C, bulk density, apparent porosity and volume change of these mixtures do not change appreciably as shown in Figures 3.6 and 3.7. This is due to the high sinterability of ultrafine alumina which causes the shrinkage at relatively low temperature, and, less amount of produced spinel, as shown in Figure 3.9. The shrinkage counteracts the volume expansion at about 1200°C. The densification mechanism and microstructure will be discussed in next section.

At 1600°C, the MUA series samples are highly densified. With more ultrafine alumina, the bulk density increases and apparent porosity decreases. This is attributed to the reactivity of ultrafine particles which can produce fine spinel crystal and sinter easily. The sample with MgO/Al_2O_3=28/72 doesn't exhibit great expansion because at 1600°C the sintering shrinkage is able to compensate for it.

Reviewing the procedure of sintering in the compacts, we can find that the raw materials (Al_2O_3 powders) determine mainly the ultimate properties of compacts because the effective factors of sinterability of raw oxides, reactivity between MgO and Al_2O_3; and sinterability of product (spinel) is decided by the raw materials characteristics. And the balance of the three factors indicates the properties of compacts. Fine Al_2O_3 powder shows a weak

sinterability and strong production of spinel before 1200°C, so a large expansion may happen. The Ultrafine alumina powder has an early sinterability which reduces the expansion of spinel formation. So the expansion and porosity can be adjusted by the nature of alumina powders and the MgO/Al_2O_3 ratio.

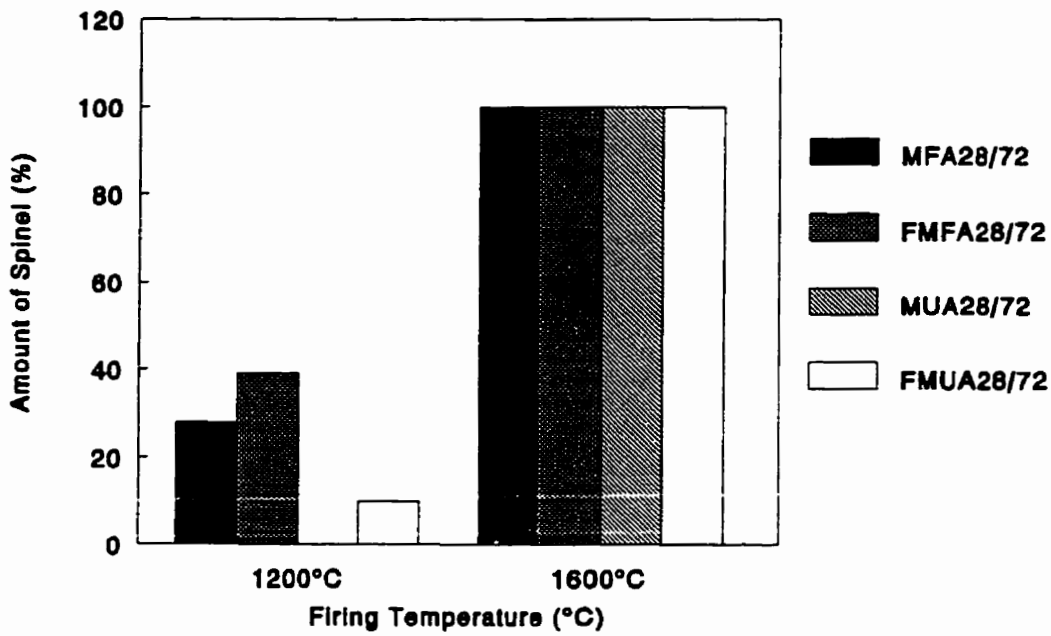

Figure 3.9 Quantity of Formed Spinel in the Stoichiometric Mixtures

3.2.2.3 Effect of Raw Materials on Properties of Stoichiometric Spinel

As shown in Table 3.6, four mixtures with the stoichiometric proportion have been prepared by using MgO (-0.1 mm) and (-0.045 mm), fine alumina and ultrafine alumina powders. Figure 3.10 illustrates the apparent porosity at different firing temperature and Figure 3.11 shows the results of volume change from 1000°C to 1200°C or 1600°C, respectively. The apparent porosity for all mixtures has a similar value at prefiring temperature of 1000°C, but the trend and evaluation is different after 1200°C. The mixtures containing ultrafine alumina (MUA and FMUA) show stronger densification and shrinkage than that containing fine alumina (MFA and FMFA). Consequently, the porosity of mixtures containing fine alumina increases and the samples with ultrafine alumina show a slight decrease. With the temperature up to 1600°C, all samples have a lower porosity than before, especially the samples containing ultrafine alumina show low porosity and considerable shrinkage. This is due to the higher sinterability of ultrafine alumina and the formation of agglomerate structure during mixing which accelerate the sintering of ultrafine alumina. The sintering of ultrafine alumina starts at a relatively low temperature and this process of sintering produces a large shrinkage, greater than the expansion due to spinel formation. But fine alumina has a less sinterability, especially at 1200°C and the mixtures produce a homogenous microstructure which can increase the contact surface between MgO and Al_2O_3 leading to the rapid formation of spinel and a large expansion.

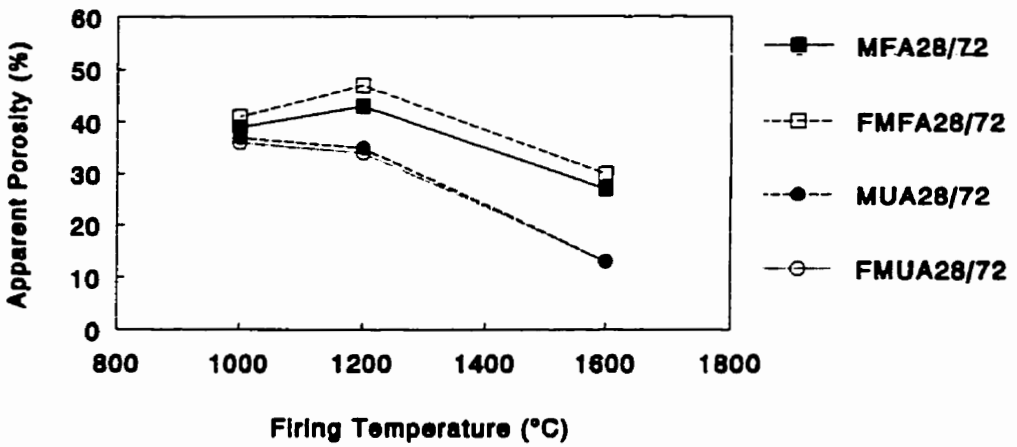

Figure 3.10 Apparent Porosity of Mixtures Containing Different Size Powders with Stoichiometric Proportion

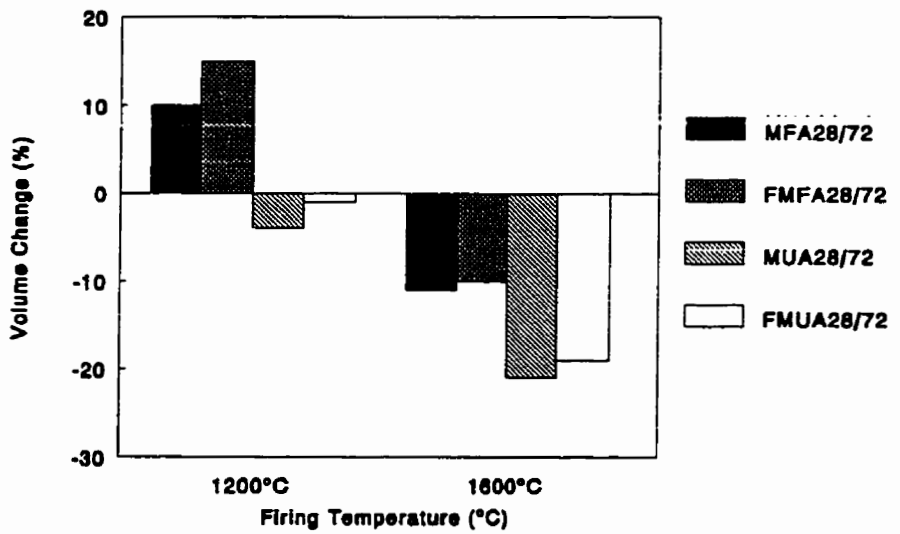

Figure 3.11 Volume Change of Mixtures Containing Different Size Powders with Stoichiometric Proportion

The spinel can be formed very well at 1600°C for all the stoichiometric mixtures, but at 1200°C, the mixture containing finer MgO (-0.045 mm) or fine Al_2O_3 produces more spinel. The finer MgO (-0.045 mm) has larger specific surface, so it is more reactive than MgO (-0.1 mm), this accelerates the formation of spinel. Fine alumina has a higher chemical activity to react with MgO than ultrafine alumina because fine alumina contains higher Na_2O, which works as mineralizer to accelerate the chemical reaction. The homogeneous dispersion between MgO and Al_2O_3 particles and lower sinterability of fine alumina itself also improve the reaction of spinel formation. The ultrafine alumina forms itself the cellular agglomerate during the dry mixing, which reduces the contact surface between MgO and Al_2O_3 particles, the agglomerates shrink rapidly to produce a dense alumina clinker during sintering, which greatly decreases the chemical activity of agglomerate, however, the mixture containing the fine alumina is homogeneously distributed between the MgO and Al_2O_3 particles. The finer MgO powder (-0.045 mm) can also accelerate the spinel formation due to the small size which can increase the contact surface between MgO and Al_2O_3, and meanwhile, which can decrease the diffusion distance of cation.

The pattern of formed spinel after firing at 1200°C from mixture of FMUA28/72 which contains MgO (- 0.045 mm) and ultrafine alumina at the stoichiometric ratio is shown in Figure 3.12. Spinel (bright thin ring) begins to form around the alumina agglomerates. The agglomerates does not show evident shrinkage at this temperature.

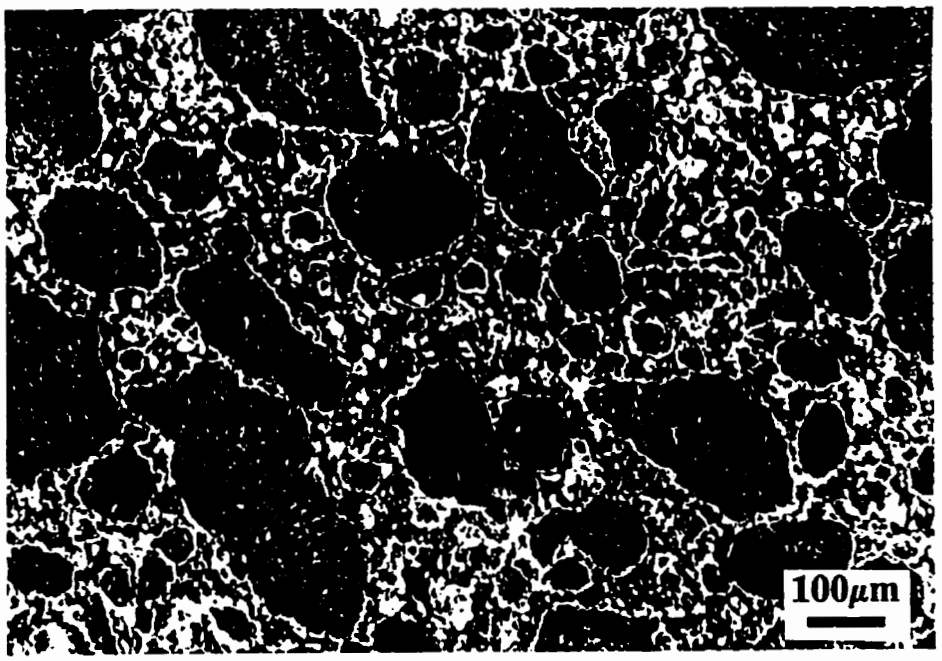

Figure 3.12 Mixture with Finer MgO and Ultrafine Alumina fired at 1200°C; spinel, as white ribbon, surrounds the alumina agglomerates

However, fine alumina has a relatively bigger size than ultrafine alumina, so the solid reaction between MgO and Al_2O_3 is relatively slow which leads to the increase of reaction temperature and time, and delays the start of sintering. Consequently, a high porosity and low shrinkage sample is produced.

The fineness of magnesia shows a greater effect on the densification at 1200°C than at 1600°C. More contact points between MgO and Al_2O_3 particles produces rapidly a great quantity of spinel at low temperature and causes larger expansion, so that the densification become difficult at 1200°C. Following the increasing temperature from 1200°C to 1600°C, the difference of density, porosity and volume change between the mixtures with different magnesia powders decrease slightly, because the alumina plays a more important role.

The microstructure of mixtures after firing at 1600°C has been observed and the MgO powders (-0.045 mm and -0.1 mm) have not evident influence on microstructure, but the two alumina powders show a strong effect on microstructural characteristics. Figures 3.13a shows a homogeneous and porous microstructure of mixture MFA28/72. It is possible to see the original MgO grains which have not been totally transformed to spinel, as confirmed by the X-ray diffraction analysis (a strong spinel peak and weak periclase and corundum peaks). At high magnification, as in Figure 3.13b, the clear unreacted MgO grains are separated from the matrix by gaps. These gaps are formed during cooling due to the difference of thermal expansion coefficient between MgO and spinel. The matrix has lots of pores. In the matrix, some spinel crystals can be observed, but these spinel crystals have not perfectly grown into the standard cubic pattern, meanwhile, some unreacted fine alumina crystals are still in the matrix.

The microstructure of mixture containing ultrafine alumina consists of sintered agglomerate which is more likely cellular. The individual agglomerate has a strong sintering shrinkage and densification after firing at 1600°C, but the micro cracks or gaps between the agglomerate cell exist. Two kinds of pattern of agglomerate can be observed. One with a dense centre is shown in Figure 3.14a and another agglomerate is with a hollow centre, as in Figure 3.14b. The dense agglomerate has a very hard and bright core in the centre produced by sintering. Around the core, there is a thick ring. The ring is denser near the core and less dense at the edge of agglomerate. The electron micro-probe analysis (EMPA) indicates that the bright central zone is nearly pure alumina, and the thick ring is dense spinel, as shown in Figures 3.15a and 3.15b. The edge of agglomerate is shown in Figure 3.14c, at magnification of 400 times. Some cubic likely spinel crystals can be identified and the micro pores exist between these crystals. In the gaps between agglomerates, some residual MgO grains can be observed. The small agglomerates are transformed mostly to spinel. Some agglomerates can also be found in the form of hollow centre due to the high sintering and diffusion rates (Figure 3.14b), if the initial agglomerates contain some pores.

Nakagawa et al [6] reported their sintering curve of compacts with stoichiometric ratio, with magnesia under 0.5 μm and alumina between 10 and 15 μm. The sintering behaviour always shows an expansion up to 1500°C and during soaking time, no evident shrinkage appears. But our results show an evident shrinkage at 1600°C which is different with theirs. The reason probably is the raw materials, and the sintering temperature. Nakagawa used coarse alumina and fine magnesia, while we used fine alumina and coarser magnesia. Alumina mainly controls the sintering shrinkage due to the evident difference of activity with the size

change, so the ultrafine alumina can greatly decrease the expansion.

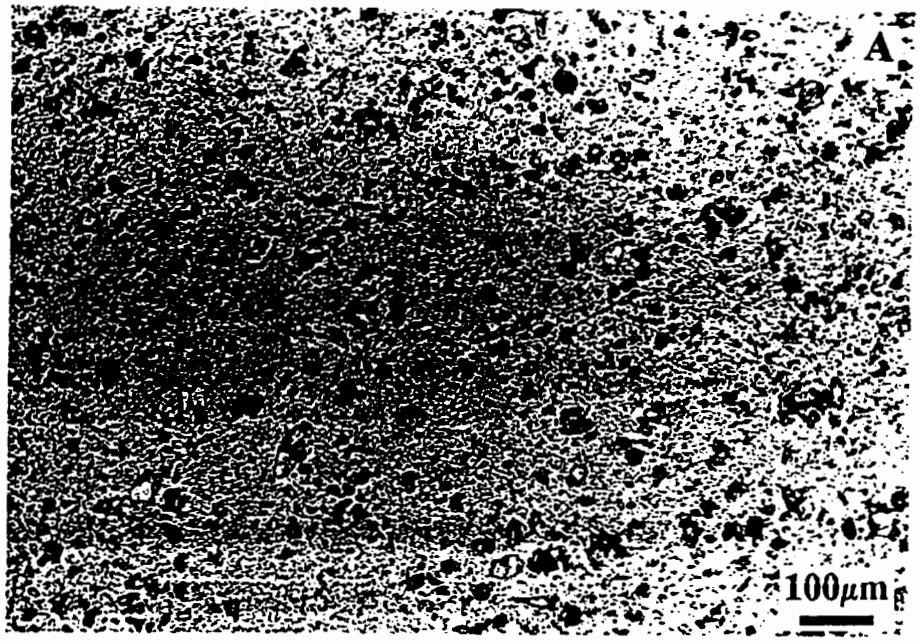

Figure 3.13a Microstructure of Mixture MFA28/72 which contains under 0.1 mm MgO and Fine Alumina Powder.

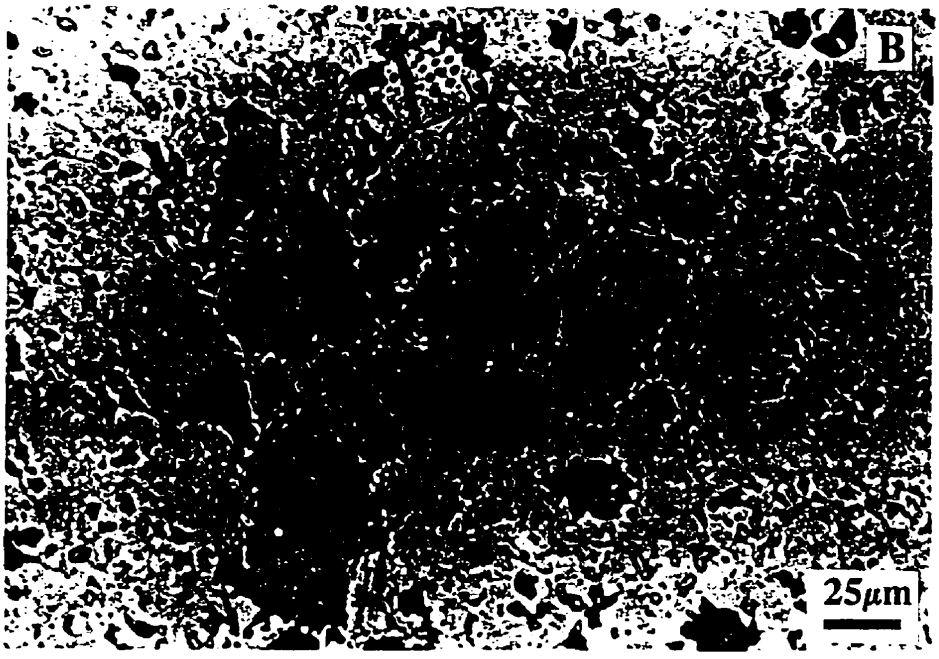

Figure 3.13b Microstructure of Mixture MFA28/72 which contains under 0.1 mm MgO and Fine Alumina Powder. a: is under 50x; b is under 200x.

Figure 3.14a and 3.14b Microstructure of Mixture MUA28/72 which contains under 0.1 mm MgO and Ultrafine Alumina Powder. a and b: is under 50x; c is under 400x.

Figure 3.14c Microstructure of Mixture MUA28/72 which contains under 0.1 mm MgO and Ultrafine Alumina Powder. a and b: is under 50x; c is under 400x.

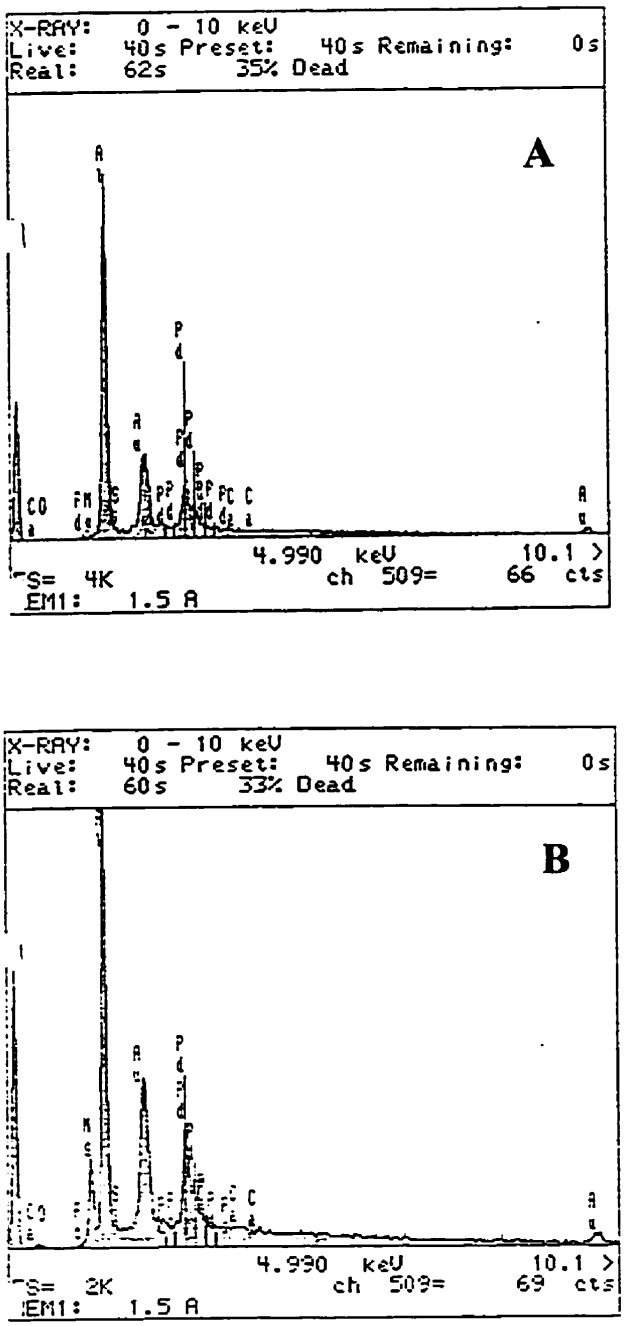

Figure 3.15 EMPA Results on the Agglomerate Composition

a is in the bright core of agglomerate and b is in the thick ring zone (see figure 3.14a)

3.2.2.4 Characteristics of Sintered Mixtures Containing Coarse Grains

The chemical reaction with +0.125 mm MgO or Al_2O_3 grains is more difficult and complex, so the formed spinel amount in the mixture is very difficult to determine; and the porosity and volume change are not clearly related to MgO/Al_2O_3 ratio. Physical properties of such mixtures are indicated in Table 3.8.

Table 3.8 Physical Properties of Mixtures Containing Big Grains

No.	Composition	1000°C		1200°C			1600°C		
		D (±0.05)	P (±1)	D (±0.05)	P (±1)	ΔV (±1)	D (±0.05)	P (±1)	ΔV (±1)
CM-FA	28%CM and 72%FA	2.39	37	2.39	37	0	2.67	28	-11
CM-UA	28%CM and 72%UA	2.53	33	2.67	30	-5	2.89	21	-13
FM-CA	28%FM and 72%CA	2.90	24	2.87	25	1	2.18	40	33

Note: CM: MgO grain with 0.125-1.41 mm, FM: fine MgO powder of under 0.045 mm, FA: fine alumina, UA: ultrafine alumina, CA: fused alumina with 0.125-1.41 mm; D: bulk density (g/cm³), P: apparent porosity (%), ΔV: volume change.

Mixtures of magnesia aggregates 0.125 - 1.41 mm with fine and ultrafine alumina at stoichiometric ratio were fired at 1000°C, 1200°C and 1600°C, respectively. The apparent porosity of mixture (CM-UA) containing big MgO grains and ultrafine alumina is always less than that (CM-FA). This probably is due to the stronger shrinkage of ultrafine alumina during sintering to form a dense matrix to decrease the porosity, and meanwhile, the expansion from spinel formation is less due to the difficulty of chemical reaction with big grains.

The microstructure of mixture CM-FA is represented in Figure 3.16a. The matrix is homogeneous and porous. Spinel is mostly formed near the MgO grains which shows a bright and dense line around MgO grains. The matrix consists of alumina-rich spinel which is identified by EMPA in Figure 3.16b. The continuous crack is formed around MgO grains which separate the matrix and magnesia grains. This cracks or gaps between matrix and MgO grains is produced during the cooling by the different thermal expansion of MgO and spinel.

The mixture containing CM MgO grains and UFA alumina shows a different microstructure in figure 3.17, comparing it with mixture containing -0.1mm MgO grains in figure 3.11 which forms the agglomerate microstructure. Due to the existence of big MgO grains, the alumina agglomerate is broken during mixing, so the microstructure consists of big MgO grains and dense matrix. The alumina in matrix mostly converts to spinel, but some dense matrix zone which is farther from MgO grains can find some sintered alumina core in Figure 3.17. Some cracks and pores can also observed. Figure 3.18 is the EMPA results in the interface of a MgO grain and matrix. From Figure 3.18, a gap is formed between MgO grain and matrix. The MgO grain edge is still highly purity MgO and the matrix around the grain is spinel.

Figure 3.16a Microstructure of Mixture Containing Big MgO Grains and Fine Alumina

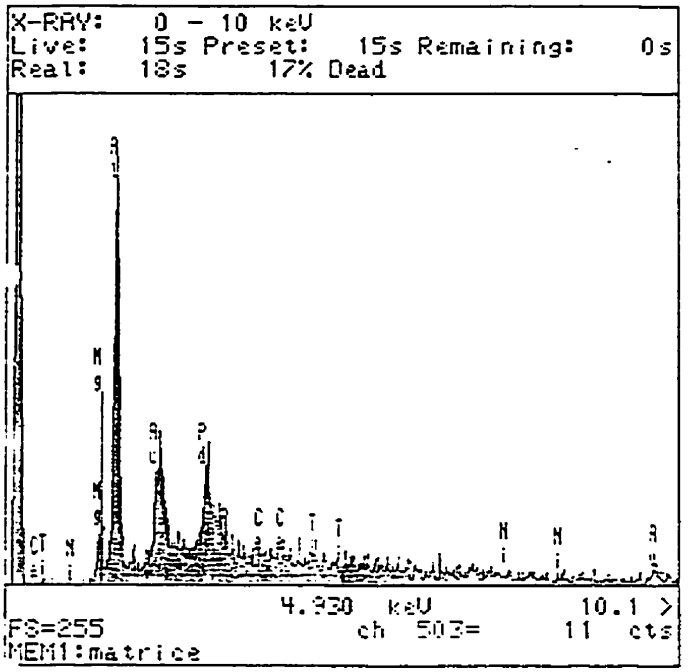

Figure 3.16b Result of EMPA in the Matrix

Figure 3.17 Microstructure of Mixture Containing Big MgO Grains and Ultrafine Alumina after Firing at 1600°C

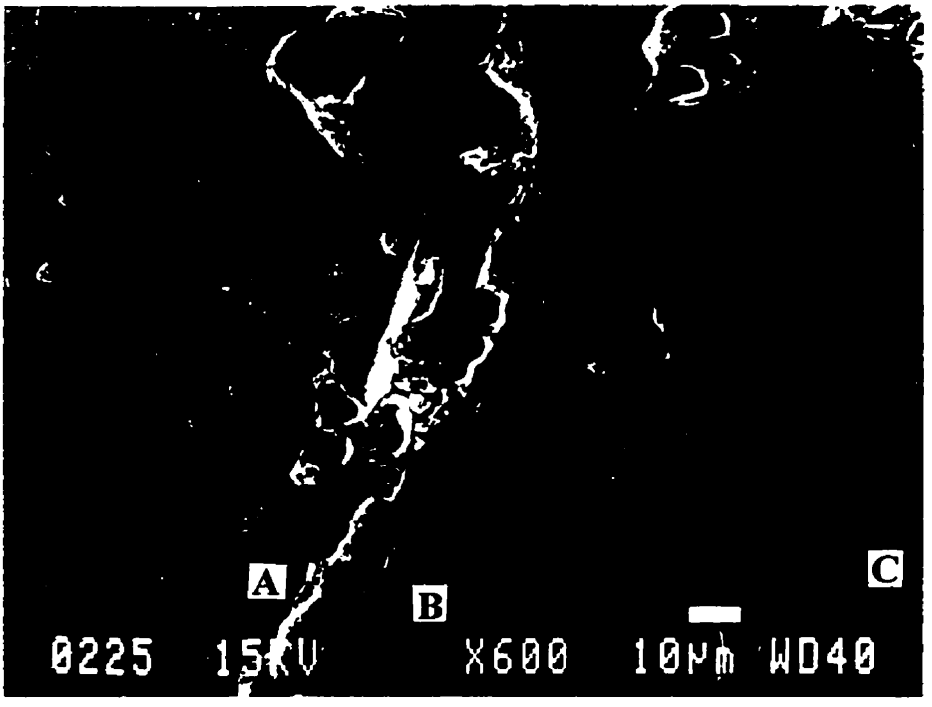

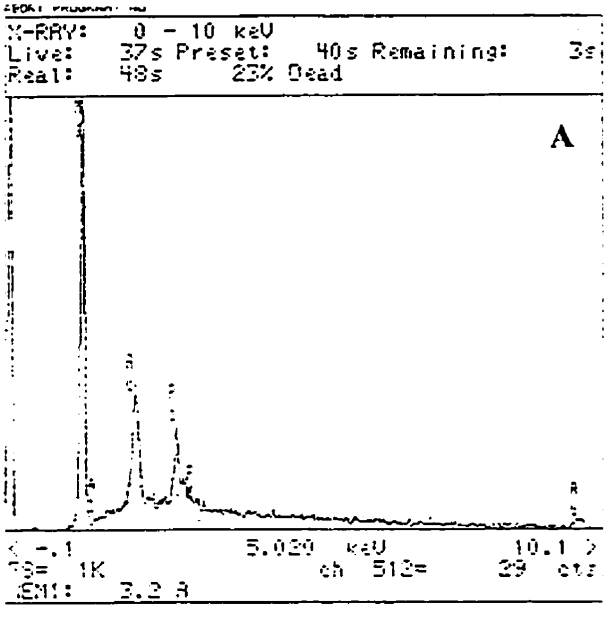

Figure 3.18a Microstructure of Mixture Containing Big MgO Grains and Ultrafine Alumina Alumina; and SEM and EMPA Results at the Interface between MgO Grain and Matrix.

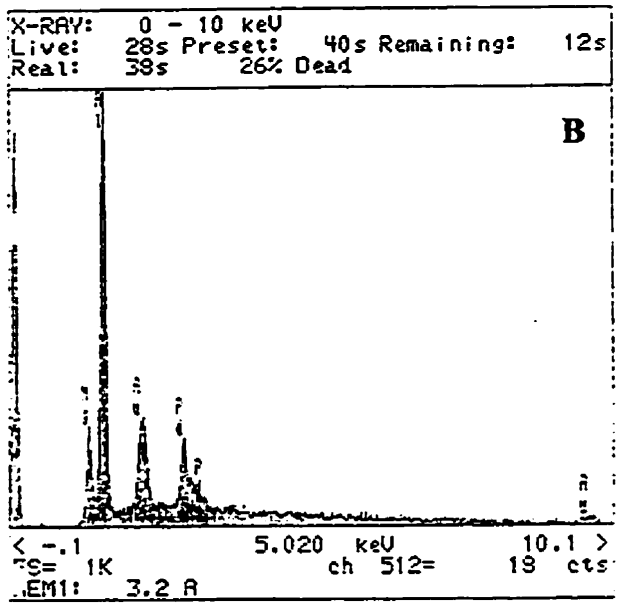

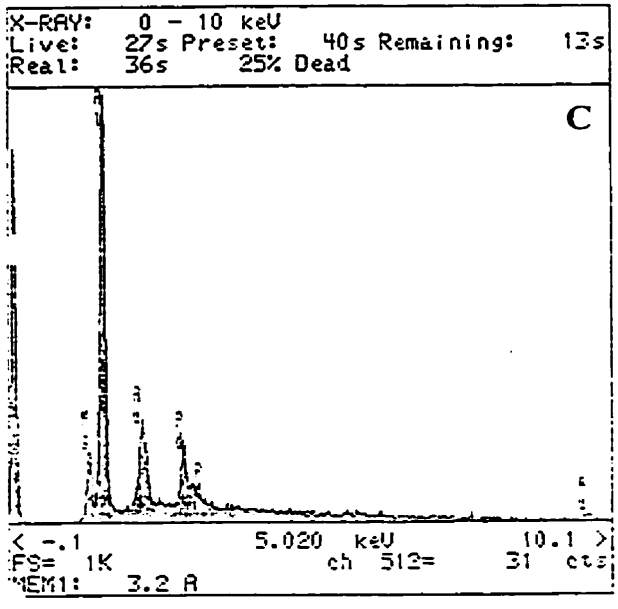

Figure 3.18b and 3.18c Microstructure of Mixture Containing MgO Grains and Ultrafine Alumina; and SEM and EMPA Results at the Interface between MgO Grain and Matrix.

a: at the MgO grain edge, b: in denser matrix near MgO grain, c: in matrix a little far from the MgO grain.

The mixture which consists of big fused alumina grains with size of 0.125-1.41 mm and fine magnesia powder of under 0.045 mm is more difficult to densify because the density decreases continuously and porosity increases with the increasing temperature. Especially at 1600°C, the porosity value is much higher than that at intermediate temperature. The reason probably is that the reaction between big alumina grains and fine MgO powder can start at 1200°C. X-ray diffraction results confirm that such is the case. This reaction is controled by the diffusion of Mg^{2+} and Al^{3+} cations into big alumina grains. The spinel production accompanies a volume expansion, so the density shows a continuous decrease until 1600°C.

The microstructure of this mixture fired at 1200°C is represented in Figure 3.19a. The spinel can be observed around the fused alumina grains. The matrix shows a low strength due to no evident sintering and/or bonding formation. After firing at 1600°C, the matrix is very porous and lots of large cracks are produced between matrix and grains. The spinel in Figure 3.19b is formed around fused alumina grains and connects tightly on unreacted alumina which is different with the mixture containing big MgO grains and alumina powder, where the MgO grains separate with spinel matrix. This is due to the great different thermal expansion between MgO and alumina or spinel, so the gap or crack always produces between MgO and spinel, and spinel adheres to the alumina.

Figure 3.19 Microstructure of Mixture Containing Big Fused Alumina Grains and Under 0.045 mm Magnesia Powder. a: firing at 1200°C, b: firing at 1600°C.

3.2.3 Recapitulation on $MgO-Al_2O_3$ Mixtures

First, the effect of MgO/Al_2O_3 ratio on the expansion-shrinkage behaviour and apparent porosity of compacts is reported. The largest expansion occurs at the ratio of 60% MgO and 40% Al_2O_3 at 1200°C in the mixtures of under100μm MgO and fine alumina (D_{50} of 4 μm) series; due to rapid formation of spinel determined by the contact point between MgO and Al_2O_3; less sintering shrinkage of product (spinel) and less sintering shrinkage of raw material (MgO and Al_2O_3);. Because of the size ratio between MgO and Al_2O_3, the 60M/40A ratio produces the most contact points between MgO and Al_2O_3 particles, so the more produced spinel leads to the maximal expansion. The apparent porosity and bulk density of compacts also change following the expansion-shrinkage behaviour with the different MgO/Al_2O_3 ratio.

At 1600°C, sintering plays an increasing role which causes large shrinkage for most mixtures except the stoichiometric ratio. At this ratio, a great deal of spinel is produced which leads to a large expansion, meanwhile, no excess MgO or Al_2O_3 is available to form some solid solution with spinel. The solid solution can accelerate the densification as reported by Chiang and Kingery [99]. Nakagawa [6] also got a similar result with the stoichiometric mixture having the largest expansion.

Large expansion in refractories will lead to cracking, so controlling the expansion is important. The ultrafine alumina is useful for that purpose. All mixtures containing UA show shrinkage at 1200°C, even at the stoichiometric ratio. Further densification and shrinkage can be obtained at 1600°C.

Due to the special feature of stoichiometric spinel, more mixtures with stoichiometric ratio have been investigated. Alumina shows a stronger influence on the sintering shrinkage

than magnesia. At 1200°C, mixtures containing fine alumina experienced an expansion, but those containing ultrafine alumina showed shrinkage. On the other hand, the high chemical activity of fine alumina and the uniform distribution between fine alumina and magnesia particles also leads to strong expansion, due to great deal of produced spinel at 1200°C. Ultrafine alumina has an effective shrinkage at 1200°C which causes the slight shrinkage of mixture.

The microstructures of mixtures containing fine alumina and ultrafine alumina show great different. The former forms a homogeneous and porous microstructure, but the later produces a dense agglomerate structure which begin to be formed at 1200°C and continue to densify at 1600°C.

The purpose of this study was to investigate the reactivity between coarse aggregates and fine powders which always exists in the matrix of real refractory castables. Due to the local (grain surface zone) and incomplete chemical reaction between coarse grains and fine powder in matrix, the quantitative description will be difficult, so the microstructural observation is major in this section. The mixtures with fine alumina lead to an homogeneous and porous matrix in the mixture at 1600°C and a spinel ring around MgO grains is produced. For ultrafine alumina mixtures there is a strong sintering in the matrix and some unreacted alumina core produced by sintering are surrounded by thick spinel layer. A denser structure is formed. The mixture containing coarse Al_2O_3 and fine MgO has an expansion trend from 1000°C to 1600°C. This is attributed to the spinel formation and very weak sinterability of fine MgO powder which occupies a high fraction in matrix, so the high porosity is produced in mixture.

It has been proven that the expansion-shrinkage can be controlled. The main factors influencing the expansion-shrinkage behaviour have been discussed. By optimizing the raw materials ratio in castable, the production of no- or less-expansion castable will be possible.

3.3 Effect of Fume Silica and Calcium Aluminate Cement on Properties of Sintered Mixtures

Some cement or some silica fume were added into the mixtures in order to investigate their effect on the properties of refractory matrix. The mixtures are made from under 0.1 mm MgO powder and ultrafine alumina at two ratio: MA-MgO rich (50%MgO) and MA-Al_2O_3 rich (80%Al_2O_3). The amorphous fume silica is added at level of 3%, 7% and 10%, and the cement Lafarge Secar 80 is added at level of 5%, 10% and 15%. Mixtures compositions are shown in Table 3.9. The physical properties after firing at different temperatures are indicated in Table 3.10. In Table 3.11 are results of X-ray diffraction for some selected mixtures, after firing at 1200°C and 1600°C.

3.3.1 Addition of Fume Silica

As shown in Figure 3.20. Fume silica addition do decrease the porosity of mixtures. At 1600°C, mixtures containing high amount of silica have a very low porosity. The silica is in liquid phase at high temperature, so the liquid phase accelerates the densification. The microstructural picture in figure 3.21 of AMS2 (7% silica) after firing at 1600°C shows lots of glassy phase. In the existence of liquid phase, the mixture can produce very beautiful cubic spinel crystals. The silica is in glassy phase after cooling since not peak of SiO_2 is detected by X-ray diffraction while very strong spinel peaks are present.

Table 3.9 Composition of Mixtures Containing Silica or Cement

	MgO (<0.1 mm) (%)	Ultrafine Alumina (%)	Fume Silica (%)	Cement (%)
AM	20.00	80.00		
MA	50.00	50.00		
AMS1	19.40	77.60	3.00	
AMS2	18.60	74.40	7.00	
AMS3	18.00	72.00	10.00	
MAS1	48.50	48.50	3.00	
MAS2	46.50	46.50	7.00	
MAS3	45.00	45.00	10.00	
AMC1	19.00	76.00		5.00
AMC2	18.00	72.00		10.00
AMC3	17.00	68.00		15.00
MAC1	47.50	47.50		5.00
MAC2	45.00	45.00		10.00
MAC3	42.50	42.50		15.00

Table 3.10 Physical Properties of Mixtures Containing Fume Silica and Cement

	1000°C		1200°C			1600°C		
	D (±0.05)	P (±1)	D (±0.05)	P (±1)	ΔV (±1)	D (±0.05)	P (±1)	ΔV (±1)
AM	2.35	39	2.41	37	-3	3.18	8	-26
MA	2.46	34	2.44	34	0	2.98	15	-17
AMS1	2.43	36	2.54	33	-4	3.13	6	-22
AMS2	2.38	36	2.46	33	-3	3.05	1	-22
AMS3	2.33	36	2.38	34	-2	2.89	1	-19
MAS1	2.51	32	2.49	31	1	3.04	14	-17
MAS2	2.42	33	2.45	32	-1	2.69	23	-10
MAS3	2.37	33	2.43	32	-2	2.42	30	-2
AMC1	2.44	36	2.48	34	-2	3.04	15	-20
AMC2	2.42	36	2.48	33	-2	3.03	16	-20
AMC3	2.39	37	2.48	33	-4	2.95	17	-19
MAC1	2.53	32	2.48	32	2	2.97	13	-15
MAC2	2.49	32	2.45	32	2	2.92	14	-15
MAC3	2.47	32	2.46	31	1	2.94	13	-16

Note: D: bulk density (g/cm^3), P: apparent porosity (%), ΔV: volume change (%).

Table 3.11 X-ray Diffraction Results for Some Selected Samples

	Major Phases	Minor Phases	Trace Phases
AMS2 after 1600°C	Spinel		
MAS3 after 1200°C	Periclase, Spinel	Corundum, Cristobalite, Forsterite	
MAS3 after 1600°C	Spinel, Periclase	Forsterite	Corundum
AMC2 after 1600°C	Spinel	CA_6	Corundum
MAC2 after 1600°C	Spinel, Periclase		CA

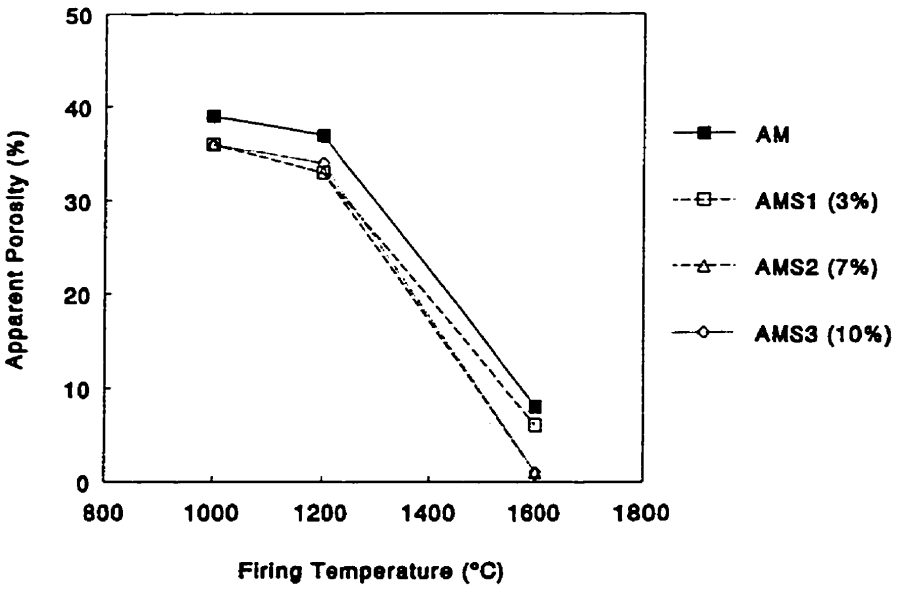

Figure 3.20 Effect of Silica on Apparent Porosity of Mixture with Alumina-Rich Ratio

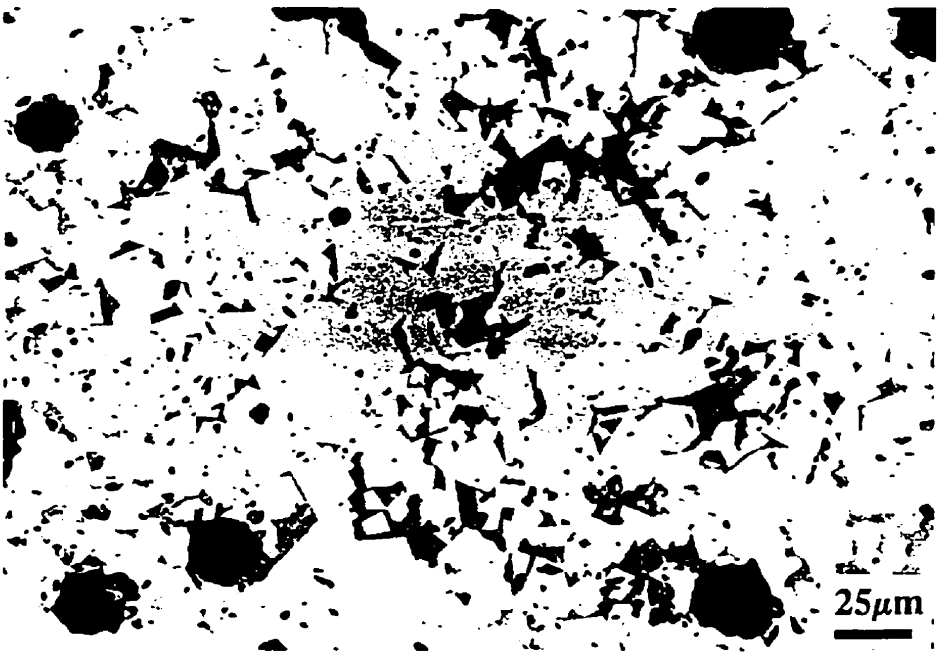

Figure 3.21 Microstructure of Alumina-Rich Mixture Containing 7% Silica

The mixtures with constant ratio between MgO and Al_2O_3 at 50/50 and 3%, 7% or 10% fume silica addition are produced to estimate their physical properties. The apparent porosity is shown in figure 3.22. The silica addition mixtures have a lower porosity than that without silica in the firing temperature of 1000°C and 1200°C. This is due to the amorphous silica which is very active. The fume silica has four roles during firing at intermediate temperature. First, it can react with MgO to form the forsterite at relatively low temperature, second, the amorphous silica will transform to cristobalite crystal, third, the presence of silica can accelerate the formation of spinel, and forth, the silica can accelerate sintering shrinkage. The X-ray diffraction results for mixture MAS3 after firing at 1200°C indicate that a certain amount of spinel has been produced and the cristobalite and forsterite also present at this temperature. At 1600°C, a great deal of spinel is produced and nearly all silica transfers to forsterite, always from the X-ray diffraction data. The porosity increases with the increasing amount of silica. This is due the existence of multiphases in mixture because the more addition of silica leads to the production of spinel, periclase and forsterite. The three minerals have different thermal expansion, so lots of cracks will be formed during cooling due to the mismatch among them. Figure 3.23 shows the microstructure of mixture MAS2 after firing at 1600°C. The co-existence of unreacted MgO, formed spinel and forsterite can be observed.

Reviewing the function of silica in MgO-rich mixture, it can be concluded that small amount of silica can accelerate the densification, for example MAS1, by the improvement of sintering, but more silica will lead to the great deal of forsterite which increases the mismatch among the different minerals in the mixture, so the structure will be loose.

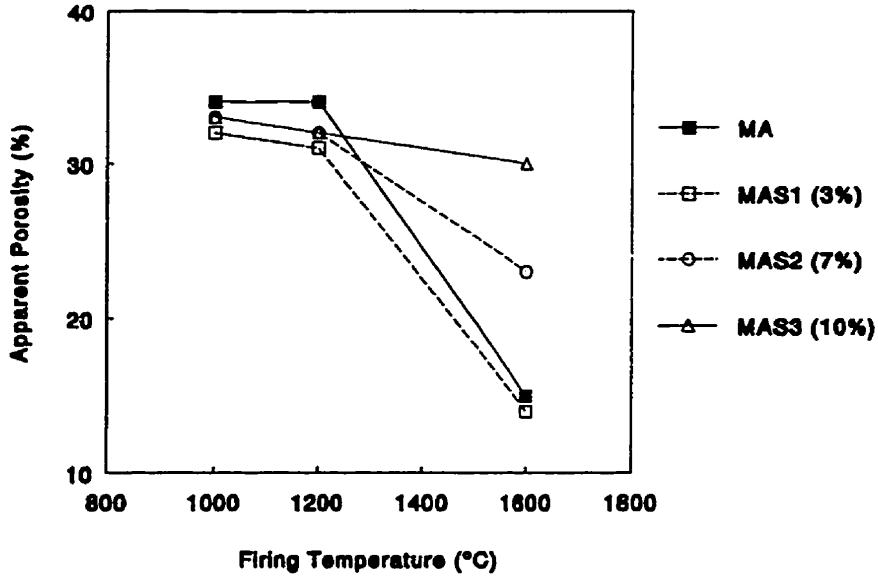

Figure 3.22 Effect of Silica on the Apparent Porosity of Mixture with MgO-Rich Ratio

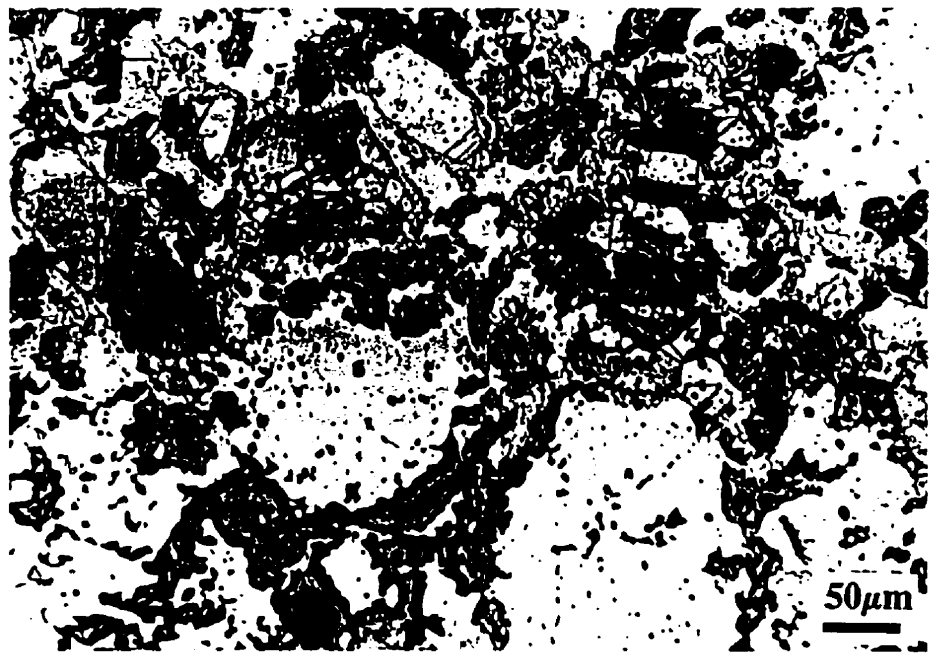

Figure 3.23 Microstructure of MgO-Rich Mixture (MAS2) with Silica Addition

3.3.2 Addition of Calcium Aluminate Cement

The different amount of cement with 80% Al_2O_3 has been added in alumina-rich mixture. The apparent porosity is represented in figure 3.24. The addition amount from 5% to 15% results in a similar porosity value. At intermediate temperature, the cement can decrease the porosity, but at 1600°C, the porosity of mixture containing cement increases. The microstructure of mixture (AMC2) after firing at 1600°C which contains 10% cement shows an agglomerate structure in figure 3.25. Most MgO has converted to spinel and certain amount of CA_6 has been found by X-ray diffraction in table 3.11. The formation of CA_6 accompanies a slight volume expansion. The CA_6 presents between the agglomerates, so CA_6 can limit the sintering shrinkage between the agglomerates to some extent. For this reason, a high porosity is produced in the mixture.

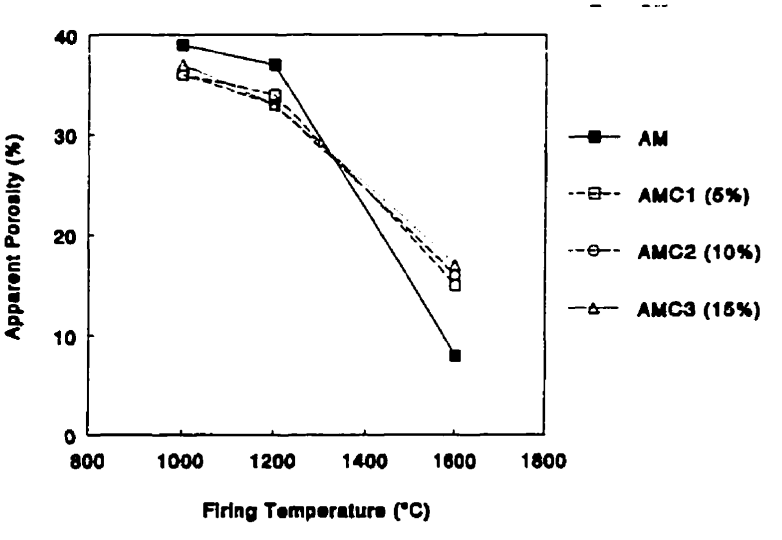

Figure 3.24 Effect of High Alumina Cement on Apparent Porosity of Alumina-Rich Mixture

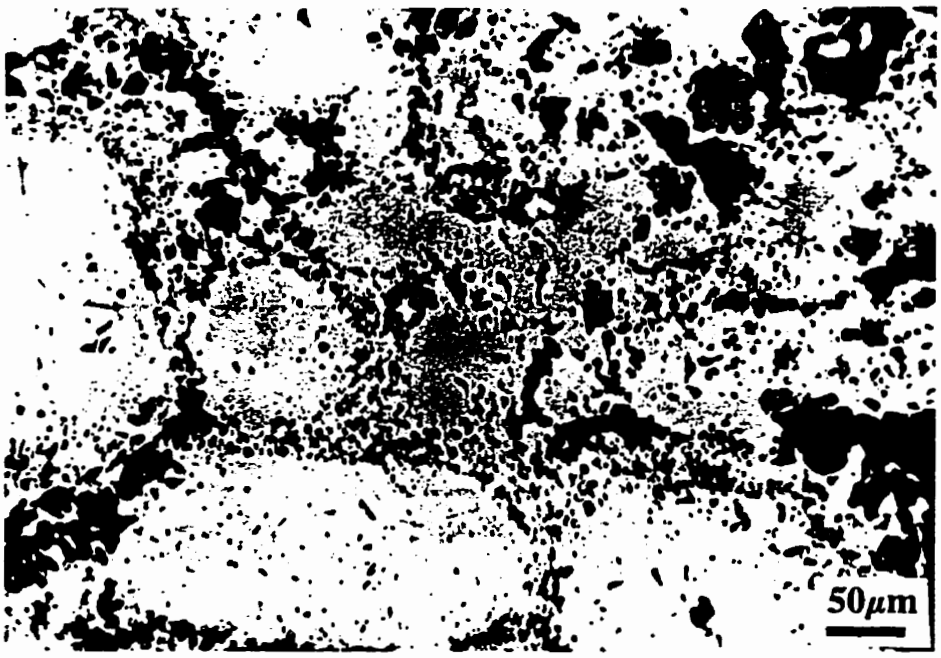

Figure 3.25 Microstructure of Alumina-Rich Mixture with Cement Addition

Figure 2.26 exhibits the effect of cement on the porosity of MgO-rich mixture. The cement addition can slightly decrease the porosity for all the firing temperatures tested. But between them, no evident influence happens. The X-ray diffraction finds great amount of spinel and unreacted periclase, and very less CA for the sample (MAC2) after firing at 1600°C. CA comes from cement and does not react with magnesia or alumina, because most alumina combines with MgO to form spinel and no more free alumina exists in mixture. CA can accelerate the formation and growth of spinel, so the clear cubic spinel crystals can be identified in figure 3.27. Some CA in glassy state dispersed in the void of spinel crystals has been observed.

The CA cannot find the free alumina in the mixture to react to form CA_6, for this reason, the CA probably is in liquid phase at 1600°C. The liquid CA can easily penetrate and disperse into the matrix and accelerates the spinel formation and crystalline growth, and meanwhile, the densification and sintering shrinkage.

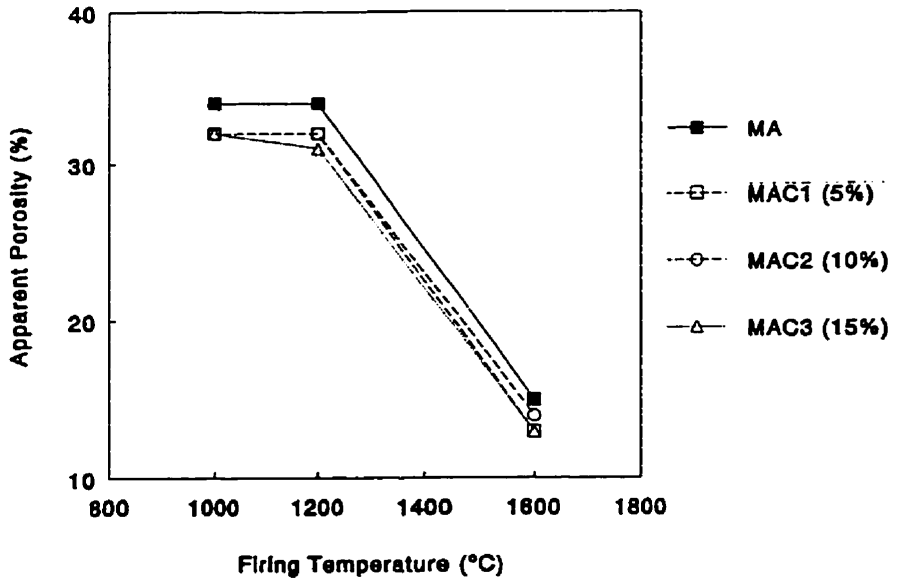

Figure 3.26 Effect of High Alumina Cement on Apparent Porosity of MgO-Rich Mixture

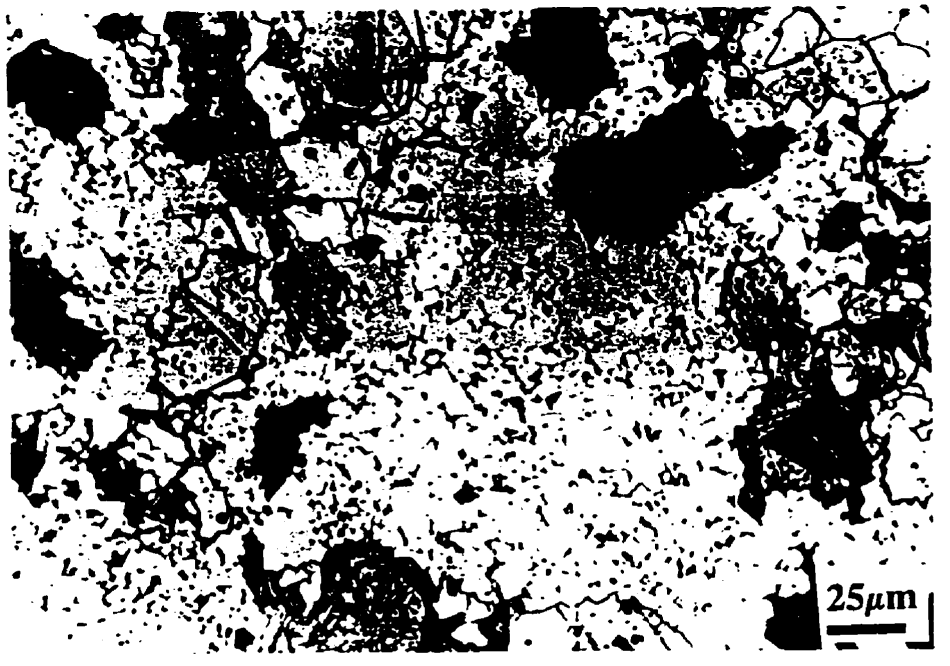

Figure 3.27 Microstructure of MgO-Rich Mixture with Cement Addition

CHAPTER 4 CEMENT-FREE CASTABLES FORMULATIONS, PHYSICAL AND MECHANICAL PROPERTIES

In previous chapter, the formation of spinel with the MgO and Al_2O_3 fine powders was discussed. The strategy is to master the feature of spinel formation and the physical performance. In this chapter, the mixes containing aggregates, fine powders and binder, more similar to the vibratory castables, are produced. The mixes are designed to satisfy some specific prospective requirements of steel making refractories, for example, strong corrosion resistance (mainly dissolution resistance) and acceptable mechanical strength.

The formulation and preparation of mixes is first discussed in this chapter. The optimal granulometry, the use of fine and ultrafine powders, the replacement of cement by hydratable alumina to decrease the CaO content, have been controlled without considering the rheology, the setting and the hardening times.

The physical and mechanical properties of castables have been measured and optimized first through the use of the proper amount of alumina powders.

4.1 Preparation of the Mixes

The magnesia based mixes consist of magnesia aggregate and magnesia-alumina fine powders as matrix. In matrix, more alumina and less magnesia are co-mixed. To realize an ideal formulation, the size distribution is first discussed by the use of Andreasen's equation and the optimum exponent n is found for our system. Then the formation of mixes is

introduced that includes binder, mixing, pouring, drying. etc.

The size distribution of bulk mixes greatly influences the compacity of products, and also some mechanical properties. To optimize the compacity, the Andreason's equation is chosen.

The size distribution is designed by use of Andreasen's equation: $CPFT=(d/D_{max})^n$ in our investigation. By changing the exponent (n), the components, and ratio of aggregates and fine particles show a continuous and variable distribution. Figure 4.1 shows the exponent (n) with the value of 0.25, 0.35, 0.37, 0.40 and 0.45.

The popular alumina based castables, which consist of fused alumina aggregate, fine alumina, silica fume and CA cement, are first investigated in order to find the best exponent for alumina system and use it as a reference. The magnesia based castables will be compared with it. The purpose is to find the influence of raw materials on the compacity, because the magnesia as aggregate to produce castables is a new trial.

The relation between the size distribution and green body's properties is studied. In Tables 4.1 and 4.2 are the mixtures' composition of corundum and magnesia systems, respectively. In these mixes, the CA cement is chosen as binder since the main purpose is to concentrate on the compacity at this stage. The alumina based castable contains constant amount of cement (5%) and fume silica (5.5%). With the increase of exponent (n), the castable contains more coarse aggregates and less fine particles. The added water increases with the increasing fine particles amount. The magnesia based castables have a constant amount of fine MgO powder (7.6%) and cement (2.6%), and the added water is also same for the three mixtures. The apparent porosity and mechanical strength for these castables are

indicated in table 4.3.

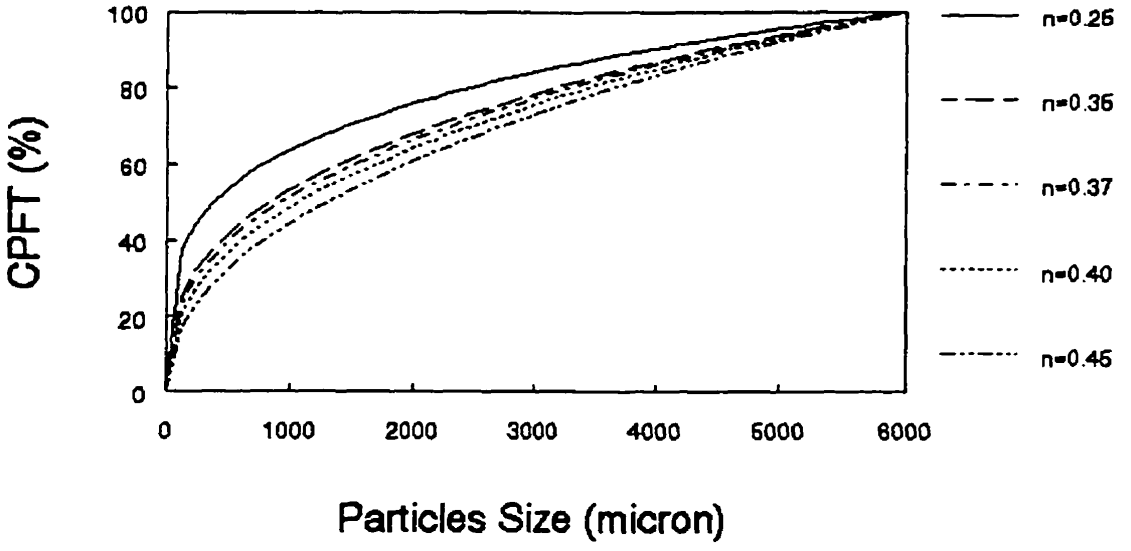

Figure 4.1 Size Distribution of Andreasen's Equation

Table 4.1 Composition of Corundum Based Castable

No.		A1	A2	A3	A4
Exponent of Andreasen's Equation		n=0.25	n=0.35	n=0.37	n=0.45
Corundum	5660 - 210 μm	58.4	71.5	73.6	80.9
Corundum	<149 μm	8.1	7.3	7.0	5.5
Fine Alumina	<45 μm	23.0	10.7	8.9	3.1
Fume Silica	<0.3 μm	5.5	5.5	5.5	5.5
Cement(71%Al_2O_3)	<80 μm	5	5	5	5
Water		5	3.56	3.5	3.44

Table 4.2 Composition of Magnesia Based Castable

No.		M1	M2	M3
Exponent of Andreasen's Equation		n=0.35	n=0.37	n=0.40
Magnesia Clinker	4760 - 125 μm	73.4	72.8	75.5
Magnesia Clinker	<125 μm	7.6	7.6	7.6
Fine Alumina	<45 μm	16.4	17.0	14.3
Cement (71%Al_2O_3)	<80 μm	2.6	2.6	2.6
Water		5.33	5.33	5.33

Table 4.3 The Green Body's Apparent Porosity and Mechanical Strength (MOR) for Both Alumina and Magnesia Based Castables

	Alumina Based Castables				Magnesia Based Castables		
	A1	A2	A3	A4	M1	M2	M3
Porosity (±2 %)	9	4	2	8	15	14	14
MOR (±0.5 MPa)					2	5	4

The apparent porosity in green body after drying at 110°C is shown in figure 4.2 for both corundum based castable and magnesia based castable. Both series castables show a minimal apparent porosity with the exponent of 0.37 which is agreeable to Dinger and Funk's theoretical calculation [108]. The green body's mechanical strength of magnesia based castables shows a best value with exponent of 0.37 also (Table 4.3). The densest structure with n=0.37 leads to the highest mechanical strength. Comparing the alumina based and magnesia based castables, the magnesia based castables have a higher porosity. This is due to the relatively high viscosity caused by fine MgO and lack of ultrafine particle likely silica

fume, so a weak workability and less filling decrease the compacity.

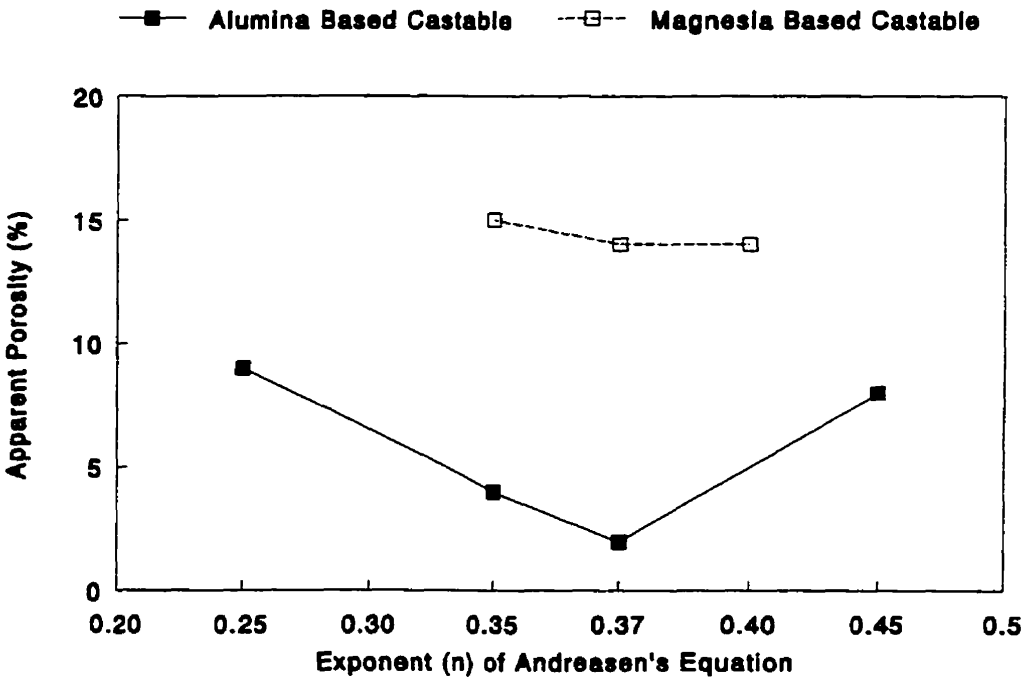

Figure 4.2 Effect of Size Distribution on Apparent Porosity of Castables

The magnesia-alumina mixes were prepared using high purity periclase aggregate and ball milled MgO grain with some fine and ultrafine aluminas and active alumina (hydratable alumina) to replace the CA cement. This was done in order to improve the refractoriness of the mixes, the high temperature mechanical properties and the corrosion resistance.

The MgO aggregates used in this series of castables is sintered seawater magnesia of 99% purity, 4 sizes: 3-6 mesh; 6-14 mesh; 14-48 mesh; under 48 mesh, and ball milled

magnesia powder produced in the laboratory. The size distributions of under 48 mesh and ball milled powders are shown in Figure 4.3. The chemical composition of the magnesia has been given in Chapter 3. The information about the alumina and the additives powders has also been introduced in Chapter 3.

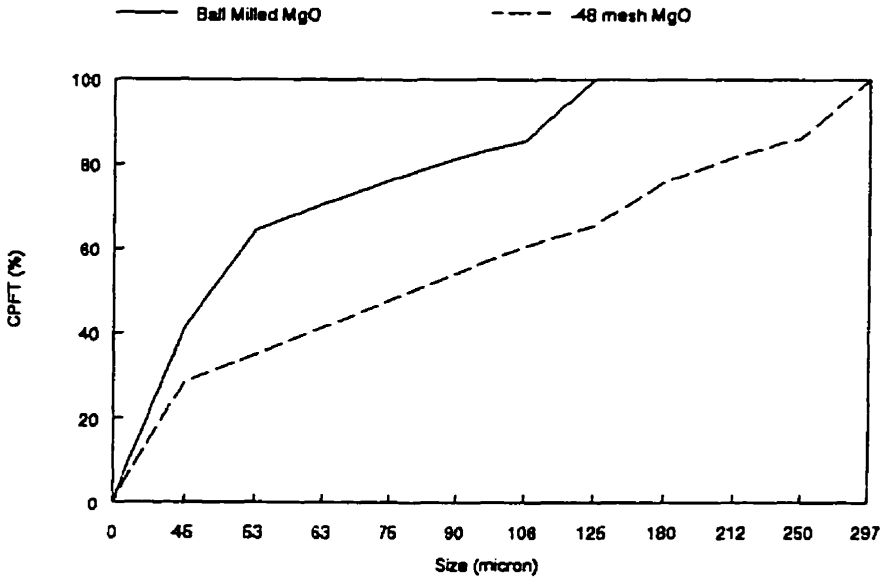

Figure 4.3 Size Distribution of Magnesia Powders

Hydratable alumina is a rather new product, introduced into refractory castables as binder, to substitute for the CA cement to produce cement-free castables [105, 109-111]. Hydratable alumina is composed of about 95 wt% chi-alumina which is very high active and

5% low crystalline alumina [105]. When mixed with water, it hydrates to form Bayerite and Boehmite gel, as following [110]:

Al_2O_3 (Hydratable) + $H_2O \Rightarrow Al_2O_3.3H_2O$ (Bayerite) + Al_2O_3. $1\text{-}2H_2O$ (Boehmite gel)

Mixing is processed in an Hobart's mixer. The batched raw mixture with certain additives or deflocculants is pre-mixed dry for 30 seconds and then suitable water is added. Total mixing time varies for 7 to 12 minutes. The fluidity of wet mixture is determined by the ball-in-hand method, according to ASTM C860-88. The wet mixture with acceptable fluidity are casted in moulds of 230×54×64 mm, further densification is done by vibration (60Hz, 0.5 to 0.7 mm) for 5 minutes. Each mix can produce 6 pieces of castables. The curing is 24 hr. at the room temperature in the mould. After demount, the castables are dried at 110°C for 24 hr. and fired respectively at different temperature for 6 hrs.

Four mixtures are made with constant alumina amount (18%), but different ratio of active/fine alumina to investigate the effect of alumina binder and alumina powders on the properties of castables. Details of the composition of such castables are to be found in Table 4.4. This constitutes the series B1 to B4. Amount of added water in castables increases with active alumina content.

The main purpose in this section is to differentiate the effect of fine alumina and ultrafine alumina; and the effect of total amount of alumina in castables. This constitutes series F of samples. These castables contain only one kind of alumina powders (fine or ultrafine alumina) with constant amount of active alumina 5% as binder, compositions are shown in Table 4.5.

Table 4.4 Composition of Castables with Active Alumina Binder

No.		B1	B2	B3	B4
		wt%	wt%	wt%	wt%
Magnesia Clinker	3360 - 106 μm	66.32	66.32	66.32	66.32
Magnesia Powder	<106 μm	15.68	15.68	15.68	15.68
Fine Alumina	D_{50}=3.65 μm		2.00	5.00	7.00
Ultra-Fine Alumina	D_{50}=0.46 μm	8.00	8.00	8.00	8.00
Active Alumina	D_{50}=50 μm	10.00	8.00	5.00	3.00
Water		10.0	6.7	5.8	5.4

Table 4.5 Composition of Castables Containing Different Alumina Powders

No.		F1	F2	F3	F4	F5
		wt%	wt%	wt%	wt%	wt%
Magnesia Clinker	6730 - 3360 μm					22.55
	3360 - 106 μm	66.19	65.23	64.27	65.23	49.80
Magnesia Powder	<106 μm	18.81	14.77	10.73	14.77	7.65
Fine Alumina	D_{50}=3.65 μm				15.00	
Ultra-Fine Alumina	D_{50}=0.46 μm	10.00	15.00	20.00		15.00
Active Alumina	D_{50}=50 μm	5.00	5.00	5.00	5.00	5.00
Water		5.3	5.0	5.8	8.3	5.0

Castables F1, F2 and F3 contain increasing amount of ultrafine alumina (10%, 15% and 20%) with constant content of active alumina binder (5%). The MgO aggregate quantity in these castables is similar , but the fine MgO powder decreases with the increase of alumina. The mixture F6 contains the same amount of alumina with F2, but the maximal aggregate size is increased to 6.73 mm (3 mesh). The added water can be controlled between 5% to 6%. The castables F4 contains 15% fine alumina which substitutes the ultrafine alumina and the active alumina binder is same. The amount of mixing water for F4 has a great increase, due to the fine alumina addition. The reason probably is attributed that the ultrafine alumina can absorb on the surface of fine MgO particles during dry mixing that limits the fine MgO particles' hydration, meanwhile, the absorbing alumina layer can reduces the contact chance between fine MgO particles, so the viscosity of matrix is decreased. For this reason, the amount of added water is reduced. The fine alumina powder has a relatively big size and it absorbs less on the fine MgO particles surface, so the high viscous matrix produced by fine MgO needs more water to fluidify.

The adsorption of ultrafine alumina on the MgO particles has been observed in figure 4.4. The mixture consists of 50% MgO small particles with 45-70 mesh and 50% ultrafine alumina. The mixture is produced by mixing dry in a plastic bottle for 40 minutes in the Turbula mixer. The picture a is the pure MgO particles and b is the mixture in macro-photograph. Picture c is a MgO particle with adsorbed ultrafine alumina particles.

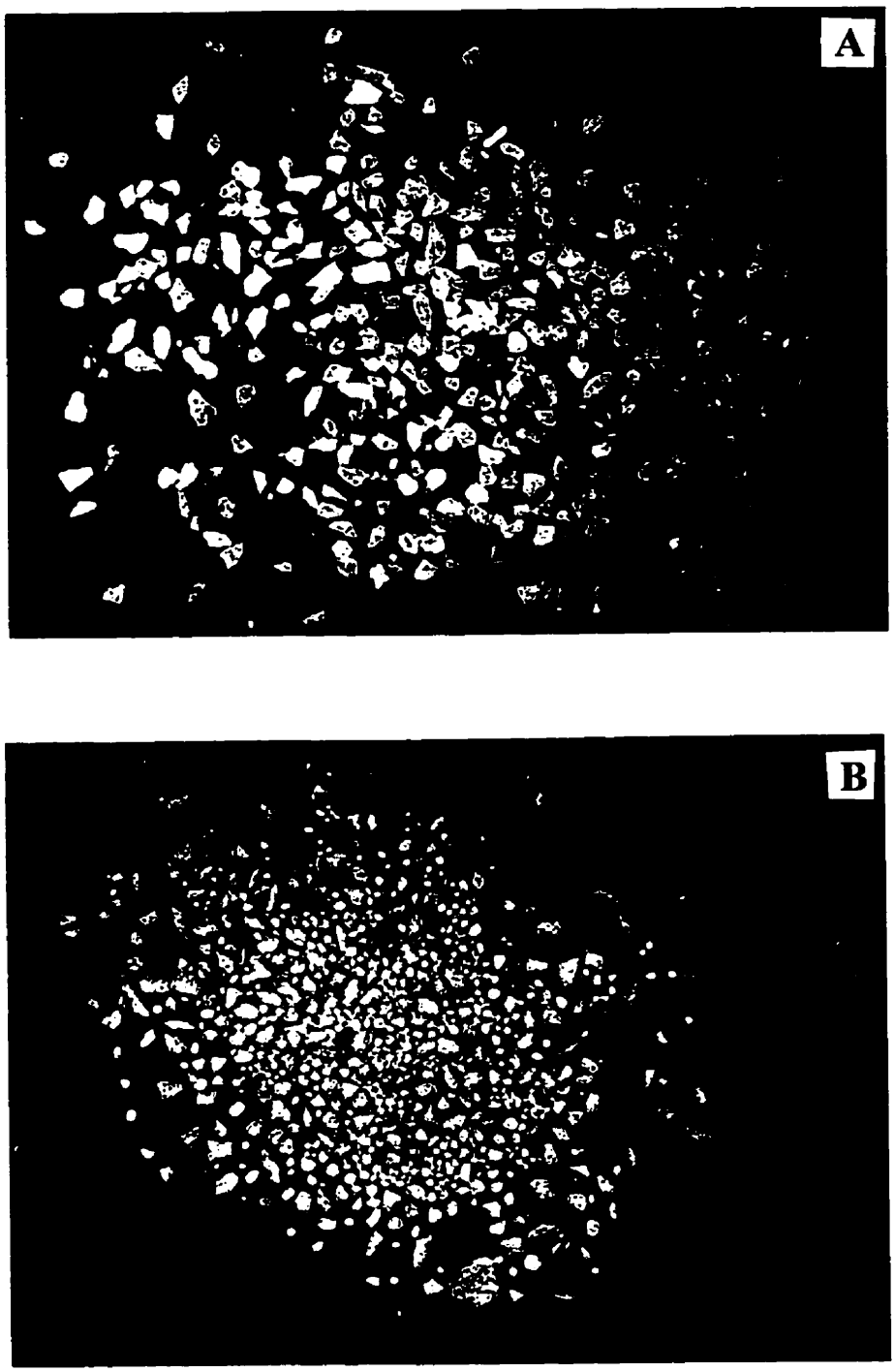

Figure 4.4a and 4.4b Macro- and Micro-structure of MgO Particles with Adsorbed Ultrafine Alumina Particles.

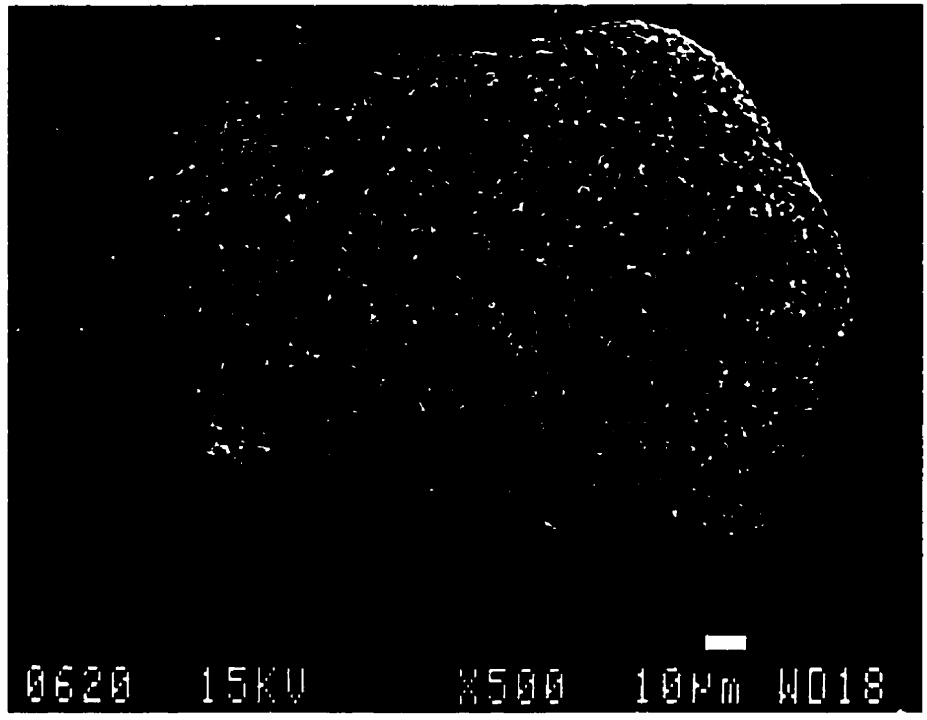

Figure 4.4c Macro- and Micro-structure of MgO Particles with Adsorbed Ultrafine Alumina Particles.

4.2 Physical and Mechanical Properties

The aim of this part of the work is to understand and master the properties of magnesia based castables.

Apparent porosity and bulk density: The apparent porosity and bulk density are measured by the method of ASTM Standard Test of Vacuum Pressure (C830-88) with specimens about 50×46×64 mm cut from the original specimens. The bulk density (D) and apparent porosity (P) are calculated by following equations:

$$D=\frac{m_{dry}}{m_{sat.}-m_{imm.}}\rho_l$$

$$P=\frac{m_{sat.}-m_{dry}}{m_{sat.}-m_{imm.}}\frac{\rho_l}{\rho_L}$$

where m_{dry} is the weight of the dry specimen (g), $m_{sat.}$ is the weight of the specimen saturated with a liquid, determined by weighing in air (g), $m_{imm.}$ is the weight of the specimen saturated with a liquid, determined by weighing the specimen immersed in the liquid (g), ρ_l is the density of liquid used for the saturation of the specimen (g/cm^3) and ρ_L is the density of the liquid for the weighing of the immersed specimen (g/cm^3). The liquid for the saturation and for immersion is water in this test, so the ρ_l and ρ_L is 1 g/cm^3.

Permanent linear change: PLC is determined by measuring the change of sample length before and after firing with general meter and the accuracy is controlled in 0.5 mm.

Dynamic modulus of elasticity (in reference to ASTM C1198-91), E_d, is measured with a Grindo-Sonic apparatus, to determine the resonant frequency (in Hz), and then calculate the E_d by the equation $E_d = 1.28fml^3/bh^3$ where f is the frequency, m is the mass of castable, l,b,h are respectively the length, width and height.

Modulus of rupture: MOR is tested in three points bending by the method ASTM C133-94 and calculated with $MOR = 3Fl/2bh^2$. The distance of support (l) is 180 mm.

Hot modulus of rupture: HMOR is tested with the three points bending method in high temperature furnace according to ASTM C583-80. The specimens about 160×24×28mm are prefired at 1600°C for 6 hr. and then tested at 1500°C. The heating rate is set at 60°C/hr.

Microstructural observations: Optical microscope and scanning electron microscope have been used to observe the microstructure. The optical microscope used is a Nikon (EPI-ILLUMINATOR "M") reflection microscope with magnification between 50 to 400 times. The SEM is JEM280 with EDS.

The previous properties have been systematically measured for series B and F castables. Results are indicated in Tables 4.6 and 4.7. All results are the average values of two samples at the same testing condition. The results are analysed to determine the suitable precision and bias. Clearly B3 composition is the best in B series; it contains 5% hydratable alumina. F2 is a good compromise; it contains 15% UFA better than B3 (with 8% UFA - 5% FA).

Table 4.6 Physical and Mechanical Properties of Castables as a Function of Active Alumina Content

No.		B1	B2	B3	B4
Apparent Porosity (±2%)	Green Body	20	12	10	14
	Fired at 1000°C	27	22	21	19
	Fired at 1200°C	27	21	19	22
	Fired at 1600°C	23	17	15	16
Bulk Density (±0.5g/cm^3)	Green Body	2.7	2.9	2.9	2.9
	Fired at 1000°C	2.6	2.7	2.8	2.8
	Fired at 1200°C	2.5	2.7	2.7	2.7
	Fired at 1600°C	2.7	2.9	3.0	3.0
Permanent Linear Change (±0.5%)	Fired at 1000°C	0.0	+0.2	+0.4	+0.9
	Fired at 1200°C	+1.1	+1.2	+2.0	+2.6
	Fired at 1600°C	-1.4	-1.3	-0.9	-0.5
Modulus of Elasticity (±1GPa)	Green	27	70	79	76
	Fired at 1000°C	1	4	4	4
	Fired at 1200°C	2	5	7	4
	Fired at 1600°C	7	20	24	22
Modulus of Rupture (±0.5MPa)	Green	3.1	10.4	9.7	8.4
	Fired at 1000°C	0.4*	1.2	1.2	1.5
	Fired at 1200°C	0.6	2.1	2.6	1.6
	Fired at 1600°C	2.1	6.6	8.7	7.5

*Note: * The minimum value is 0 with the consideration of error.*

Table 4.7 Physical and Mechanical Properties of Castables Affected by Different Sizes of Fine Aluminas (FA and UFA)

No.		F1	F2	F3	F4	F5
Apparent Porosity (±2%)	Green Body	10	10	13	19	12
	Fired at 1200°C	20	21	23	26	19
	Fired at 1400°C	17	17	21	28	18
	Fired at 1600°C	13	15	17	19	15
Bulk Density (±0.5 g/cm^3)	Green Body	3.0	3.0	2.9	2.8	3.0
	Fired at 1200°C	2.8	2.8	2.7	2.6	2.8
	Fired at 1400°C	2.9	2.9	2.8	2.5	2.8
	Fired at 1600°C	3.0	3.0	2.9	2.8	3.0
Permanent Linear Change (±0.5%)	Fired at 1200°C	+1.4	+1.4	+1.5	+2.3	+1.1
	Fired at 1400°C	-0.7	0	+1.5	+2.8	+0.9
	Fired at 1600°C	-1.0	-0.7	-0.7	-0.4	-0.4
Modulus of Elasticity (±1GPa)	Green Body	75	79	78	41	80
	Fired at 1200°C	9	13	12	4	10
	Fired at 1400°C	25	25	19	4	15
	Fired at 1600°C	10	26	31	13	17
MOR (±0.5MPa)	Fired at 1200°C	4.4	5.7	5.3	0.5	3.4
	Fired at 1400°C	10.0	8.9	7.5	1.2	5.0
	Fired at 1600°C	6.5	8.7	9.9	3.9	4.1
HMOR (±0.5MPa)	at 1500°C	2.1	2.3	2.5	1.6	1.4

4.3 Discussion

4.3.1 The Optimum Amount of Active Alumina Binder

The permanent linear change and apparent porosity of these castables are illustrated in Table 4.6 and Figure 4.5, respectively. With increasing fine alumina and decreasing active alumina, a trend of expansion for the samples after firing at temperature of 1000°C and 1200°C, and less shrinkage for that after firing at 1600°C occurs. The difference of PLC between 1200°C and 1600°C is large for all mixtures, indicating a risk of cracking under a temperature gradient. With increasing fine alumina amount, this difference of PLC augments. It is believed that fine alumina will lead to great expansion at intermediate temperature due to the formation of in-situ spinel, however, active alumina changes to $Al(OH)_3$ or hydrate alumina gel in the green body and after firing, the water will go out and a shrinkage will occurs which can diminish a part of expansion from the reaction between alumina and MgO.

For the green body, B3 has a minimum apparent porosity in Figure 4.5. This probably is due to the better binder/fine particles ratio or size distribution. At 1000°C, porosity increases significantly due to the dehydration. After 1000°C, porosity decreases with increasing ratio of fine/active alumina. This is line with the fact that the greater amount of active alumina, the more combined water there is, having more pores after firing up to 1000°C. After firing at 1200°C and higher, the apparent porosity is minimum for sample B3. Samples B1 and B2 of lower fine/active alumina ratio contain more active alumina which requires more water. The sample B4 of higher fine/active alumina ratio, contains more fine alumina which produce larger expansion than the other samples during spinel formation. The minimum in porosity for B3 is a result of a compromise between hydration porosity and

expansion porosity. In Chapter 3, the effect of alumina on expansion and porosity of dry mixes has been discussed. It was found that fine alumina increases the expansion at intermediate temperatures; this is still the case for the castables in this chapter.

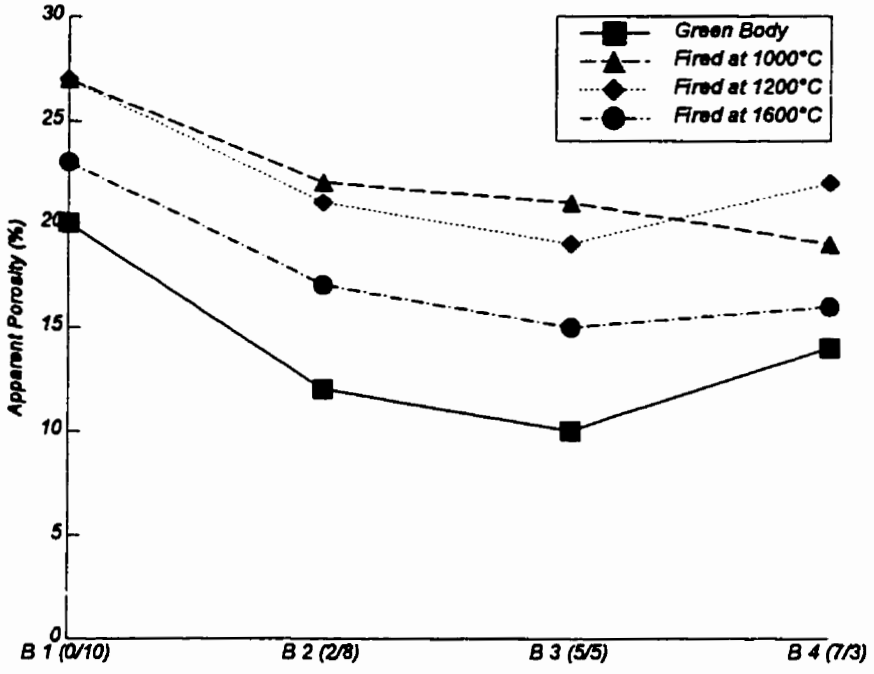

Figure 4.5 Effect of Ratio of Fine/Active Alumina on the Apparent Porosity
0 Ratio of Fine/Active Alumina*

The modulus of rupture shown in Table 4.6 at different treatment temperatures represented in Figure 4.6. From this it can be said that the increasing amount of active alumina can enhance the mechanical strength of green body (castables B2, B3 and B4). B1 shows a very weak strength because of too much added water which is needed by the hydration of great deal of active alumina, so a high porosity and loose structure is produced. After firing at intermediate temperature, all samples have a low strength, but B3 exhibits a bigger increase than others at 1600°C. The final strength at 1600°C of B3 is still best, due to the dense structure in Figure 4.5.

The low strength at intermediate temperature is due to the dehydration of binder and no enough ceramic bond formation at this time. Following the increasing temperature, the ceramic bond is formed which leads to the gradual pick-up in strength. Overviewing the mechanical strength of these magnesia based castables after firing at high temperature, it can be said that our magnesia based castables have a significantly lower strength than now available alumina-mullite castables. The main reason is due to the great difference of thermal expansion between spinel matrix and magnesia aggregates which causes the separation of matrix and aggregates during cooling. Form the observation of rupture section, the magnesia based castable almost show intergranular fracture. But according to the concept of thermal shock resistance, this materials should display good thermal shock resistance.

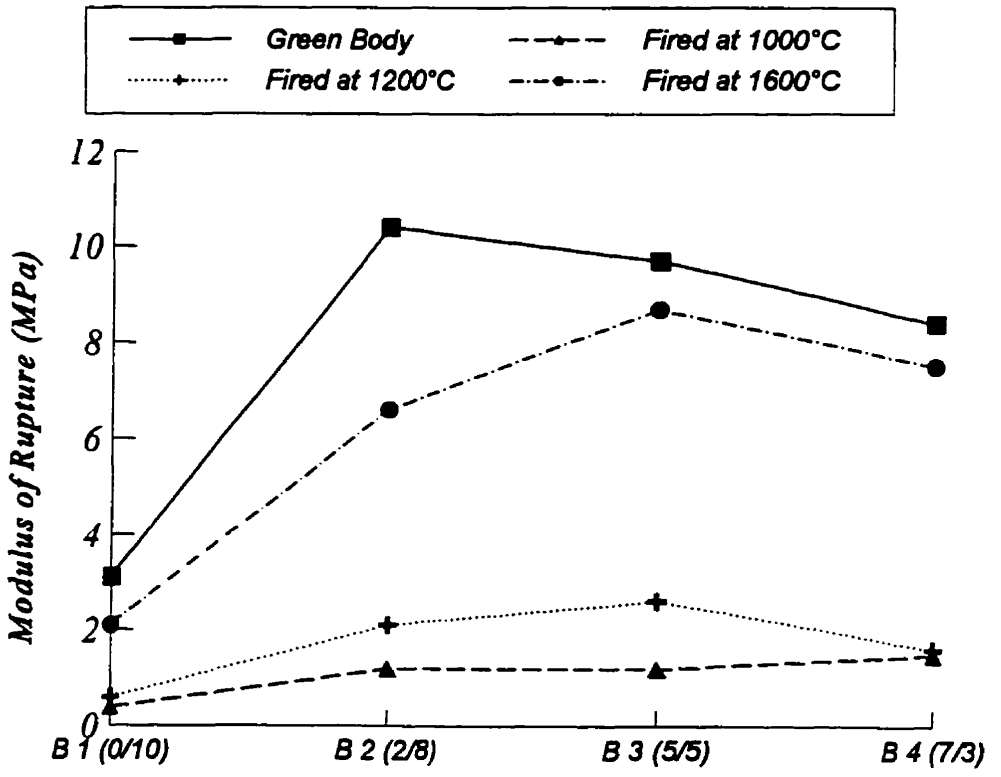

Figure 4.6 Effect of Ratio of Fine/Active Alumina on the Mechanical Strength
*() * Ratio of Fine/Active Alumina-From Table 4.6*

4.3.2 Effect of Ultrafine Alumina on Physical and Mechanical Properties

The effect of fine and ultrafine alumina on physical and mechanical properties of castables defined in Tables 4.5 and 4.7 will be discussed in this section.

Values of apparent porosity of castables with 10%, 15% and 20% ultrafine alumina powders are represented in Figure 4.7. Castables containing 10% and 15% ultrafine alumina show a similar low porosity, but 20% alumina increases the porosity for fired or no-fired samples. The higher porosity of F3 in green body probably is caused by slightly high water

addition. After firing, due to the formation of spinel which accompanies an expansion, the porosity is higher than the castables with less amount of alumina.

All three samples show a positive PLC after firing at 1200°C, but at 1400°C, F1 has a shrinkage, F2 reduces expansion near zero and F3 still shows great expansion in Figure 4.7. So the amount of ultrafine alumina shows strong influence on PLC at 1400°C, e.g. following the increase of alumina, a great expansion occurs due to a great deal of in-situ formed spinel which compensates sintering shrinkage and delays the temperature of beginning shrinkage. After firing at 1600°C, all samples appear shrinkage, and F1 expresses a little stronger than others. Comparing the difference of PLC at different firing temperature, only F2 shows a gradual change from 1200°C to 1600°C, and F1 has a great drop from 1200°C to 1400°C, great drop of F3 is between 1400°C and 1600°C. The gradual PLC with the temperature gradient can reduce thermal stress and improve the stability of structure.

Mechanical strength and strength ratio between 1600°C and 1200°C are indicated in Figures 4.8 and 4.9, respectively. Mechanical strength (Figure 4.8) after firing at 1400°C has a rapid augmentation for sample F1. This is probably due to the less amount of alumina which can rapidly transfer to spinel at this temperature and then leads to strong sintering to improve its microstructure. As shown in Figure 4.7, the great drop of PLC between 1200°C and 1400°C can confirm this sintering shrinkage. At 1600°C, F1 has a relative low strength. This is probably due to a shrinkage of the matrix, while, no ceramic bonding (spinel) is produced, so large mismatch appears between aggregates and matrix. For the samples containing more alumina, ceramic bonding (spinel) can still be formed at 1600°C, so the MOR shows an increase from low temperature to high temperature, for example F3. At 1400°C,

with increasing amount of alumina from F1 to F3, MOR decreases because more alumina produces more spinel and a volume expansion is accompanied, which reduces the strength. With increasing temperature to 1600°C, castable containing more alumina shows a high strength because a great deal of ceramic bonding (spinel) has well formed.

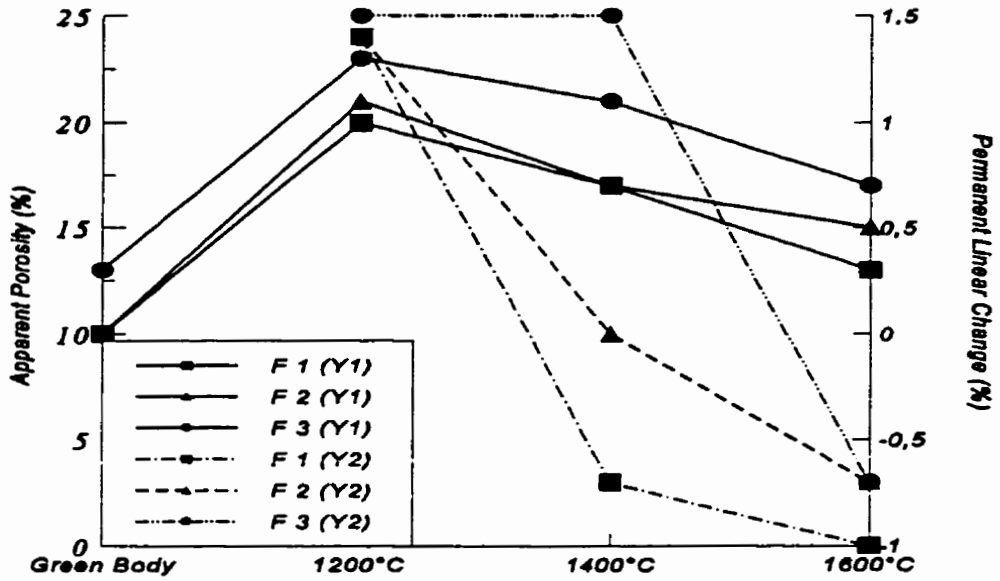

Figure 4.7 Effect of Amount of Ultrafine Alumina on Apparent Porosity and Permanent Linear Change of Castables

Strength ratio (Figure 4.9) of MOR at 1600°C and at 1200°C are investigated. F1 and F2 have a low value, but F1 has a very high ratio between 1200°C and 1400°C. Low strength ratio means good resistance to thermal spalling under the thermal cycles. Excess high

strength at high temperature zone and excess low strength at intermediate temperature zone will produce stress concentration at the weakest layer and cracks parallel to the hot face, then spalling takes place.

The hot strength in Table 4.7 of the three castables shows an acceptable value at this temperature. With increasing amount of alumina, the HMOR has slight elevation, due to the more ceramic bonding formed in the castable with more alumina addition.

Reviewing the mechanical properties of magnesia based castables, a relatively low strength is generally produced, comparing with alumina based castables. The main reason for this phenomenon is the cohesion stress between grains and matrix. Due to the great thermal expansion mismatch between MgO grains and spinel matrix, the large cracks or gaps occur around MgO grains. So the castable strength is only the matrix strength which is separated and reduced by grains. The cracks or gaps in the microstructure of F2 fired at 1600°C can be clearly observed in Figure 4.10. Around big or small MgO grains, lots of cracks are formed. In the observation of the rupture section after three points bending test, all the samples is in intergranular rupture mode.

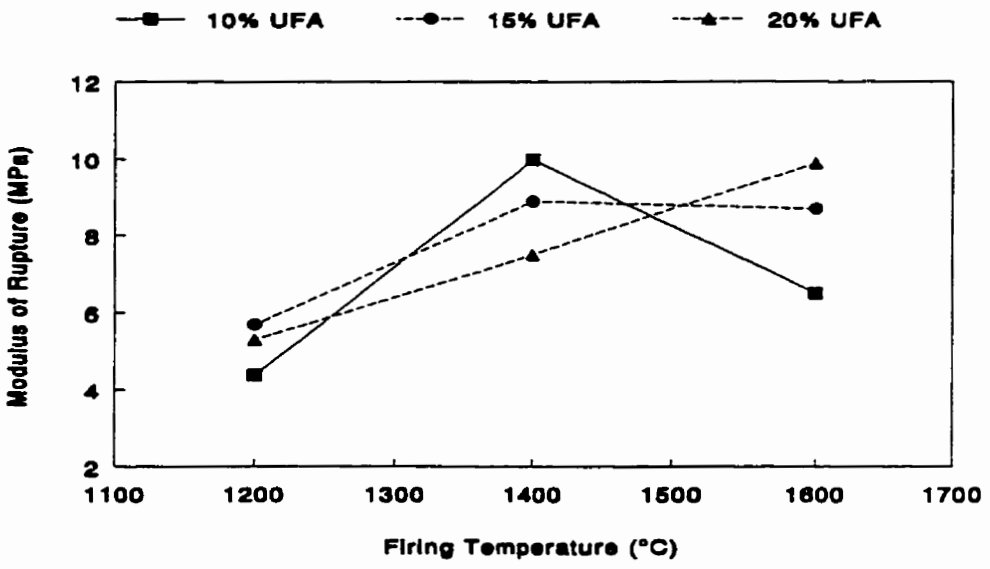

Figure 4.8 Effect of Amount of Ultrafine Alumina on Modulus of Rupture

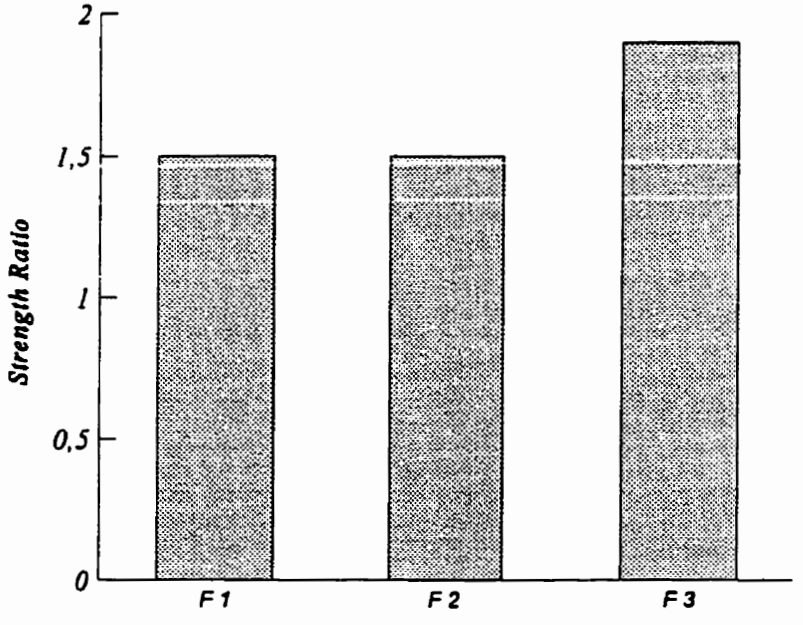

Figure 4.9 Effect of Amount of Ultrafine Alumina on Strength Ratio between 1600°C and 1200°C

Figure 4.10 Microstructure of Magnesia Based Castable (F2) After firing at 1600°C

4.3.3 Effect of Alumina Nature on Physical and Mechanical Properties of Castables

Castables F2 and F4 contain same total quantity, but different kinds of alumina. The castables have the same granulometric fraction of magnesia aggregates, and 5% active alumina as binder. F2 contains 15% ultrafine alumina and F4 contains 15% fine alumina. Comparison of physical and mechanical properties is now considered.

The apparent porosity and permanent linear change of mixture F2 and F4 are indicated in Figure 4.11. Castable containing fine alumina powder always shows a high apparent porosity than that containing ultrafine alumina, thus ultrafine alumina powder

improves the microstructure of green body and leads to more densification. After firing, matrix composed of fine alumina and MgO powder shows a greater difficulty to sinter than when it contains ultrafine alumina. Castable containing ultrafine alumina reaches maximum porosity and PLC at 1200°C, and then begins to shrink and densify by sintering, but castable containing fine alumina reaches maximum porosity and PLC at 1400°C, and at 1600°C, still shows a high porosity and a small shrinkage.

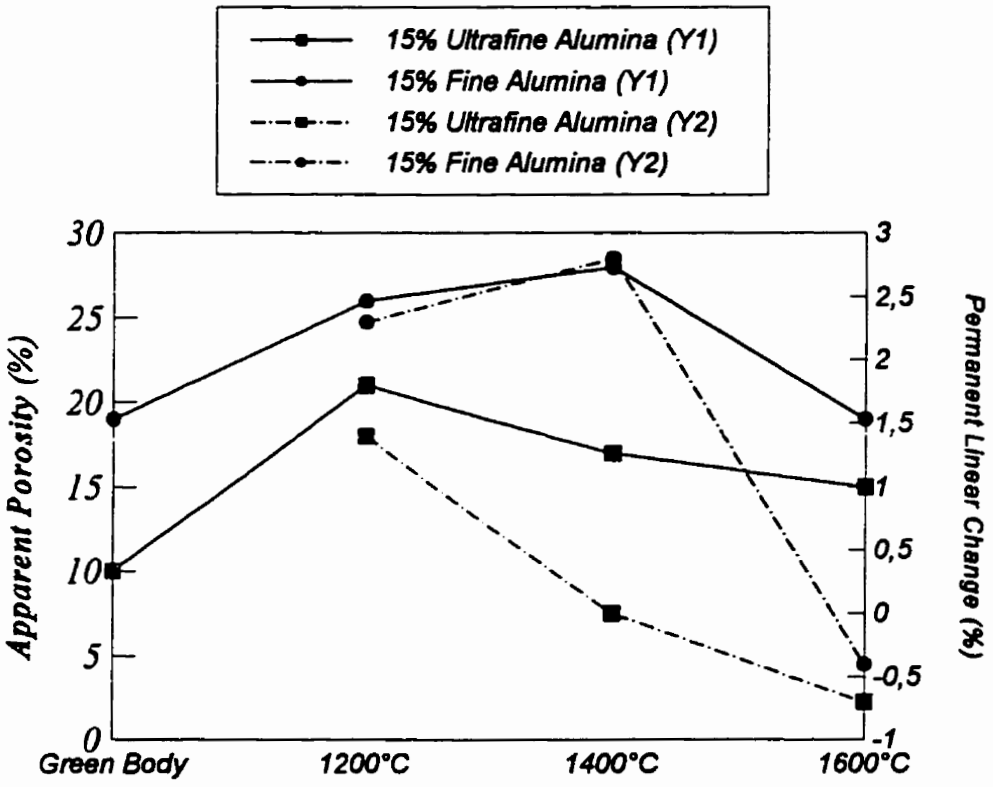

Figure 4.11 Effect of Alumina Powder Fineness on Apparent Porosity and PLC

The sintering behaviour of (50×20×20 mm) samples, cut from the two castables, have been measured using the dilatometer up to 1500°C; as shown in Figure 4.12. Castable containing ultrafine alumina has an early expansion behaviour and then follows a rapid shrinkage. This shrinkage is very strong to lead to a ultimate shrinkage. The castable containing fine alumina shows a relatively late and small expansion, and the sintering shrinkage is limited, so the ultimate linear change is a small expansion value. This result clearly indicates the sinterability of ultrafine alumina.

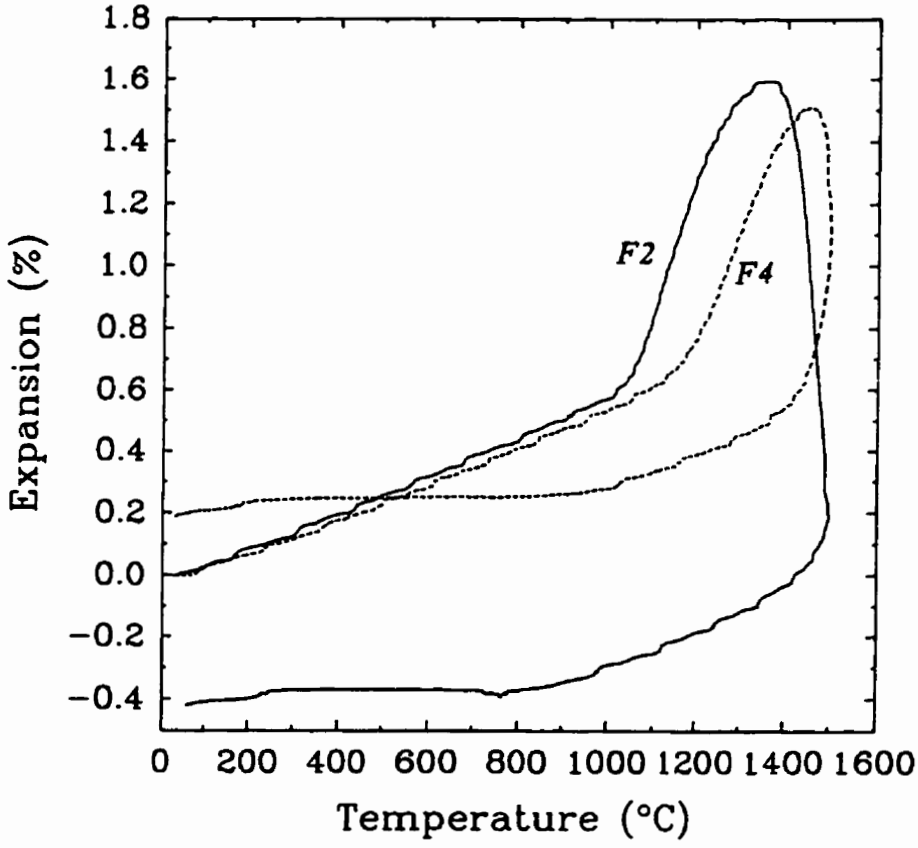

Figure 4.12 The Sintering Behaviour of the Castables Containing Ultrafine (A) and Fine (B) Alumina Powders

The mechanical strength of F2 and F4 measured by their modulus of rupture, is shown in Figure 4.13. Castable containing ultrafine alumina powder has the strongest mechanical strength. The reason is that the ultrafine alumina can form spinel ceramic bonding rapidly and produce strength earlier. This greatly enhances the strength at intermediate temperature. Further sintering improves the strength. Fine alumina has a bigger size than ultrafine alumina, so this alumina produces ceramic bonding (spinel) slowly. The difficulty of sintering for this castable leads to a loose microstructure and weak ceramic bonding strength.

The strength ratio of MOR between 1600°C and 1200°C can be calculated from Table 4.7. Castable containing ultrafine alumina (F2) has a low value which is believed to improve the thermal cycle shock for the lining application. Castable containing fine alumina (F4) shows a very high value, due to the very weak strength at 1200°C, this would be a risk to produce cracks parallel to the hot face during thermal cycle shock.

Results of hot modulus of rupture at 1500°C for samples prefired at 1600°C×6hr are indicated in Table 4.7. Castable containing ultrafine alumina has a slightly higher value due to more ceramic bonding. Both castables, F2 and F4, show acceptable HMOR values, that is attributed to their high purity.

4.3.4 Effect of Big Magnesia Aggregate Addition on Physical and Mechanical Properties

Magnesia has a great coefficient of thermal expansion which often causes the micro cracks between the magnesia aggregates and matrix during cooling, because the matrix has a low thermal expansion. In these castables, the matrix converts to spinel after first firing which has a coefficient of thermal expansion of 6 to 7×10^{-6}/°C, but magnesia is about

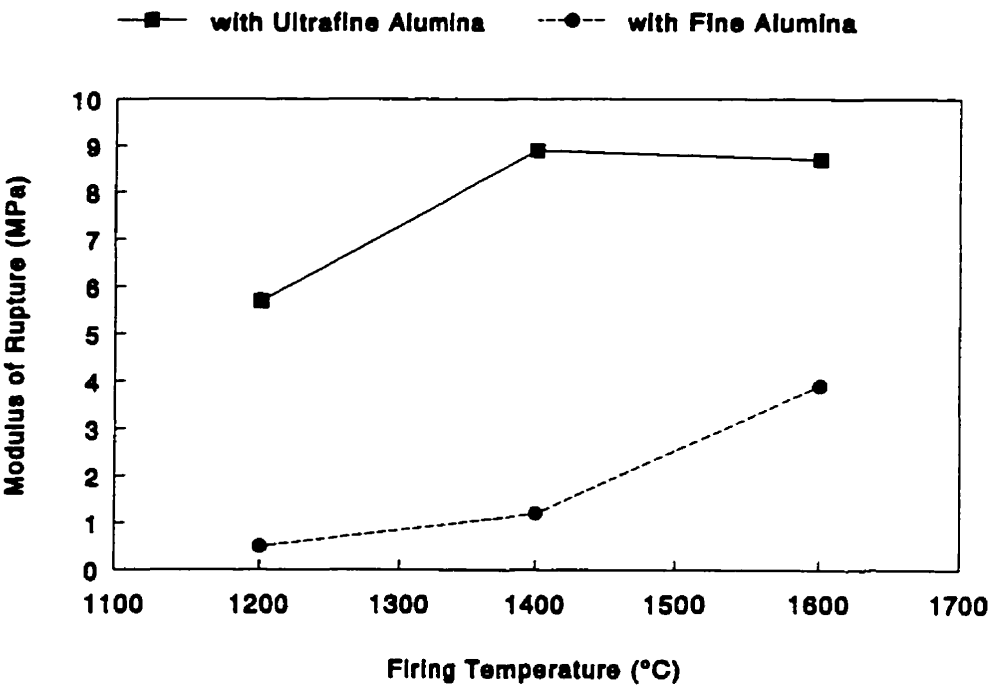

Figure 4.13 Effect of Fineness of Alumina Powders on Mechanical Strength

13.5×10^{-6}/°C. This large mismatch between them can be believed to produce micro cracks which can improve the thermal shock resistance, but meanwhile, it also leads to the drop of strength. This section will discuss the effect of some big magnesia aggregates on physical and mechanical properties.

The castable (F5) containing certain amount of big grains with maximum size of 6.73 mm (3 mesh) has been prepared to compare with the castable containing small aggregates ($D_{max.}$=3.36 mm). The effect of big aggregates on the porosity is indicated in Figure 4.14.

The big grains have less influence on porosity, but an evident influence on PLC. The addition of big grains decreases relatively the fine MgO amount in castable, so the reaction

between MgO and Al_2O_3 reduces, for this reason, less expansion occurs at intermediate temperature. At higher firing temperature, the big aggregates will limit the shrinkage of castable.

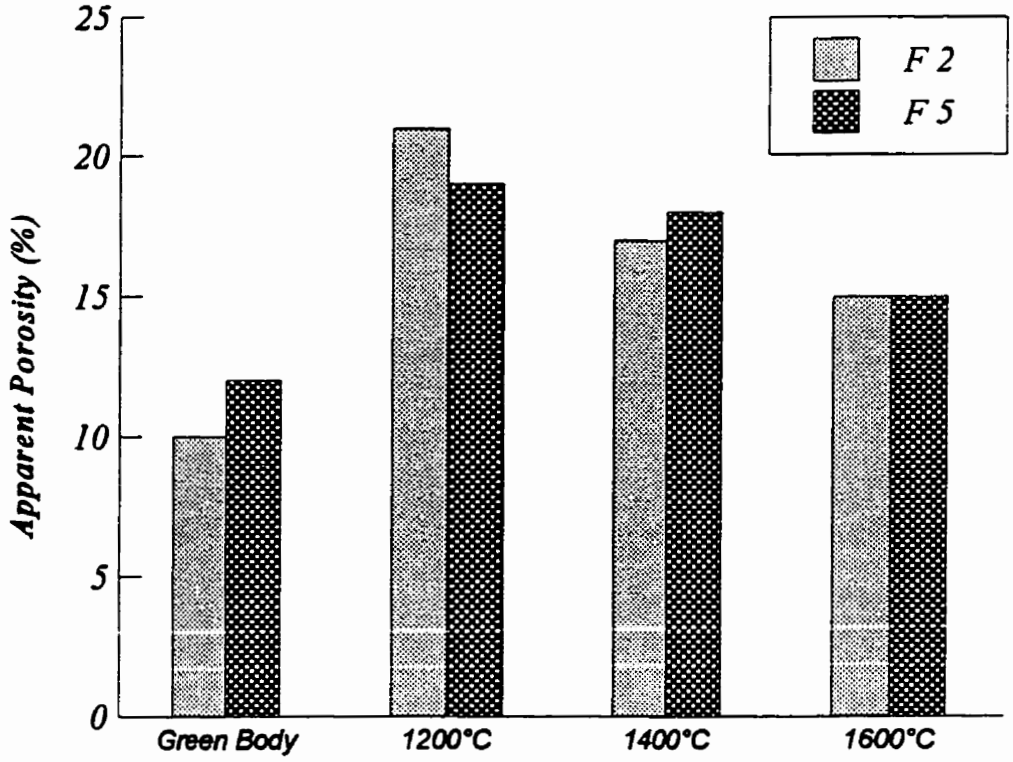

Figure 4.14 Effect of Big Aggregates on Apparent Porosity

The modulus of elasticity, modulus of rupture, strength ratio and hot modulus of rupture are shown in Figures 4.15, and 4.16, respectively. The difference of E_d between the castable with and without big aggregates for green body is very small but increases as the temperature rises. This is attributed to the large shrinkage of big magnesia grain during

cooling which causes the micro cracks between the matrix and aggregates, so the E_d decreases. The MOR has an evident drop for castable containing big aggregates. One reason probably is that F5 contains less fine magnesia powder which decreases the amount of ceramic bond; another reason is due to the existence of large cracks between aggregates and matrix that decreases the strength of castable. The micro cracks may decrease the strength ratio due to more reduction of MOR after firing at higher temperature, so the thermal shock resistance can be improved. HMOR follows the same trend as MOR when big aggregates are used. The reason probably is that the sample is prefired at 1600°C, so the micro crack occur during cooling. These micro cracks decrease the strength.

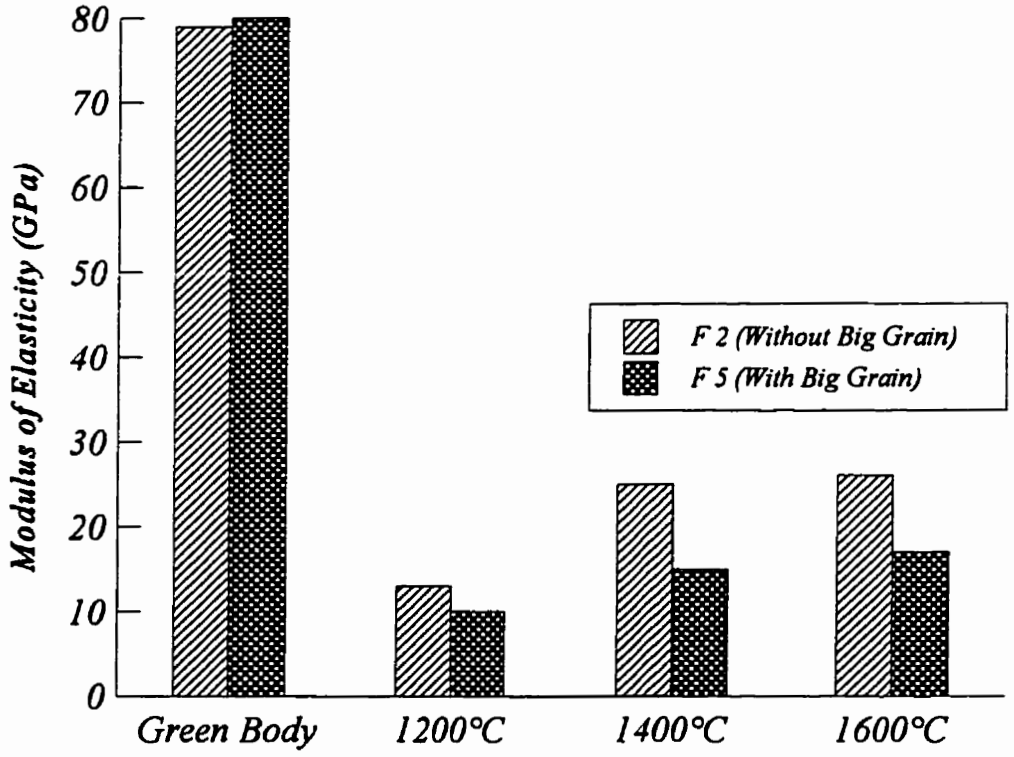

Figure 4.15 Effect of Big Aggregates on Modulus of Elasticity

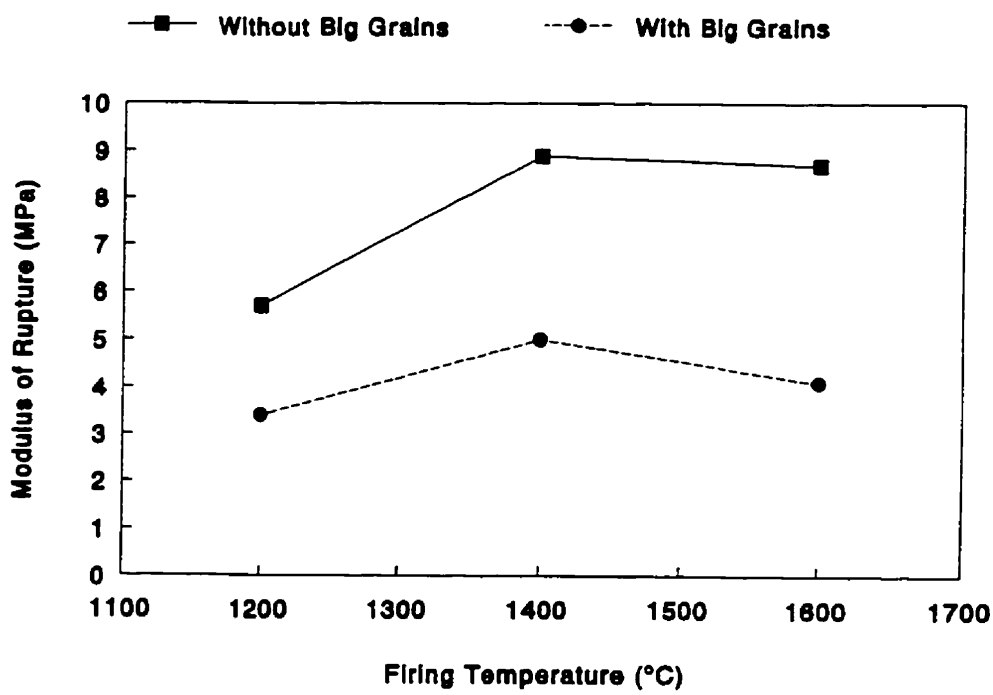

Figure 4.16 Effect of Big Aggregates on Modulus of Rupture

4.3.5 Recapitulation

It was found that a suitable amount of active alumina, likely 5% or 8%, can diminish the apparent porosity of green body, as well as improve the mechanical strength. Excessive addition of active alumina will require more water. Too little active alumina binder will not produce enough hydratable bond in green body and a good mechanical strength. According to this investigation, 5% active alumina is the recommended amount.

The amount of ultrafine alumina has a direct effect on physical and mechanical properties. More alumina addition increases the porosity and PLC at intermediate temperature. Less alumina leads to high strength at intermediate temperature, but strong drop occurs at high temperature. More alumina produces a gradual increase of strength from intermediate temperature to high temperature. The alumina amount controls the production of bond which indirectly affects the strength, so a suitable quantity of ultrafine alumina (15%) is needed for an optimum mechanical resistance.

The castable containing ultrafine alumina shows a lower porosity than that containing fine alumina by improving the densification. The PLC shows a gradual decrease from 1200°C to 1600°C for the castable containing ultrafine alumina, but the castable containing fine alumina has a great drop between 1400°C and 1600°C, due to the rapid sintering. This will increase the local thermal stress and leads to a decrease of thermal shock resistance.

Bigger magnesia grains have a small effect on porosity, but strongly decrease mechanical strength, due to microcracking during cooling.

The investigation on physical and mechanical properties in this chapter indicates an evidently different characteristic between magnesia based castables and traditional alumina

based castables. The magnesia based castables generally have a high porosity and low mechanical strength. This is determined by their microstructure. Some effective factors have been discussed and documented which will be favourable to design these castables.

CHAPTER 5 CORROSION RESISTANCE

The corrosion resistances of various castables are compared in this chapter: our magnesia based castables with commercial alumina based castables. The corrosion mechanisms are discussed, and further works suggested.

5.1 Experimental Conditions

Corrosion testing was done following the rotary slag test method according to ASTM standard C874-85. In one test, 6 samples are used, as shown in Figure 5.1. The thickness of each sample is about 38 mm. The 6 samples are fixed by mortar applied outside and then placed in the rotary furnace filled with insulating powder between the sample and lining. The gas-oxygen burner is used to heat inside the furnace. The increasing temperature rate is controlled by experience and generally it is about 500°C to 800°C per hour according to the testing requirement for the inside lining of samples. The temperature of lining is measured with an infrared radiation thermometer for non-contact temperature measurements (Minolta/Land Cyclops 152).

Two testing slags in Table 5.1 have been used: slag1, with a basicity ratio of 2.5, and a very high percentage of Fe_2O_3; and slag2, with a higher basicity 3.2 and a normal Fe_2O_3 content. Two types of prefiring samples are considered: one is prefired in 1600°C with 6 hours and then test in rotary corrosion furnace, which is called totally prefired sample; the other is prefired in rotary corrosion furnace at hot face with 1200°C and then test the

corrosion at 1600°C. In total, 6 groups of tests have been done. Two groups have been tested under the same testing condition, using totally prefired samples with slag1. These castables are B2, B3, B4, F1, F2, F3, FSilica, BCement and commercial alumina-based castables S1, A1, A3. Another group of totally prefired samples have been tested in high basicity slag-slag2; castables B4, F1, F2, F3, A1 and A2. Three groups of partially prefired samples have been tested in slag1, but with different corrosion cycle times of one cycle, two cycles and three cycles, respectively. Samples correspond to F2, F4, A1, S2, S3 and S4. Compositions of samples are indicated in Tables 5.2 and 5.3. The increasing temperature rate is about 800°C per hour. When it reaches the 1600°C, the slag is charged. The temperature is mostly controlled at about 1600°C, but the slight decrease can happen during charging slag. The temperature drop is less than 50°C and normally it can recover to 1600°C in 5 minutes. The slag is charged each 30 minutes with 200g until the end of test. The cooling is in the air. For the multi-cycle test, this procedure is repeated on the second day.

Table 5.1 Chemical Composition of Chosen Slag

	CaO	SiO_2	MgO	Al_2O_3	Fe_2O_3	Other*	C/S
Slag 1	32.8	13.1	12.4	4.5	33.7	3.5	2.5
Slag 2	50.9	16.0	7.6	8.5	15.3	1.7	3.2

* *Other oxides are Na_2O, K_2O, TiO_2, MnO, P_2O_5, Cr_2O_3, V_2O_5 and ZrO_2.*

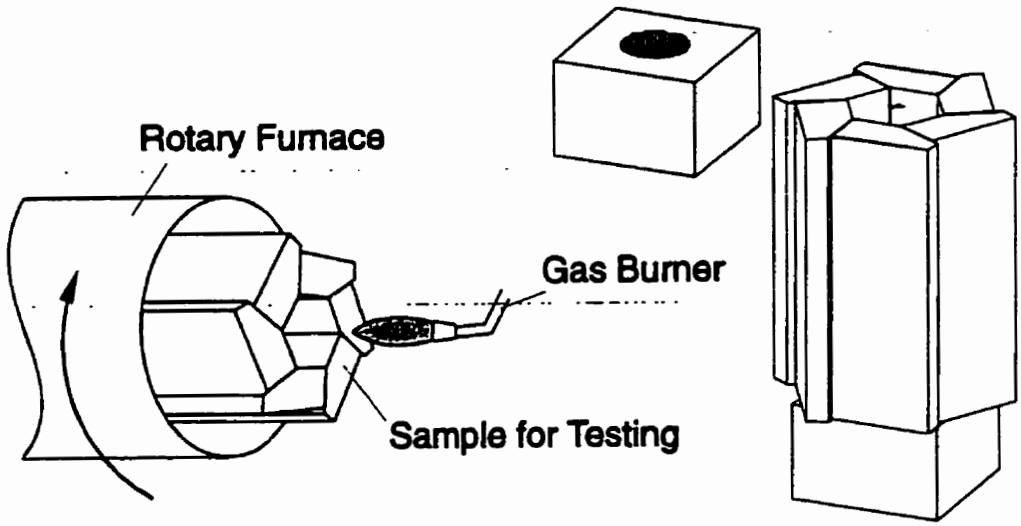

Figure 5.1 Corrosion Test in Rotary Furnace

Table 5.2 Composition of Basic Castables

	MgO Clinker (6-48 mesh)	MgO Powder (-48 mesh)	Fine Alumina	Ultrafine Alumina	Active Alumina	High Alumina Cement	Others	Spinel	Water
B2	59.85	22.15	2	8	8				6.7
B3	59.85	22.15	5	8	5				5.8
B4	59.85	22.15	7	8	3				5.4
BCement	59.85	21.15	5	10		4*			5.5
F1	59.23	25.77		10	5				5.3
F2	58.97	21.03		15	5				5.0
F3	58.72	16.28		20	5				5.8
F4	61.82[+]	18.18		15	5				5.0
FSilica	58.97	21.03		13	5		2[a]		5.6
S1	68.50	7.5		14	4			10[s]	4.7
S2	58.99[+]	11.01		15	5			10[ss]	5.0
S3	60.19[+]	12.81		10	3	1**		13[ss]	5.0
S4	57.70[+]	7.3		15	5		5[b]	10[ss]	5.0

Note: 1) The major raw materials are respectively described in chapter 3 and 4.

2) *: Lafarge Secar 71, **: Secar 80 Cement. [+]: $D_{max.}$ of MgO clinker is 3 mesh. [s]: Prepared spinel in our laboratory. [ss]: Commercial spinel. [a]: Fume silica. [b]: Fused alumina with 45-70 mesh.

Table 5.3 Chemical Composition of Commercial Castables

No.	Type	Al_2O_3	MgO	SiO_2	Others
A1	High Al_2O_3	96.3	1.9	0.1	1.7
A2	Al_2O_3-MgO	86	10	2	2
A3	Al_2O_3-MgO-Spinel	89	9	-	2

The cross section of corroded sample is shown in Figure 5.2. The eroded part is determined by the difference before and after corrosion testing. The penetration thickness is determined by macro-observation and measurement of altered layer, and also, confirmed by measurement under optical microscope. The depth of penetration is determined by depth at which a liquid or glassy phase inside the brick is detected. The penetration depth of Fe element (FeO or Fe_2O_3) is determined by the colour change at the macro-level. Chemical analysis is done at different thickness for some selected samples, cut at 0-5 mm, 5-10 mm ,10-15 mm from hot face and cold face, as well as X-ray diffraction on the same samples.

As shown in Table 5.2. B2, B3 and B4 contain same amount and grade of magnesia aggregates and ball mill fines; the ultrafine alumina quantity is also the same, at 8%. The complete amount of fine and active alumina is constant, but the ratio of fine/active alumina varies from 2/8, 5/5 to 7/3. The required amount water increased with the amount of active alumina in castables.

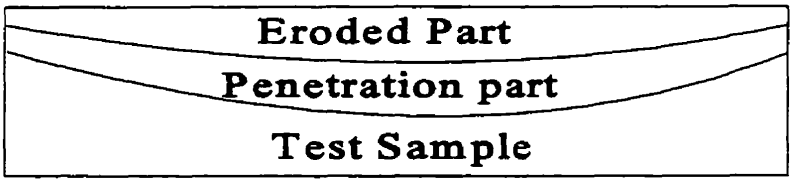

Figure 5.2 Cross Section of the test Sample after rotary corrosion test

Samples F1, F2 and F3 are with constant amount of active alumina binder 5%, and the amount of ultrafine alumina varies from 10%, 15% to 20%. No fine alumina is added in these castables. F4 contains same amount of alumina as F2, but increasing the maximal size of aggregate to 3 mesh.

FSilica is designed to investigate the influence of silica on corrosion. 2% silica fume is added in castable in substitution to the ultrafine alumina of castable F2. The effect of calcium aluminate cement is also considered in castable BCement which 4% high alumina cement of Lafarge Secar 71 which is added to replace the active alumina binder, in a composition similar to castable B3.

S1 contains 10% preformed spinel. This preformed spinel is produced by wet mixing the ultrafine alumina and $Mg(OH)_2$ in the stoichiometric MgO/Al_2O_3 ratio, after drying, it is fired at 1600°C for 10 hours. After crushing and sieving, the under 48 mesh powder is used in S1 castable. Castable S2, S3 and S4 have addition of commercial spinel: FUSED

MAGNESIA ALUMINA SPINEL 25 (MgO % content) from C-E Minerals Company. The typical chemical composition is 73.70% Al_2O_3, 25.40% MgO, 0.35% SiO_2, 0.35% Na_2O, 0.20% CaO. The major phase is spinel and minor phase is alumina. The size of spinel powder used in our castables is under 200 mesh. Castable S4 contains 5% fused alumina grain with size 45-70 mesh.

5.2 Results and Discussion

The corrosion tests results are shown in Tables 5.4 and 5.5, according to their prefiring conditions. The penetration depth is indicated in slag penetration and $FeO(Fe_2O_3)$ penetration, because the $FeO(Fe_2O_3)$ show an evidently restricted layer on the surface in magnesia based castables.

5.2.1 Effect of Total Alumina Content

B2, B3 and B4 contain the same type, but different amount of alumina: 15%, 20% and 25%, respectively. These castables are magnesia based castables with in-situ spinel bonding to be compared with alumina based castables. Two alumina based castables are used. They are commercial alumina-spinel-(magnesia) castables. The composition of basic castables is indicated in table 5.2 and the chemical composition of commercial castables is shown in table 5.3. Because all samples are prefired, the phase composition in the magnesia based castables will be MgO-spinel and that in alumina based castables will be Al_2O_3-spinel.

Figure 5.3 shows the erosion resistance with different amount of alumina. The evident trend is that erosion resistance decreases with the increasing alumina quantity in castables. This agrees with the chemical stability of these oxides to resist the basic slag, e.g. MgO more stable than spinel, and spinel more stable than Al_2O_3 in basic slag environment. The phase composition of F1 contains more MgO and less spinel than F3, so F1 shows a stronger erosion resistance. For the alumina based castables, A3 contains more spinel and less Al_2O_3 than A1, so a less erosion in A3 occurs.

Table 5.4 Corrosion Test Results of Totally Prefired Specimens

	Erosion Thickness (±0.5 mm)	Penetration Depth of Slag (±2 mm)	Penetration Depth of $FeO(Fe_2O_3)$ (±2mm)	Deteriorated Thickness (±2mm)
Slag 1				
B2	2.6	21	10	24
B3	2.6	20	10	23
B4	2.9	22	10	25
F1	0.4	23	18	23
F2	0.9	23	15	24
F3	2.7	23	10	26
FSilica	3.9	21	9	25
BCement	2.6	25	9	28
S1	5.6	23	16	29
A1	13.9	8.5	6	22
A3	10.1	13	5	23
Slag 2				
B4	5.2	26	13	31
F1	1.7	25	15	27
F2	1.2	27	14	28
F3	3.5	24	8	28
A1	25.5	7	6	33
A2	12	16	15	28

Table 5.5 Corrosion Test Results of Partially Prefired Specimens

	Erosion Thickness (±0.5 mm)	Penetration Depth of Slag (±2 mm)	Penetration Depth of FeO(Fe_2O_3) (±2mm)	Deteriorated Thickness (±2mm)	Coating Thickness (±1 mm)
Slag 1 and 1 cycle corrosion (8 hours)					
F2	0	17	12	17	2
A1	11	8	7	19	0
Slag 1 and 3 cycle corrosion (5 hours)					
F2	3.9	12	8	16	9.5
F4	3.9	11	9	15	9.5
Slag 1 and 2 cycle corrosion (5 hours)					
S2	4.7	16	15	21	5
S3	4.8	18	15	22	5
S4	5.7	15	14	20	5

The penetration depth in Figure 5.3 indicates that the magnesia based castables have almost the same level of penetration. The value can reach about 23 mm, where the slag may solidify at this temperature. This means that these refractories have no penetration resistance and the only penetration resistance is a fuction of the temperature gradient. The alumina based castables have a better penetration resistance, especially the high alumina castable. The mechanism of corrosion resistance of alumina-spinel castables has been discussed in Chapter 2. Hereby, it is confirmed again that high alumina castable has strong penetration resistance, due to the great deal of CA_6 formed by the reaction between Al_2O_3 in refractories and CaO from slag which increases the viscosity of slag leading to the low penetration. The penetration

depth of A1 is very low. One reason is that alumina castable has good penetration resistance, another reason is that the dissolution-erosion reduces the penetration layer thickness.

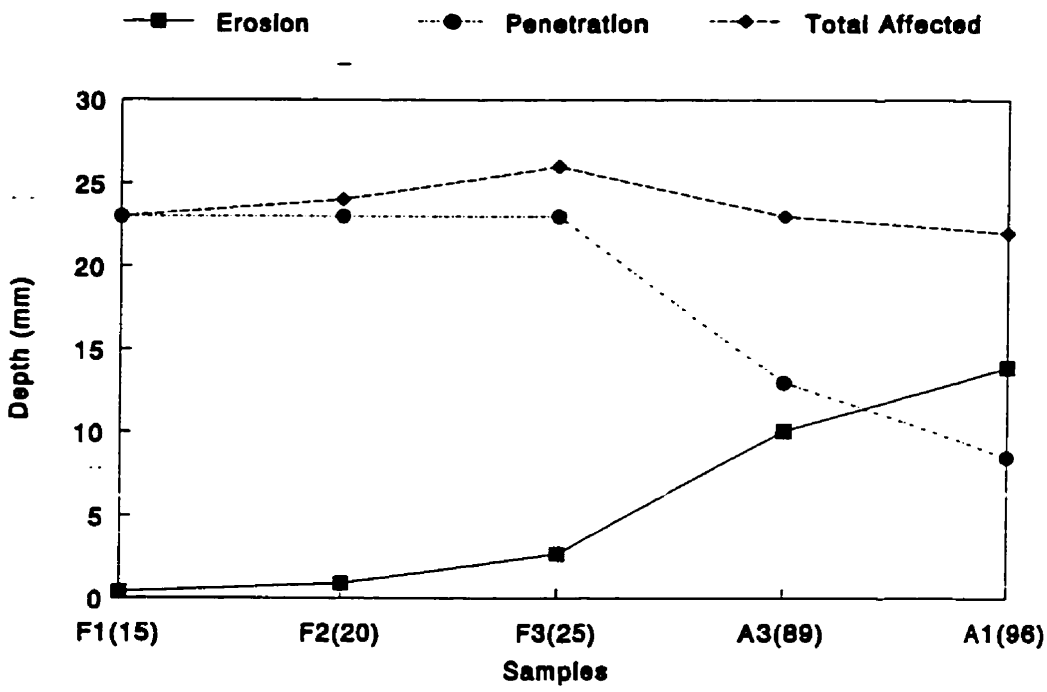

Figure 5.3 Effect of Alumina Quantity in Castables on Erosion and Penetration Resistance

( ) Total amount of alumina in castables

The slag penetration is also measured by chemical analysis from the hot face to cold face and the CaO content in magnesia and alumina based castables, shown in Figure 5.4. Results of X-ray diffraction analysis corresponding to these penetration depth are displayed in Table 5.6. The CaO penetration depth in alumina based castables is less than 10 mm. Presence of CA_6 and CA_2 at hot face zone is confirmed. The CaO penetration depth in magnesia based castable is more than 15 mm. This result agrees with the macro and micro measurements.

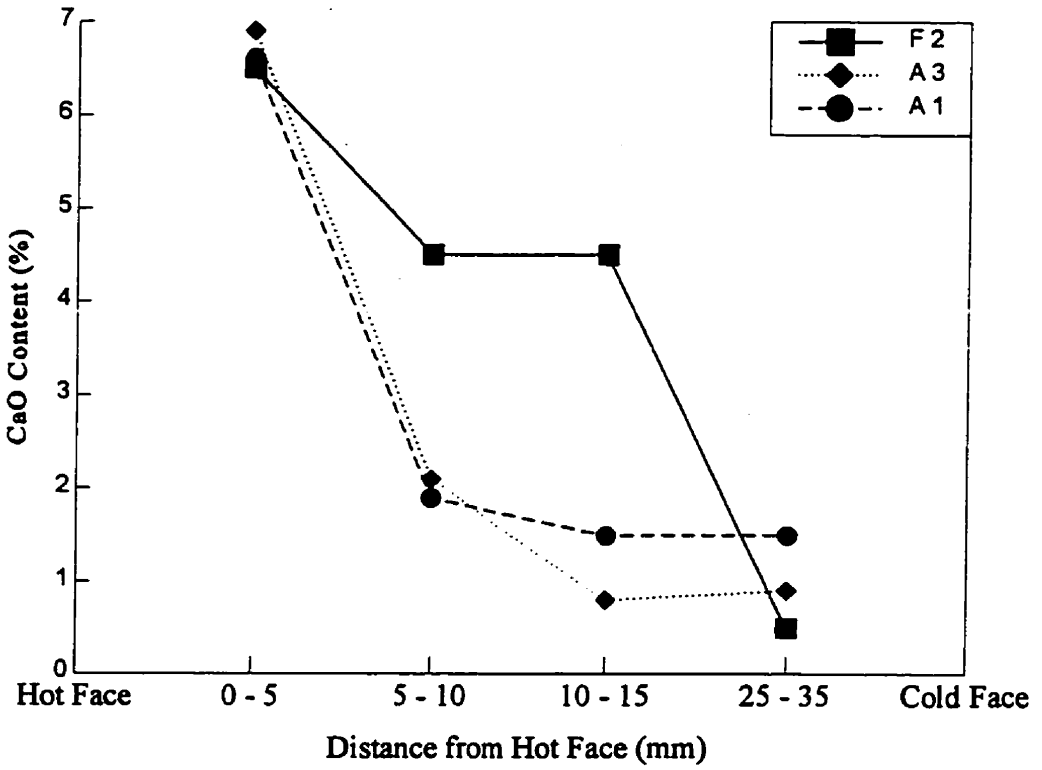

Figure 5.4 CaO Penetration Depth in Magnesia and Alumina Based Castables

Table 5.6 Phases Detected by X-R Analysis in Penetrated Zone, after Corrosion Test

	Distance from Hot Face	Major Phases	Minor Phases	Trace Phases
F2	0 - 5 mm	M, MA+MF	C_2S	C_3MS_2, CA_4F_2
	5 - 10 mm	M, MA+MF	C_2S	C_3MS_2
	10 - 15 mm	M, MA	C_2S	
	25 - 35 mm	M, MA		
A3	0 - 5 mm	A, MA+MF	CA_6	
	5 - 10 mm	A, MA	CA_6	
	10 - 15 mm	A, MA	CA_6	
	25 - 35 mm	A, MA	CA_6	
A1	0 - 5 mm	A	MA+MF, CA_6	C_3MA_2, CA_2
	5 - 10 mm	A	MA, CA_6	C_3MA_2, CA_2
	10 - 15 mm	A	MA, CA_6	
	25 - 35 mm	A	MA, CA_6	

Note: C:CaO, M:MgO, A:Al_2O_3, F:Fe_2O_3, S:SiO_2

The total deteriorated thickness is also shown in Figure 5.3. The basic castable has a slightly increasing trend with the enhancing alumina in castable because high content of alumina leads to the decrease of erosion resistance. The total deteriorated thickness of alumina based castable can reach the basic castable level, but the mechanism is totally different between them, because the major deterioration in basic castables is from penetration and the major deterioration in alumina based castables is from the erosion.

From the observation of microstructure, the magnesia based castables show a different slag-refractories reaction and slag penetration pattern as opposed to alumina based castables.

The magnesia based samples are also susceptible to penetration of iron oxide. The Fe element can be absorbed by MgO. If the penetration of Fe element is relatively shallow, CaO, SiO_2 can deeply penetrate into the refractories and a dense layer can be formed, as shown in Figure 5.5.

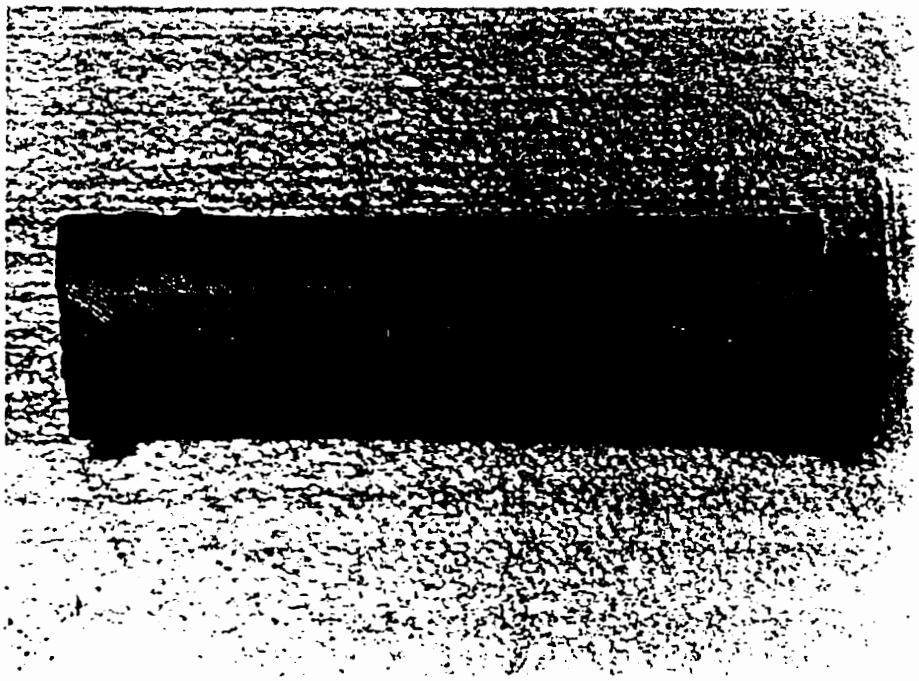

Figure 5.5 Macrostructure of the Corroded Magnesia Based Castable (F2)

Figure 5.6a, 5.6b and 5.6c exhibit the microstructure at the hot face of castable F2. Figure 5.6a shows the eroded MgO grains. Many MgO grains contain certain amount of FeO disperse in the slag. On the MgO grains, lots of bright dots, which are the secondary $MgO.Fe_2O_3$ spinel formed during cooling, dope on it. The FeO co-exists with MgO in the solid solution state at high temperature. When the (Mg,Fe)O solid solution is cooled, they transfer to the ferrian spinel ($MgO.Fe_2O_3$) and MgO, and the ferrian spinel will be doped on the grain surface with the pattern of bright dots. Between these MgO-ferrian spinel grains, some secondary spinel can be found. These spinel are also recrystallized during cooling, and some have a dark centre with a bright outside ring. The dark centre probably is $MgO.Al_2O_3$ spinel, but the bright ring maybe contain more Fe element which is the MA and MF spinel solid solution.

Figure 5.6b shows the interface between one big MgO grain and slag zone. The surface crystals in the MgO grain grow due to the slag penetration, but the centre of MgO grain still keeps the original state. The MF spinel precipitates on the surface of MgO grain and in the crystal boundary. Some MgO at the outside surface is eroded and dissolved into slag.

Figure 5.6c illustrates a MgO grain surface at high magnification. The doped MF spinel is clearly dispersed on MgO surface, and more and big MF spinel is located at the most outside layer. Some MgO grains are separated and dissolved into slag from the outside surface of big grains.

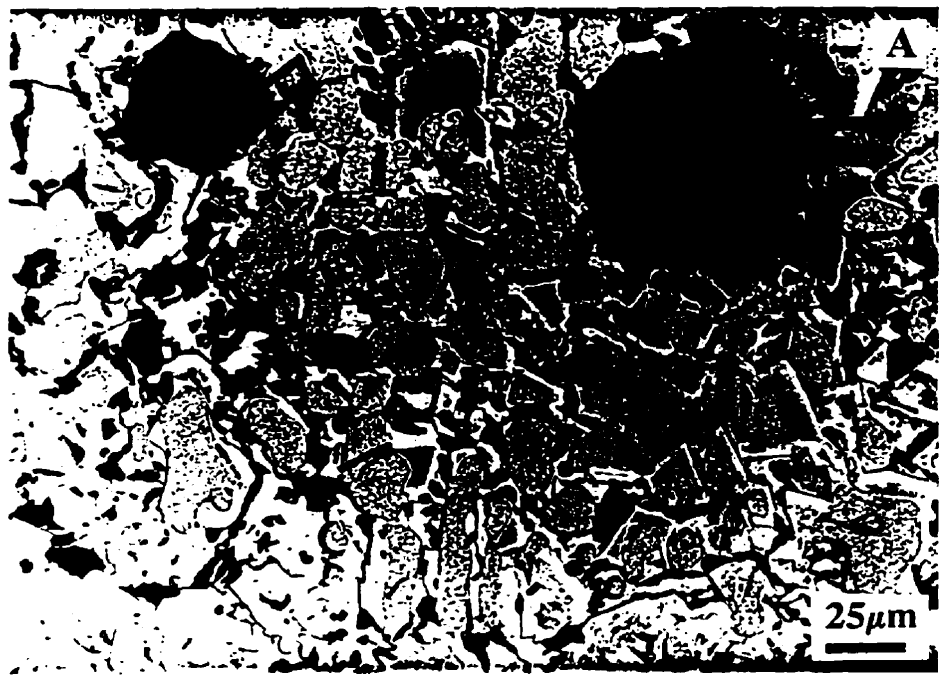

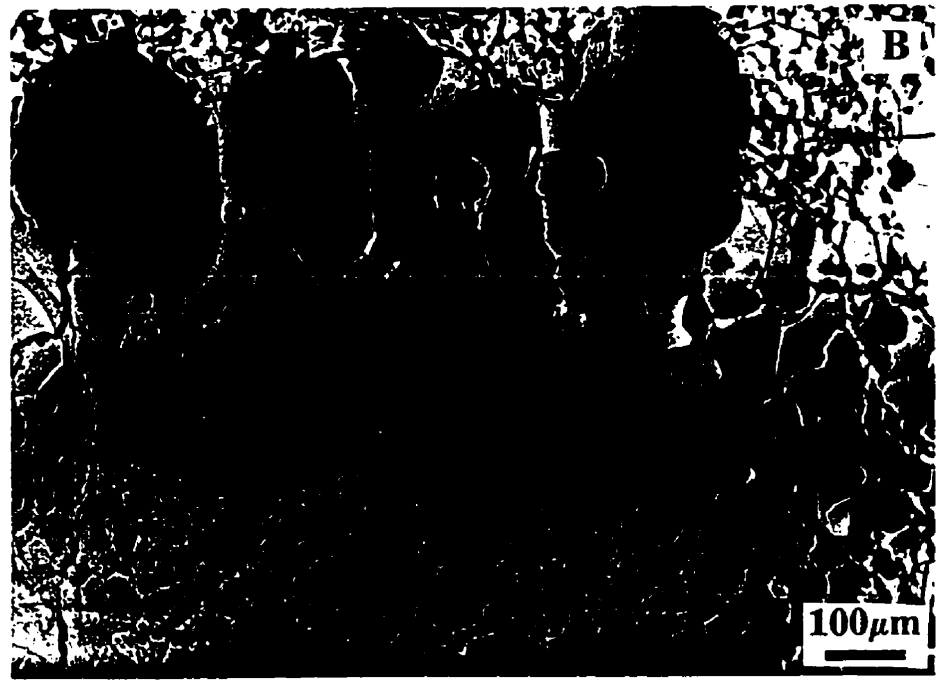

Figures 5.6a and 5.6b Microstructure in the Slag Zone of the Corroded Magnesia Based Castable F2.

Figure 5.6c Microstructure in the Slag Zone of the Corroded Magnesia Based Castable F2. a: corroded magnesia grains containing high amount of Fe; b: big magnesia grain; c: surface of big magnesia grain

Figure 5.7a illustrates the interface between matrix and slag. In the matrix, the small spinel crystals have been formed and connects each other to form a matrix net. The high magnification at slag matrix interface is shown in Figure 5.7b. At the connection face, the spinel is relatively large and dense.

Figure 5.8 is in the penetration zone. The beautiful spinel crystals have been formed and between these crystals, there is lots of pores and less glassy phase. For this reason, this

porous spinel matrix has not the capacity to suppress the slag penetration. Due to less glassy phase in penetration, this can be believed that the slag is still high basic, and this low viscous slag can rapidly recrystallize.

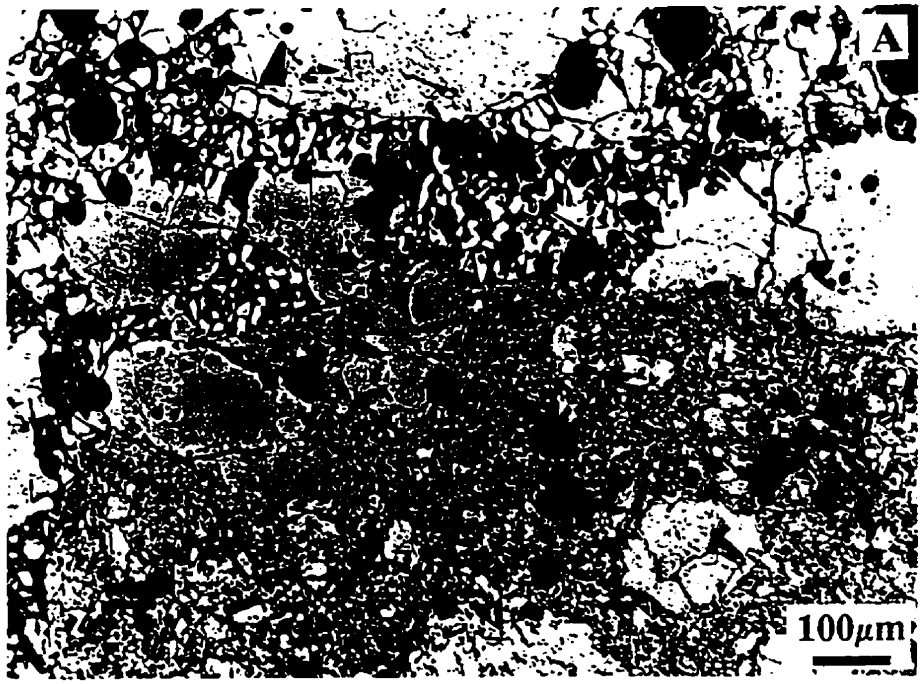

Figure 5.7a Microstructure at the Interface between Slag and Matrix for Castable F2

Figure 5.7b Microstructure at the Interface between Slag and Matrix for Castable F2
a:50x, b:200x

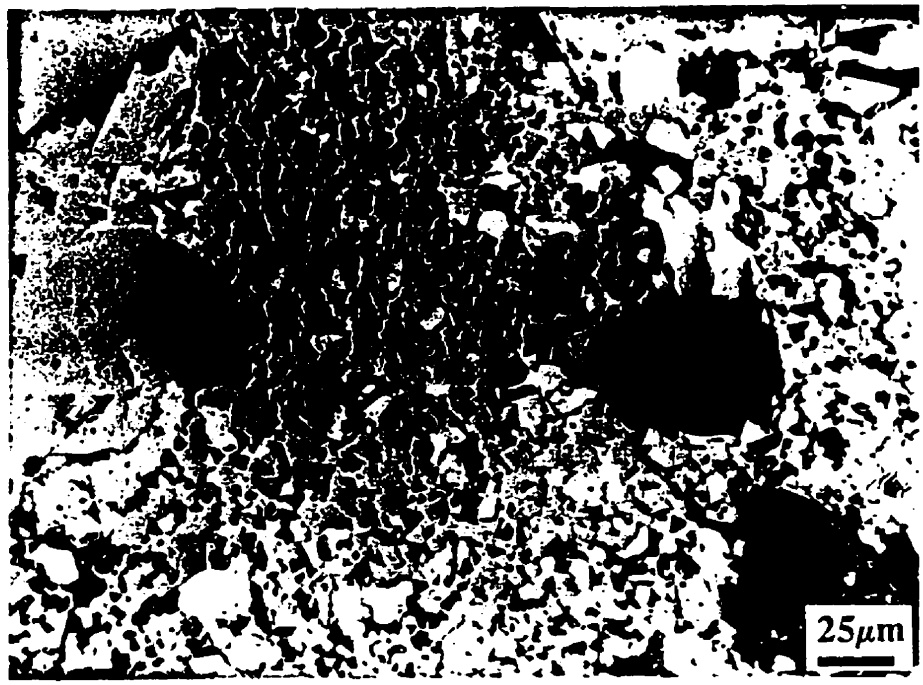

Figure 5.8 Microstructure of Porous Matrix at Penetration Zone
in Magnesia Based Castable (F2)

Figure 5.9a shows the microstructure at the cold face. The matrix is sintered and some cracks between matrix and MgO grains are formed which can be believed to accelerate the penetration. Figure 5.9b is at a higher magnification showing the cold face and the constituants of the matrix. There is some cubic spinel crystals formed, but it is not evident as the spinel crystal in the slag penetration zone. From this reason, it is beleived that the penetrated slag accelerates the spinel formation and sintering.

The alumina based castables have a stronger erosion than magnesia based castables from the macro observation. In the microstructure, a great deal of glassy phase can be observed. Figure 5.10a is the micrograph of castable A1. In the slag zone (up part), lots of glassy phase and some spinel can be found. In the refractories, the matrix and the alumina grains all are corroded. The matrix consists of needle like secondary alumina which has precipitated during cooling. The big porous alumina grains are seriously corroded and the dense alumina grains has less corroded. Under high magnification, as shown in Figure 5.10b, the dense alumina grain is corroded only on the surface and the matrix around the grain is very glassy.

In deep layer of castable A1, the strength of matrix is influenced by the penetration slag which is shown in Figure 5.11. The high strength is produced due to the penetrated slag, so the matrix can be observed, but the matrix in the no penetrated slag zone is polished out due to the weak matrix strength, for this reason, only big grains can be observed. In spite of the fact that the sample is prefired at 1600°C, the matrix strength is still weak due to less ceramic bonding, the amounts of MgO and CaO being less.

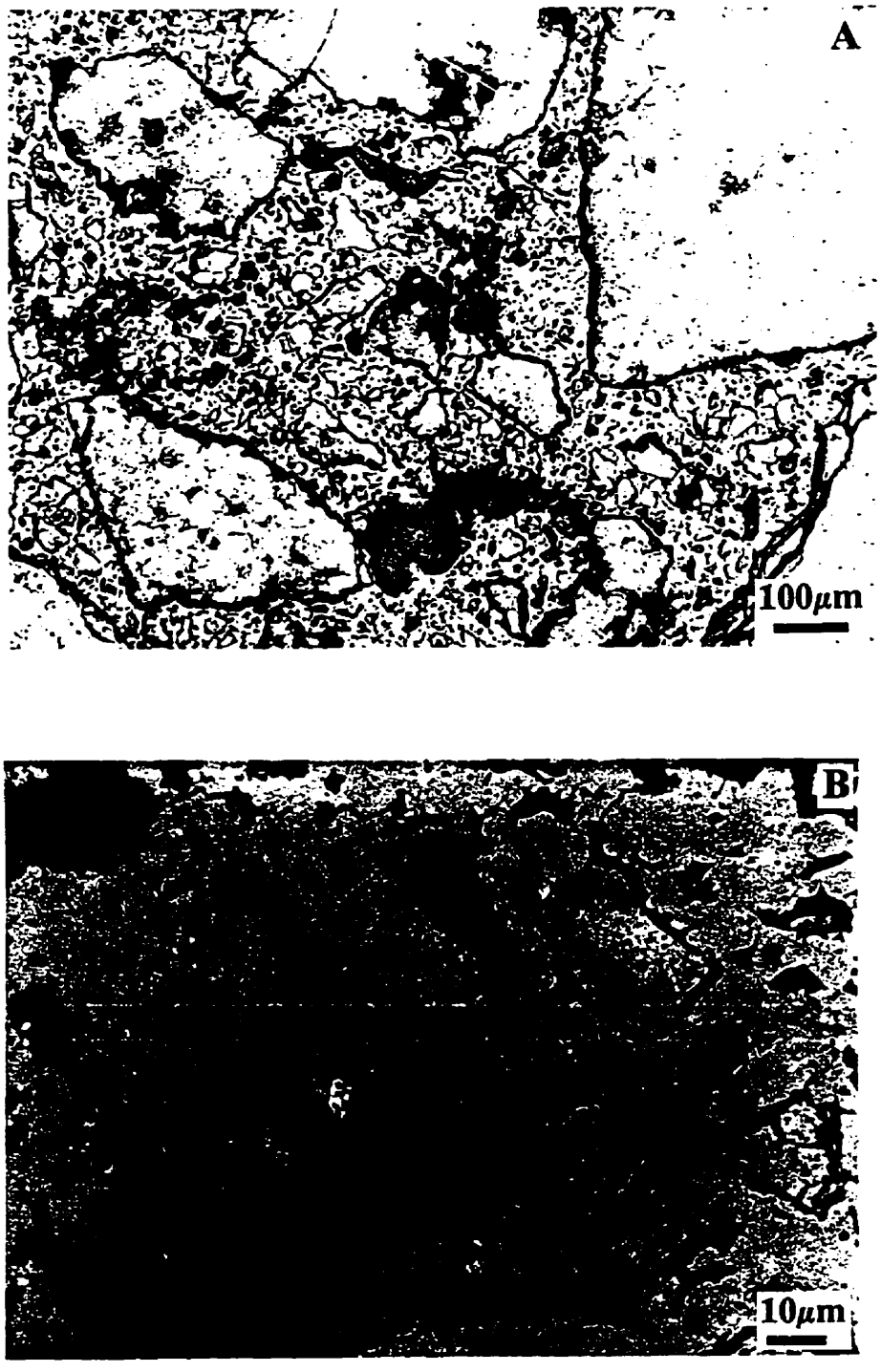

Figure 5.9 Microstructure of Castable F2 at Cold Face. a: 50x, b: 400x

Figure 5.10 Microstructure of High Alumina Castable A1 at the Corrosion Zone.

a: 50x, b: 200x.

Figure 5.11 Microstructure of Castable A1 at the Interface of Penetration and No-Penetration Zone

The microstructure of castable A3, containing certain amount of MgO for form spinel, is shown in Figure 5.12. In the penetration zone, Figure 5.12a, the matrix, a very porous structure, consists of some glassy phase and recrystallized corundum. The recrystallized corundum is clearly shown in Figure 5.12b having typical needle like shape. Some spinel particles can also be identified. Comparing the matrix of A3 and the magnesia based castables, the matrix of A3 contains more glassy phase than that of basic castables. This is due to the a greater erosion of the matrix and a higher viscosity of liquid phase penetrating, enhancing the difficulty of recrystallization. Through X-ray diffraction, a great deal of corundum, some

spinel and less CA_6 in the penetration zone, have been identified.

For Castables A1 and A3, lots of liquid phase exists in matrix, but the slag penetration at high temperature, accelerates the erosion. The castable is composed of big grains and matrix. The ability of castable corrosion resistance depends significantly on the matrix corrosion resistance, because the matrix is a porous and non-continuous component, and the multi-phases or multi-elements (low melting point) in matrix reduce greatly its corrosion resistance. The major phase in matrix determines its ability of corrosion, especially, erosion resistance. Comparing the erosion resistance of MgO, spinel and Al_2O_3 in basic steelmaking slag, MgO is better than spinel, and spinel is better than Al_2O_3, according to their thermodynamical stability. For the erosion resistance of MgO-rich, stoichiometric and Al_2O_3-rich spinel in basic slag, the MgO-rich spinel is stronger than others. This agrees with the report of Nagasoe et al. [63] who investigated the corrosion resistance of different spinel in basic slag.

Reviewing the corrosion behaviour of MgO-Al_2O_3 castables in basic slag, the MgO-rich castables have a better erosion resistance than Al_2O_3-rich castables, but the Al_2O_3-rich castables have a better penetration resistance than MgO-rich castables. The corrosion resistance mechanism in Al_2O_3 based castables can be concluded that the Al_2O_3 captures the CaO from slag to form CA_6 in Al_2O_3-rich castables, that leads to the composition of penetrated slag changing to more viscous state, so the penetration is suppressed, but the strong erosion carries out. In basic castables, the MgO and spinel (matrix) have a strong chemical stability in basic slag, which greatly decreases the chemical erosion, but the slag can penetrate deeply into the castables.

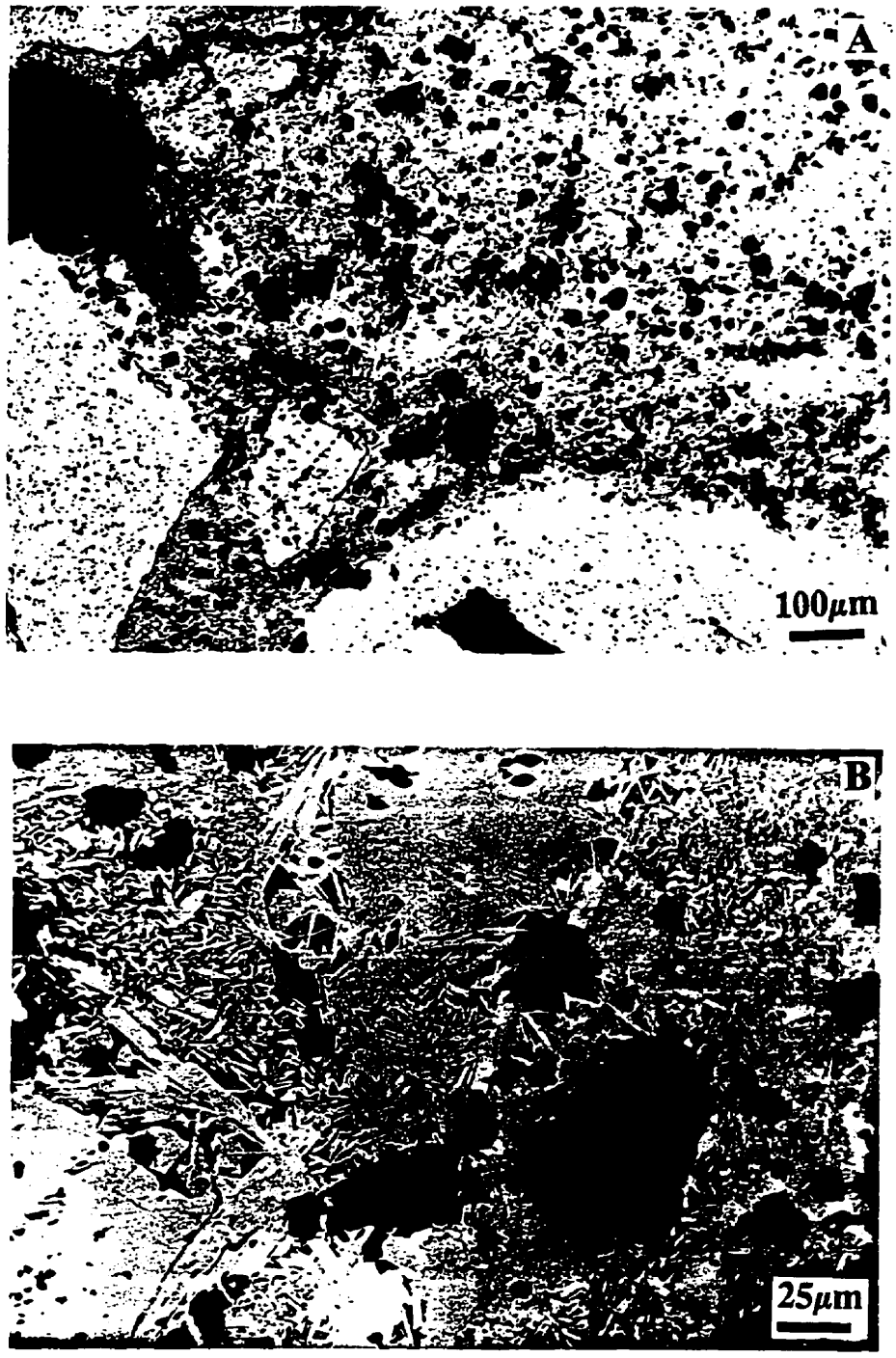

Figure 5.12 Microstructure of Castable A3 in the Penetration Zone.

a: 50x, b: 200x

5.2.2 Effect of Slag Basicity on Corrosion Resistance

In steelmaking, sometimes the very high basic slag is chosen to improve the steel quality or satisfy some special requirement. In this section, the effect of slag basicity on corrosion has been studied to compare the resistant capacity of magnesia based and alumina based castables. All specimens for this series test are totally prefired samples.

Figure 5.13 shows the macrostructure of all samples tested after corrosion; the samples are high alumina castable (A1), alumina-spinel castable (A2), magnesia castables (B4) and (F1, F2 and F3), respectively from left to right. These samples are corroded in high basic slag--Slag 2 for 8 hours. Erosion of the alumina based castables is quiet evident, especially the high alumina castable (A1) where some big alumina grains are dislodged while the magnesia based castables show less erosion, but evident penetration.

Figure 5.14 shows the erosion thickness in different slag(Slag 1 and Slag 2). The increase of slag basicity from 2.5 to 3.2 accelerates the erosion for all specimens, but the increasing value for high alumina contained castable is greater than relatively low alumina contained castables. The fine alumina addition which substitutes a part of ultrafine alumina increases the erosion, for example B4, due to the formation of spinel which has a weaker resistance to basic slag attack.

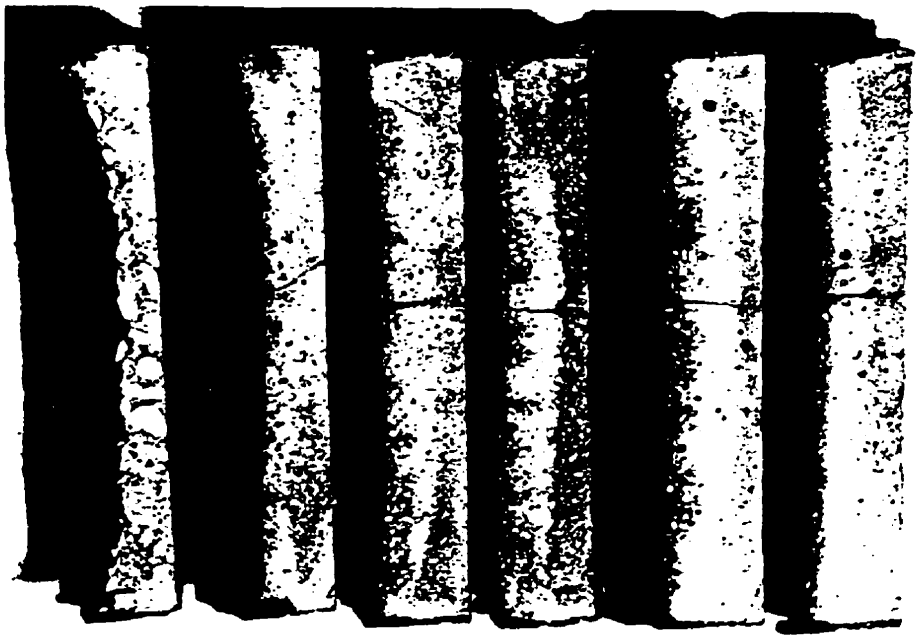

Figure 5.13 Macrostructure of a Group of Corroded Castables in High Basic Slag.

(A1, A2, B4, F1, F2 and F3 from left to right)

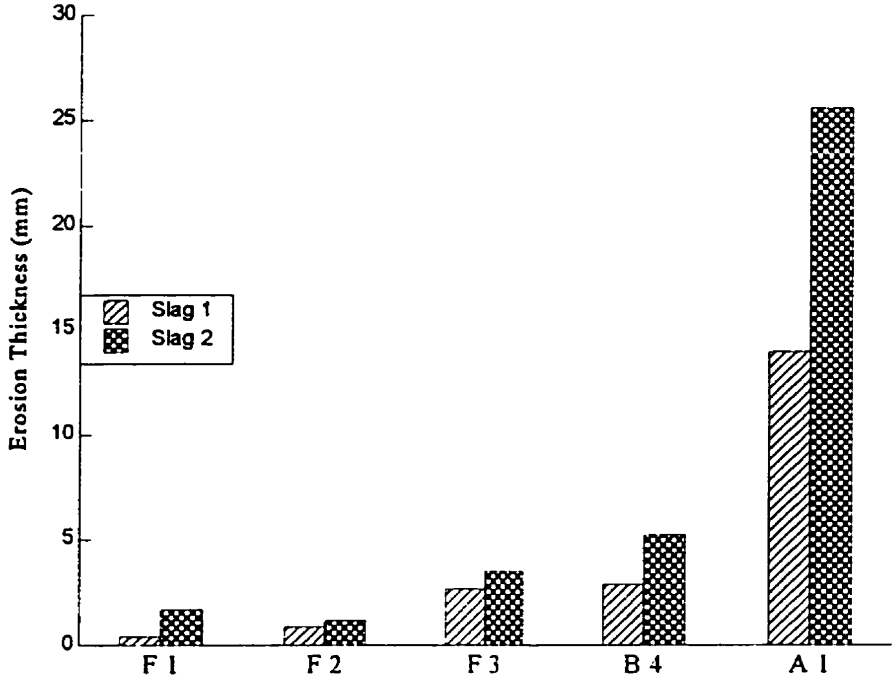

Figure 5.14 Effect of Slag Basicity on Erosion Resistance

The penetration depth is indicated in Figures 5.15 and 5.16. For the basic castables, the penetration depth has slightly increased in the high basic slag corrosion. The high basic slag has a low viscosity which can accelerate the penetration. The penetration depth nearly reaches the solidification temperature of slag. The high alumina castables are weakly penetrated in high basicity slag. The reason is that the erosion speed is faster, and the materials are simply eroded.

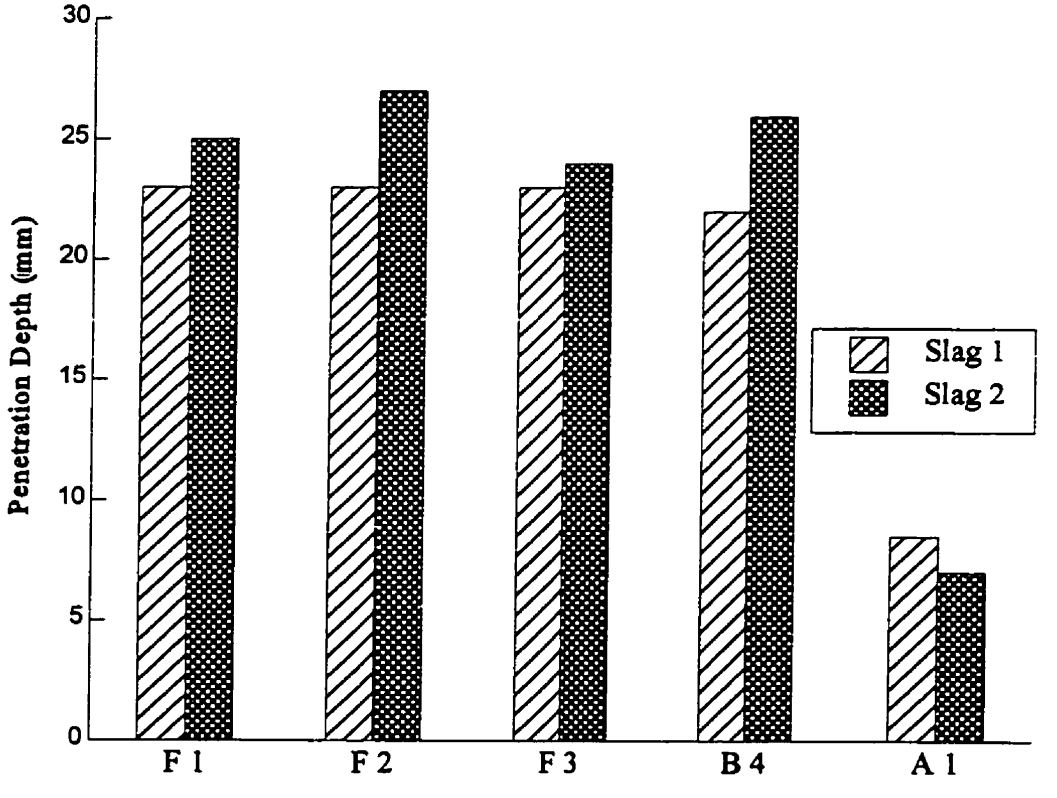

Figure 5.15 Effect of Slag Basicity on Penetration Depth

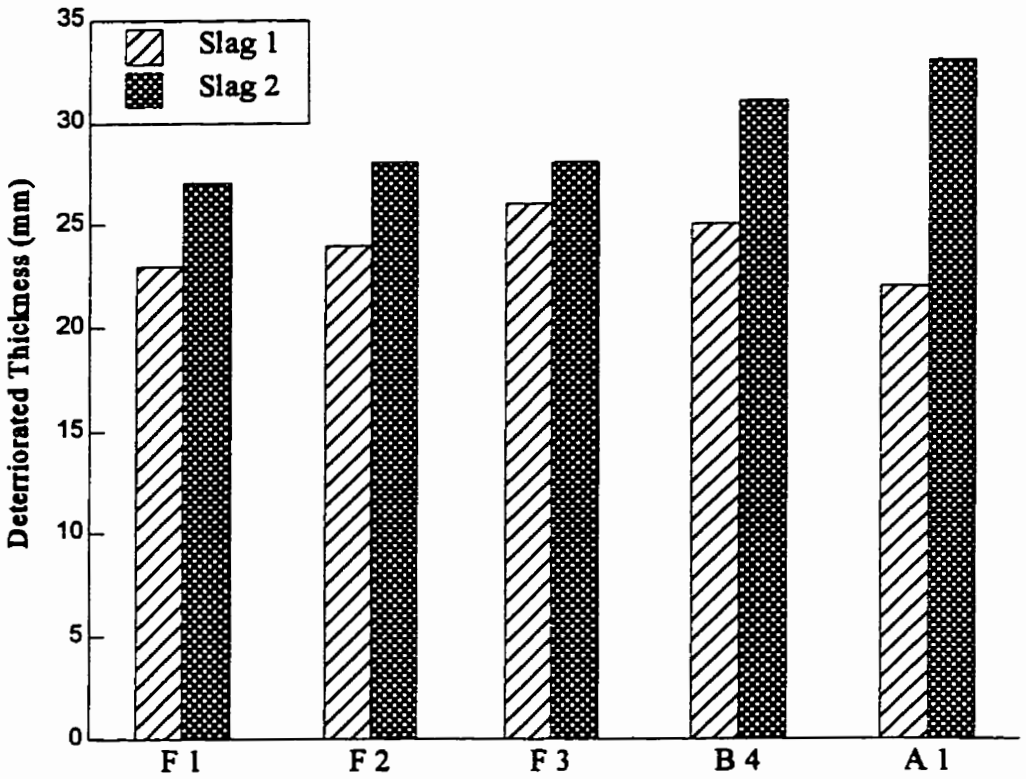

Figure 5.16 Effect of Slag Basicity on Deteriorated Thickness

5.2.3 Effect of Prefiring Condition and Testing Methods on Corrosion Resistance

In this section, the totally prefired specimens and partially prefired specimens are compared in order to know the effect of testing conditions. Cycle testing is also carried out. The testing methods have been described in section 5.1.

The effect of prefiring condition on the slag penetration is investigated with the high alumina castable A1 and magnesia based castable F2. The penetration depth is compared

according to Tables 5.4 and 5.5 . Due to the irreversible expansion of partially prefired sample during firing, the measurement of erosion thickness become impossible. For the high alumina castable, the penetration is very similar, due to the penetration value for both is already low and the major phase in castable is similar--very high alumina. F2 castable fired at 1600°C contains magnesia mostly as aggregate and spinel mainly as matrix, but alumina can not be found by X-ray diffraction as shown in Table 5.7. F2 has a porosity of about 15%. This porosity is high enough to allow for slag penetration. Also the MgO is easily wetted by the slag, because the surface energy of magnesia (1000-4000 dynes/cm) is much greater than the surface tension of molten slag (400-500 dynes/cm) according to Nishikawa's report [112]. When slag is charged during corrosion test, liquid slag has less chemical reaction with MgO and spinel, comparing with Al_2O_3, meanwhile, MgO is easily wetted by molten slag, so the penetration is very deep. The penetrated slag can slightly accelerate the densification of matrix that can decrease the penetration, but the densification is relative and limited for the preformed spinel matrix. To the partially prefired specimen, only hot face is fired at 1200°C and it is not enough to form good spinel at 1200°C according to our matrix study in chapter 3. The bonding formation of spinel is during the corrosion. Some penetrated slag participates to the formation of ceramic bond, so liquid slag greatly accelerates the spinel formation and matrix densification. On the other hand, some unreacted very fine Al_2O_3 and MgO powders are possible to dissolve into slag to increase the slag viscosity and the melt temperature.

The X-ray diffraction results in Table 5.7 find the unreacted alumina in deep layer (far from the hot face), but all the alumina in the layer near hot face transfer to spinel, and in the total prefiring sample, all alumina transfer to spinel in spite of cold face zone. The chemical

analysis results for castable F2 in the condition of total prefiring and partial prefiring indicate that more MgO and Al_2O_3 of partial prefiring sample dissolve into slag in the penetration zone than that of total prefiring sample which is shown in Figure 5.17.

Table 5.7 X-ray Diffraction for the Magnesia Based Castables in the Condition of Total and Partial Prefiring

	Distance from Hot Face	Major Phases	Minor Phases	Trace Phases
Total Prefiring	0 - 5 mm	M, MA+MF	C_2S	C_3MS_2, CA_4F_2
	5 - 10 mm	M, MA+MF	C_2S	C_3MS_2
	10 - 15 mm	M, MA	C_2S	
	25 - 35 mm	M, MA		
Partial Prefiring	0 - 5 mm	M, MA+MF	C_2S	C_3MS_2, CA_4F_2
	5 - 10 mm	M, MA+MF	C_2S	
	10 - 15 mm	M, MA	C_2S	A
	25 - 35 mm	M	MA, A	

The one cycle and three cycles testing specimens are compared to investigate the influence of testing procedure. The test results are shown in Figure 5.18. All specimens after partial prefiring contain certain unreacted small MgO and Al_2O_3 particles. The small MgO particles have larger surface area than big MgO grains and in contact with slag, during corrosion testing, they have stronger capacity to absorb FeO and form (Mg.Fe)O solid solution. The chemical analysis in the 0-5 mm hot face layer show that for totally prefired sample, Fe_2O_3 content is 18% and for partially prefired sample, 25% Fe_2O_3. The (Mg.Fe)O

solid solution has a high melting temperature, as shown in MgO-FeO phase diagram [113]. During cooling, the (Mg.Fe)O solid solution will transform to MgO and $MgO.Fe_2O_3$ (ferrian spinel). The MF spinel is localized on the grain surface, at crystal boundaries or in the internal pores of grains. With multi-cycles test, MgO will again absorbs the FeO from the slag to form (Mg.Fe)O solid solution during re-heating and MF spinel during cooling. During corrosion test, part of MF can transform to (Mg.Fe)O solid solution, but another part of MF stays as MF spinel, with a melt temperature of 1713°C. Under the slag environment, CaO and SiO_2 can greatly decrease the MF melt temperature. Also the precipitation of MF spinel

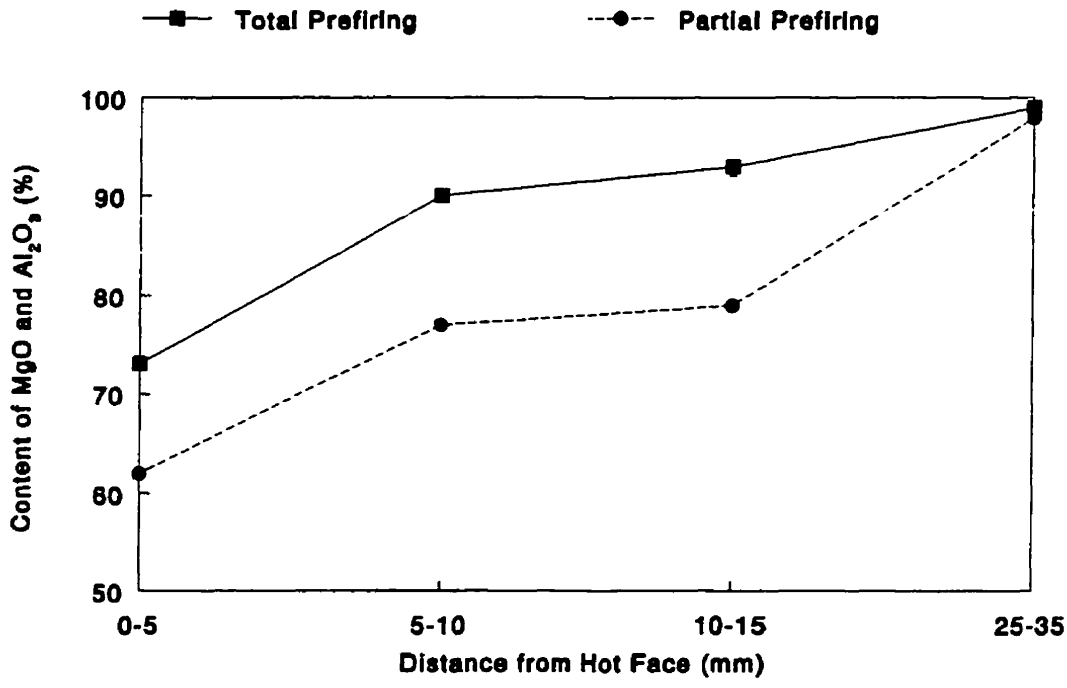

Figure 5.17 Content of MgO and Al2O3 at Penetration Zone for the Total Prefiring and Partial Prefiring Samples

accompanies a volume change, e.g. from FeO to Fe_2O_3 with a volume expansion. This volume change will produce micro cracks which increase the contact area between slag and refractories, meantime, loosen the refractory structure. The erosion increases. So cycled test samples show a weaker erosion resistance than no cycled test samples.

The cycled test samples produce MF spinel in the refractory surface layer. This coating can not completely re-melt on the second or third heating. After cooling-heating-cooling cycle, the coating thickness gradually increases with the number of cycles. The thickness for one cycle is about 2 mm and for three cycles about 9 mm. The testing temperature is always 1600°C at hot face. Due to the existence of a coating, the real temperature of refractories is relatively lower. For this reason, the cycled test sample do show less penetration. The complete deteriorated thickness of all specimens is nevertheless similar.

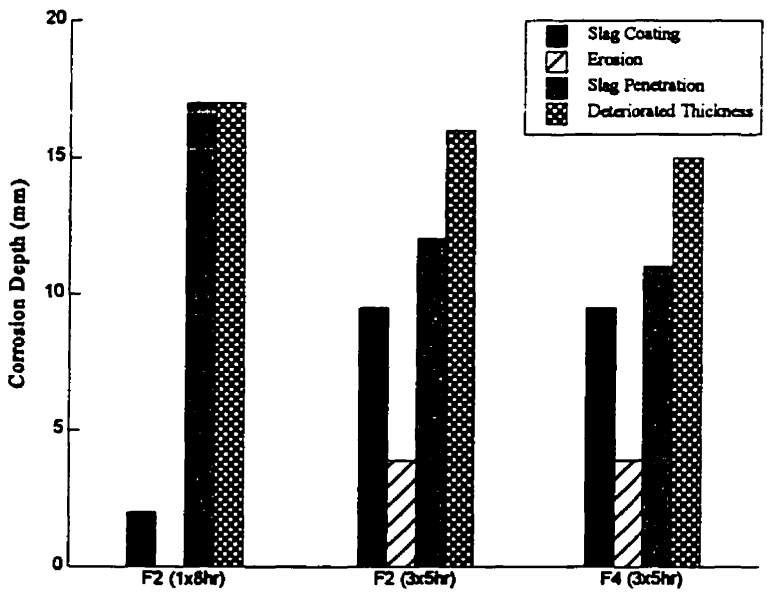

Figure 5.18 Effect of Cycle Test on Corrosion Resistance

Comparing F2 and F4 in three cycles test, no evident difference between them appears. So the big aggregate has less influence on corrosion resistance.

The Fe_2O_3 content in 0-5 mm layer for different testing methods of castable F2 is examined by chemical analysis and the results are indicated in Figure 5.19. For castable F2 in total prefiring state, the sample absorbs less Fe cation than partial prefiring samples. One cycle testing sample absorbs less Fe cation than three cycles testing sample. Most fine MgO particles in total prefiring specimen transfer to spinel or is in death burnt state which decrease the activity of MgO, such as the absorption of FeO is limited. The partial prefiring specimens contain more fine MgO particles, so they can easily absorb great deal of FeO from slag to form (Mg.Fe)O solid solution at high temperature and MF spinel can be formed with some precipitated MgO by the decomposition of (Mg.Fe)O solid solution during cooling. However, when it is heated again to high temperature, only a part of precipitated MgO combines with MF to produce (Mg.Fe)O solid solution and another part of precipitated MgO will absorb again the FeO from slag, so the Fe element amount increases with the cycle times. From the chemical analysis, it clearly displays this trend.

Figure 5.20 is the macrostructure of the three cycles corrosion sample. A thick coating layer is evidently formed on the hot face and some MgO grains move in the coating layer because the connected matrix or ceramic bonding is eroded. An evident colour element penetration occurs from black at hot face to grey in refractories. A dense layer is also identified near the hot face. With increasing the depth, the structure is looser with a weak strength. The colour elements (Fe, Mn, etc.) are captured in surface layer because the MgO absorbs the FeO to produce (Mg.Fe)O solid solution at high temperature.

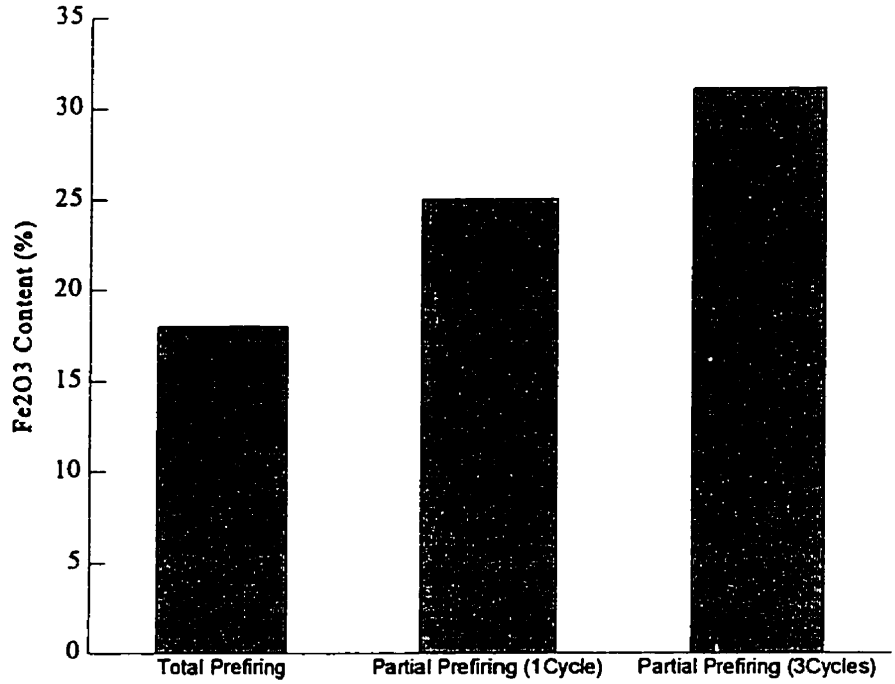

Figure 5.19 Absorbed Fe_2O_3 Amount on the Castables Hot Face Layer (0-5mm)

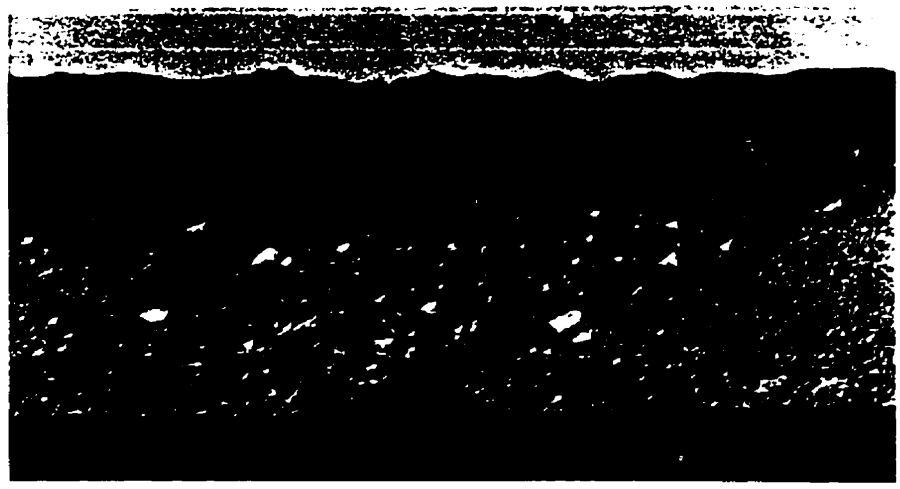

Figure 5.20 Macrostructure of a Three Cycles Testing Sample

The microstructure at the interface between the slag and refractories is shown in Figure 5.21a. In the slag zone, MgO grains with doped FM spinel and some big MA spinel grains can be observed. Between the slag zone and refractories, a dense spinel line is formed due to the liquid slag which accelerates the spinel crystals or grains growth. In the refractories (penetration zone), porous spinel matrix can be produced, but these spinel has relatively small size and they connect each other to form net. The microstructure at cold face in Figure 5.21b shows a very weak matrix. Only some big MgO grains can be observed and no evident ceramic bonding is formed.

5.2.4 Modification of Magnesia Based Castables: Effect of Addition of fume Silica, Calcium Aluminate Cement and MA Spinel on Corrosion Resistance

X-ray diffraction analysis results, for castables with silica addition (FSilica) and cement addition (BCement) after corrosion are indicated in Table 5.8. The results are obtained in a layer 5-10 mm away from the hot face.

Table 5.8 The Phases Composition between 5-10 mm from Hot Face after Corrosion of Castables Containing Silica or Cement

	Major Phases	Minor Phases	Trace Phases
FSilica	M, MA+MF	C_3MS_2, CMS	
BCement	M, MA+MF	C_3MS_2	CMS

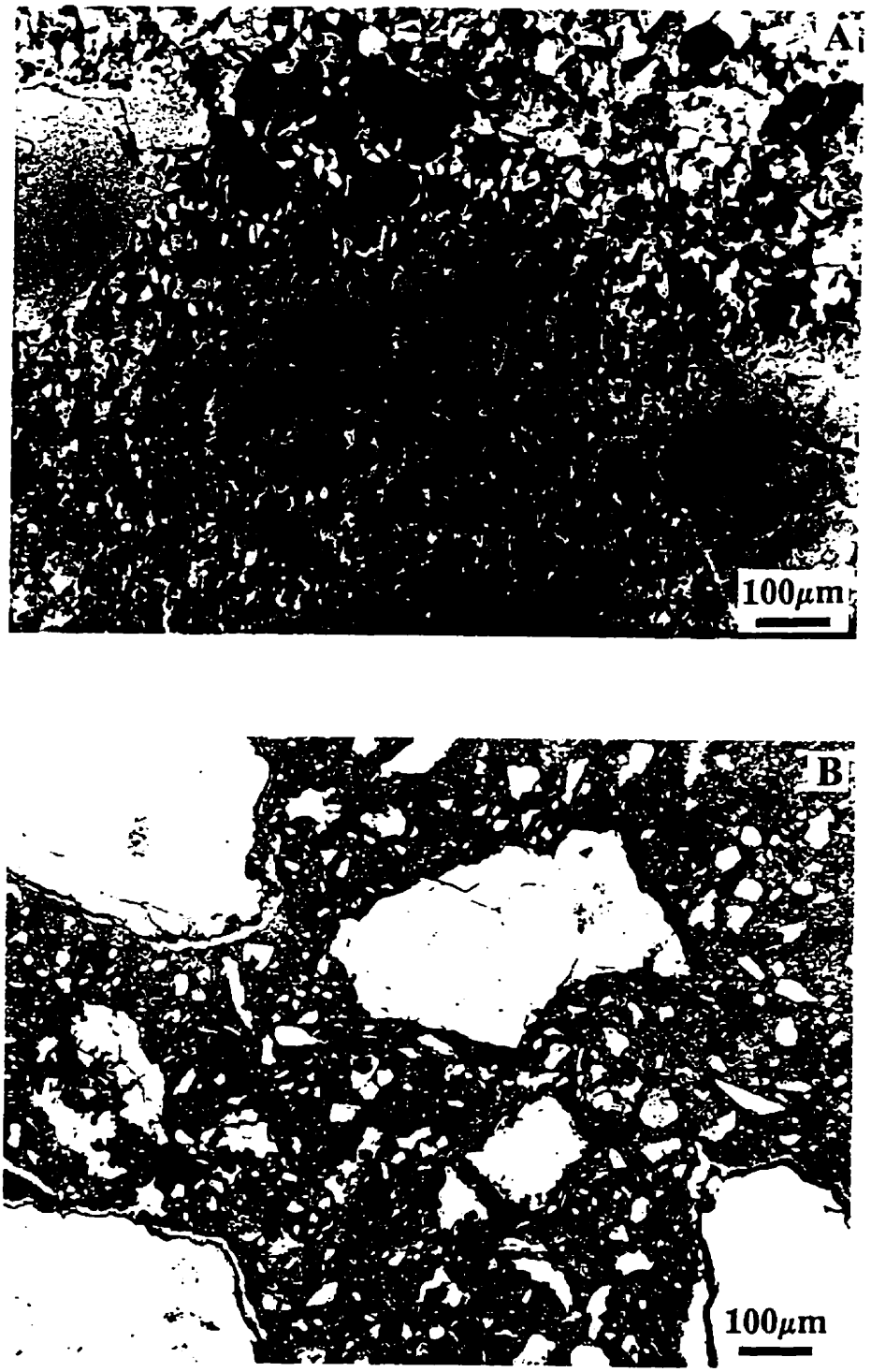

Figure 5.21 Microstructure of Partial Prefiring Sample after Corrosion Test. a: interface between slag and refractories, b: cold face.

Castable FSilica contains 2% fume silica in substitution to ultrafine alumina powder, in the composition of castable F2 (see Table 5.2). The two castables in Table 5.8 have been totally prefired. The corrosion test at 1600°C was carried out for 8 hours. The corrosion results are shown in Figure 5.22. The addition of silica evidently decreases the erosion resistance, since silica reduces the refractoriness of the castable, especially the refractoriness of matrix which contains three major oxides: MgO, Al_2O_3 and SiO_2. From the phase diagram of MgO-Al_2O_3-SiO2 [113], the minimum melting temperature between MgO and Al_2O_3 is about 1850°C, but the minimum melting temperature among MgO, Al_2O_3 and SiO_2 is about 1710°C in magnesia rich composition and much lower in the alumina rich composition. For this reason, the addition of silica reduces the melting temperature of refractories and increases the possibility of production of low melt compound in matrix, so the erosion increases. In the penetrated zone, at the microstructural level, glassy phase is clearly seen in Figure 5.23. Silica is dissolved into the slag. With the X-ray diffraction in the penetrated zone, C_3MS_2 and CMS phases are detected, both being liquid at 1600°C.

The penetration for castable containing silica is slightly reduced, but the deteriorated thickness of castable containing silica is important and the addition of silica has not improved the corrosion resistance.

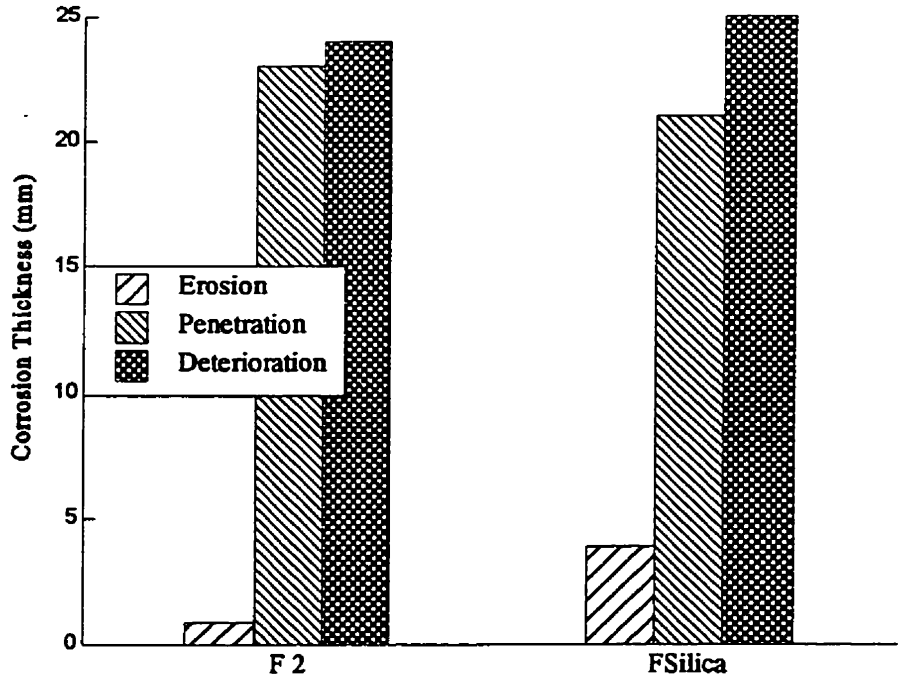

Figure 5.22 Effect of Silica Addition on Corrosion Resistance

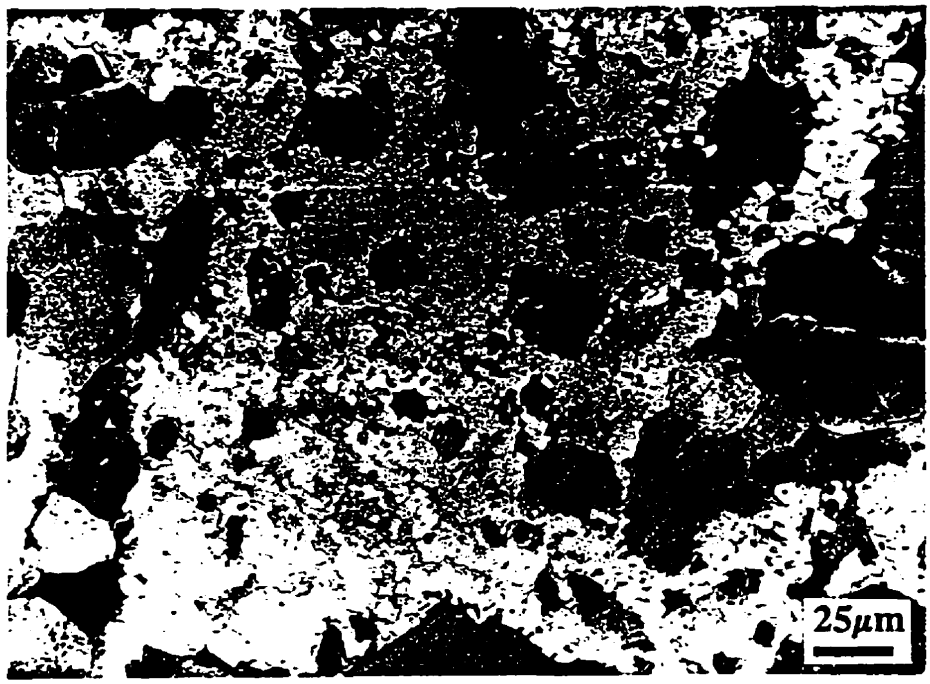

Figure 5.23 Microstructure of Castable FSilica--More Glassy Phase Occurs in Matrix

For the BCement sample, 4% high alumina cement Secar71 is added to replace the active alumina binder. The corrosion results of Castable B3 and BCement are indicated in Figure 5.24. These two castables are also in total prefiring state and their total Al_2O_3 quantity in castable is similar (about 18%). The cement addition does not change the erosion resistance appreciably, of cause there is the same amount of Al_2O_3 in each castable. However, the penetration thickness in the castable with cement is deeper than castable without cement. Hence, cement does not improve the corrosion resistance of the basic castables, as expected.

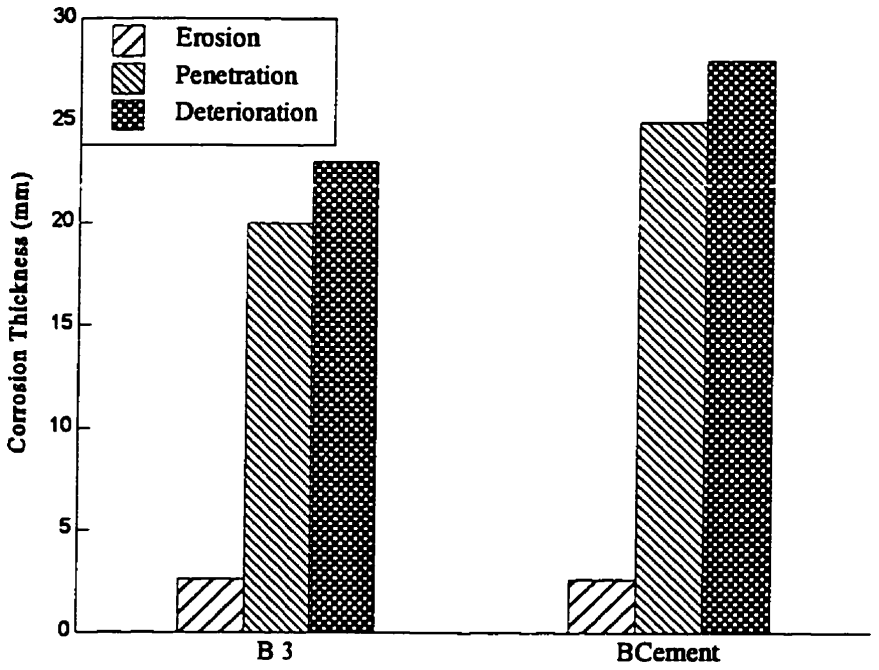

Figure 5.24 Effect of Cement Addition on Corrosion Resistance

Spinel has a better corrosion resistance to basic slag than Al_2O_3 or SiO_2, so in-situ spinel was added as bonding to improve the corrosion resistance of the F magnesia based castables series. The compositions of the S series are shown in Table 5.2. Castable F2 serves as a reference. It is partially prefired and corrosion tested for three cycles. The spinel S-castables are also partially prefired samples, but the corrosion cycle lasted two cycles. Results are shown in Figure 5.25. The erosion of castable containing preformed spinel is slightly higher, but the total Al_2O_3 amount is also a little higher. The difference in corrosion resistance of synthetic spinel versus in-situ formed spinel is not considered here a conclusive

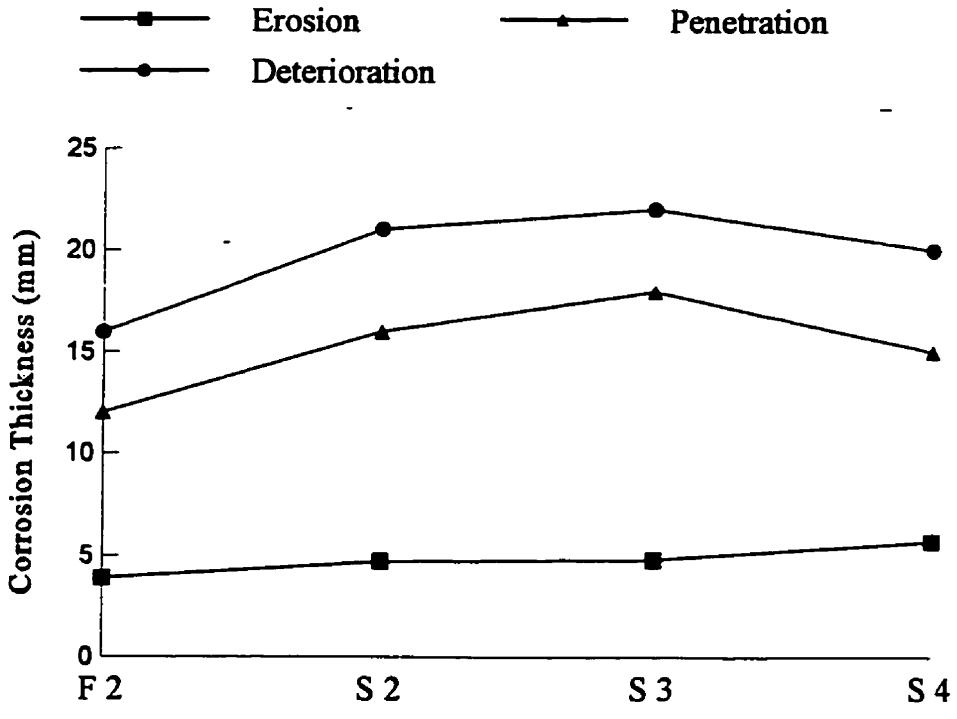

Figure 5.25 Effect of Commercial Spinel Addition on Corrosion Resistance of Basic Castables

one.

Penetration of S-castables is also higher. And the castables containing synthetic spinel has more micro pores or micro cracks between aggregates and/or between the matrix compounds. Overall, the S-series suffer from a highest deteriorated thickness even after 2 cycles instead of 3.

Two magnesia based castables with nearly same content of alumina, one is made with alumina powder and another is made with preformed spinel, are compared in the corrosion test. These two castables are totally prefired samples. Castable S1 contains 10% preformed sintering spinel with the stoichiometric ratio and 10% ultrafine, 4% active alumina. Castable F3 contains 20% ultrafine and 5% active alumina. The corrosion results are shown in Figure 5.26. The castable S1 containing preformed spinel exhibits more erosion. This is attributed to the spinel quality. The preformed spinel is in the stoichiometric ratio, but the in-situ spinel is produced with in the MgO-rich environment, so a MgO-rich spinel or MgO-spinel co-clinker is formed. This in-situ spinel has a stronger erosion resistance to basic slag leading to better performances. The penetration for both castables are similar. The higher deteriorated thickness of S1 mainly is caused by erosion.

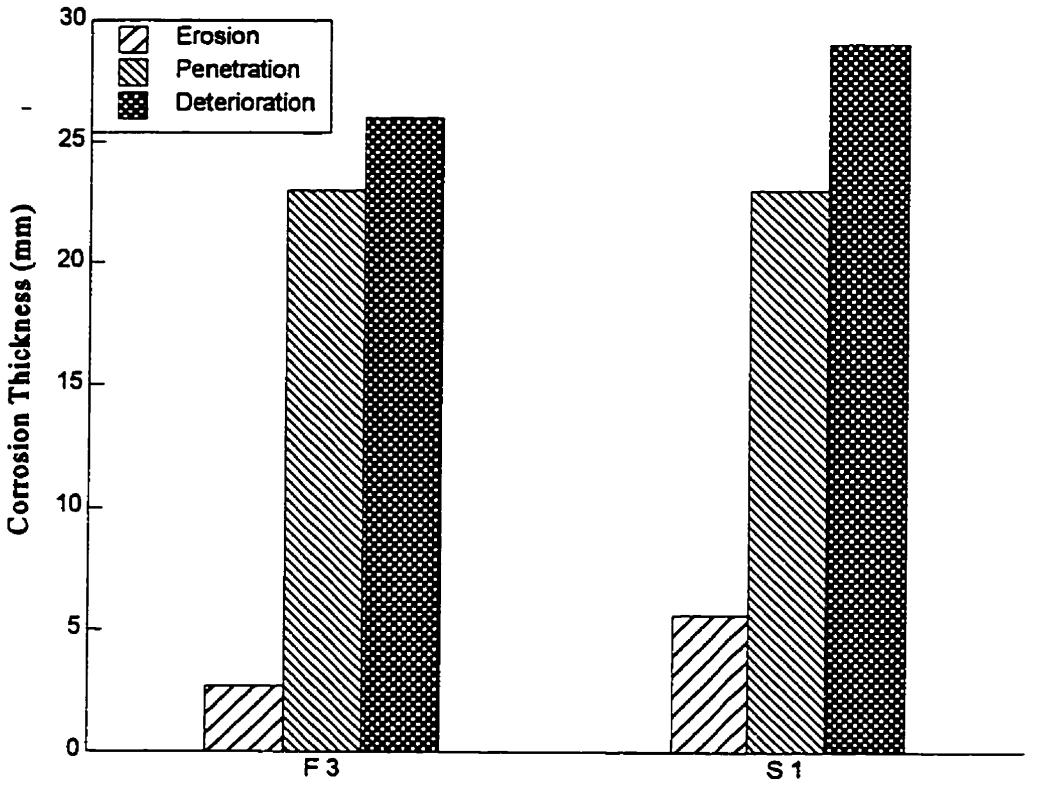

Figure 5.26 Corrosion Resistance of Castables with Preformed Sintering Spinel or In-situ Spinel

5.3 Summary on Corrosion Resistance

Basic castables have been investigated and compared with alumina based castables in the environment of basic slags. Basic castables are naturally more erosion resistance to basic slags. The erosion resistance decreases with increasing amount of Al_2O_3 in castables, as expected from the relative chemical stability of the constituents in basic slag environment (MgO more stable than spinel, spinel more stable than Al_2O_3). Also the MgO-rich spinel or MgO-spinel co-clinker seems more resistant to basic slag than stoichiometric spinel and Al_2O_3-rich spinel. The erosion resistance of Al_2O_3 based castables is very weak compared to basic castable.

Penetration of basic slag in basic castables is very pronounced. This is the service of the poor structural spalling resistance of MgO based castables. MgO is chemically stable in contact with basic slag, but it is very easily wetted and the low viscosity basic slag can penetrates into the refractories through the pores and micro cracks, present in all castables with MgO aggregates with spinel bonds. Partially prefired castables show lower penetration values. Unreacted MgO and Al_2O_3 alter the slag viscosity, but the liquid slag can also participate and accelerate the spinel bonding formation which leads to a relatively dense matrix formation.

The ultrafine alumina powder can reduce more efficiently erosion than fine alumina powder. This is attributed to the in-situ formed spinel quality. The ultrafine alumina is more uniformly dispersed in the matrix and forms spinel more readily. This spinel or MgO-spinel matrix has a more homogeneous microstructure which improve its chemical stability. The fine alumina particle with a relatively larger size are less reactive, the quality and quantity of

spinel matrix will be lower, so the resistance to erosion weaker.

The relative amount between fine and active alumina has not evident influence on the corrosion resistance. The two alumina powders seem to have a similar effect on the spinel formation and the matrix properties.

The addition of silica can not improve the corrosion resistance because the silica decreases the refractoriness of castable matrix and produce low melting compounds, consequently, the erosion resistance is reduced. The penetration of castables containing silica is not enhanced, but it can not suppress it, so the addition of silica in $MgO\text{-}Al_2O_3$ may not be advisable at the first glance.

The addition of cement is not to be recommended either. The CaO is not really welcome in the $MgO\text{-}Al_2O_3\text{-}CaO$ system to improve refractories.

Synthetic spinel addition had no positive effect on the corrosion resistance. This is still to be considered as a preliminary result. More works need to be done before a firm conclusion can be reached.

CHAPTER 6 SUMMARY AND CONCLUSION

Use of magnesia based castables has been contemplated for steelmaking vessels for many decades. But some obstacles, like the hydration of magnesia or the selection of proper binder and bonding system, have not yet been overcome. This thesis studies systematically the magnesia based with MA spinel bonded castables.

A binder plays a critical role in castables. It determines not only the physical and mechanical properties of green body, but also the characteristics at high temperatures. It has been reported that the CA cement and active alumina have been used in high alumina castables, but there is no detailed report regarding the use of active alumina in magnesia based castables. In the present work, active alumina is first introduced to magnesia based castables as a binder to substitute the traditional CA cement. This investigation indicates that a suitable amount of active alumina (suggested 5% in this thesis) leads to good physical and mechanical properties; the penetration resistance was also improved by replacing CA cement.

The synthesis of spinel has been reported since 1930s; however the spinel formation relevant to the matrix of refractory castables, especially its expansion-shrinkage behaviour and effect on refractories, has never been described. In this thesis, the spinel is formed in-situ using the refractory grade of MgO and Al_2O_3 raw materials, and the expansion-shrinkage behaviour relative to raw materials and the ratio between MgO and Al_2O_3 are investigated. The ultrafine alumina (UFA) with D_{50} under 0.5 μm is first introduced into magnesia based castables. The ultrafine alumina has a very early sintering temperature (about 1000 to

1100°C). This strong sinterability compensates the expansion due to spinel formation in the mixtures. The sintering process of MgO-UFA mixtures goes through a shrinkage at intermediate temperatures (1200°C) and more shrinkage at high temperatures (1600°C). This improves the expansion-shrinkage behaviour considerably. The volume change during spinel formation is controlled. Inversely, fine alumina (D_{50} of 4 μm) has a low sinterability before 1200°C. Due to the chemical impurity of fine alumina and homogeneous distribution between MgO and Al_2O_3 particles in the mixtures, spinel can be rapidly produced at 1200°C. A great volume expansion will cause sintering difficulty at intermediate temperature (1200°C).

The ratio of MgO/Al_2O_3 in mixture containing fine alumina strongly influences the quantity of formed spinel by controlling the contact area between MgO and Al_2O_3. However, the densification depends greatly on the spinel formation. The largest expansion was found at the ratio of 60% MgO and 40% Al_2O_3 at 1200°C, due to rapid formation of spinel; less sintering shrinkage of product (spinel) and less sinterability of raw materials (MgO and fine Al_2O_3).

The effect of additives, like fume silica and CA cement, on the expansion-shrinkage behaviour has also been investigated. When silica fume is added to alumina-rich mixture, it works as a mineralizer to accelerate the densification, due to the formation of liquid phase, but when it is added to magnesia-rich mixture, the different features are resulted in according to the addition amount. Small amount of silica (3%) leads to the densification, however, more silica (>7%) causes the formation of silicate minerals which reduce the densification. The addition of CA cement does reduce the porosity of magnesia-rich mixture from intermediate temperature (1200°C) to high temperature (1600°C), but in alumina-rich mixture, the porosity

is increased at high temperature due to the formation of CA_6. These results systematically delineate the spinel formation and its expansion-shrinkage behaviour at the refractory matrix level that would be beneficial to the development of magnesia-alumina refractory castables.

Chapter 4 studies the formation of magnesia based mixtures and their properties. The fine magnesia particles of 50μm can be used and then do not cause the hydration damage in these castables. The amount of ultrafine alumina in castable has a great influence on the properties. More ultrafine alumina (20%) leads to a higher porosity for both green body and fired samples due to the great deal of formed spinel. The amount of ultrafine alumina also affects strongly the PLC gradient from intermediate (1200°C) to high temperature (1600°C). Less amount of ultrafine alumina (10%) will cause a great PLC drop between 1200°C and 1400°C, but more ultrafine alumina leads to great PLC drop between 1400°C and 1600°C. So only a suitable amount (15%) of ultrafine alumina can produce a uniform PLC gradient from 1200°C to 1600°C. Ultrafine alumina improves the MOR (9MPa at 1600°C) also, compared with the same added amount of fine alumina (4MPa), due to good formation of ceramic bonding.

The magnesia based castables produced a relatively low mechanical strength (9MPa at 1600°C), when compare with alumina based castables (>20MPa typically). The low mechanical strength of our basic castables is attributed to the mismatch between big MgO grains and spinel matrix, due to the great difference of coefficient of thermal expansion. The cracks and gaps around MgO grains often occur, which greatly decreases the mechanical strength. Smaller D_{max} of aggregates should improve the mechanical strength. A mixture with good performance has been produced by the addition of about 5% active alumina and 15%

ultrafine alumina.

The corrosion resistance of magnesia based mixtures was investigated and compared with the alumina based castables in Chapter 5. In the basic slag, the developed magnesia based mixtures showed much better erosion resistance than commercial alumina based castables. The total amount of alumina in MgO-Al_2O_3 castables has the strongest influence on the erosion resistance to basic slags. The typical values of erosion are 1 mm for the 20% alumina and 14 mm for 96% alumina castables. Among the spinels, the MgO-rich spinel seems more chemically stable than stoichiometric and Al_2O_3-rich spinel. In basic ferrite slag, iron oxide is easily absorbed by MgO to form (Mg.Fe)O solid solution at high temperature, and $MgO.Fe_2O_3$ spinel at lower temperature.

The basic castables are characterized by a poor penetration resistance in presence of such slags, where it reaches 23 mm depth. The penetrated slag in basic castables can accelerate the crystalline formation and growth of spinel. This has been proven by microscope observation between penetration and non-penetration zone.

MgO-fine alumina castables show a worse erosion resistance than ultrafine alumina castables, due to higher porosity produced by fine alumina, and more impurity content that influences the matrix (spinel) formation.

The prefiring methods have an influence on the penetration resistance. The partially prefired samples have lower penetration depth than totally prefired samples. The reason probably is due to the dissolution of unreacted fine MgO and Al_2O_3 into the slag to change the slag properties (viscosity and melting point).

Corrosion testing under cyclic condition increases the erosion thickness. This is

attributed to the re-melt of MF spinel which crystallizes during cooling.

The addition of silica reduces the melting temperature of matrix, so the erosion increases due to the dissolution of castable, mainly matrix, into slag. Two percent silica can increase the erosion depth from 1 mm to 4 mm. The addition of cement does not markedly influence the erosion, but it increases the penetration depth from 23 mm to 25 mm (with 4% CA cement). The in-situ spinel formed castable, MgO-rich spinel, shows a stronger erosion resistance than synthetic nearly stoichiometric spinel contained castable. In summary, some magnesia based mixtures are applicable at slag ligne to resist basic slag erosion.

Throughout this work, the objective of understanding the $MgO-Al_2O_3$ system, with respect to the manufacturing of magnesia based castables, has been achieved. The spinel formation, especially the in-situ spinel relevant to refractories has been reviewed. The reaction mechanism and the effect of refractory raw materials, for example the particle size, the reactivity, the distribution of particles, etc., on the spinel formation have been discussed. The volume change versus nature of raw materials and the ratio of MgO to Al_2O_3 have been systematically investigated in Chapter 3.

The physical and mechanical properties of magnesia based castables were measured. These measurements reveal that the lower mechanical strengths and higher porosity contents of magnesia based castables, compared with the traditional alumina based castables, are originated from its microstructure. The improvement of these properties can be achieved by adjusting the proportions of the binder, ultrafine alumina, fine alumina, magnesia particles and grains. The suggested ratio of alumina to magnesia particles in this thesis leads to a relatively dense structure with acceptable physical and mechanical characteristcs. This will

need to be considered for future development of magnesia based castables. It has been clearly shown that the excessive expansion accompanying spinel formationcan can be controlled by the introduction of ultrafine alumina. This solves the difficulty of in-situ spinel formation in castables that has often led to spalling.

Only few published reports have described testing results concerning MgO-SiO_2 castables, but they do not present excellent corrosion resistance to high basic slags presently (see Chapter 2). The spinel expansion leads to fracture in MgO-Al_2O_3 castables and the addition of SiO_2 reduces the corrosion resistance. Due to these artifacts, no results can be found stating the excellent behaviour in high basic slags zone. In this thesis, the erosion resistance of magnesia based castables to basic slags posses a satisfactory value, but it is necessary to reduce the penetration. The reduction of penetration will be discussed subsequently.

Magnesia based castables can be chosen for commercial fabrication after further improvement of their penetration resistance because they have excellent erosion resistance to basic slag. The basic composition would be 70-80% magnesia and 20-30% alumina. Due to the better chemical stability of magnesia in basic slag, high contents of magnesia in castables lead to high erosion resistance. But the higher the amount of magnesia, the higher the amount of water needed, reducing the rheological property, and the physical, mechanical properties and thermal shock resistance. It is strongly suggested that CA cement be replaced by hydratable alumina when refractoriness and corrosion resistance are taken into consideration. Some ultrafine alumina is to be used because it not only controls the PLC, but it also improves the physical and mechanical properties, as well as the corrosion resistance.

This thesis provides an experimental evidence that magnesia based castables with 80% magnesia content can be produced and fired without any spalling problem during first heat-up. It also provides experimental evidence that hydratable alumina can be used as an hydraulic binder to substitute calcium aluminate cement; this is a good way to improve the refractoriness of all commercial available castables today. This thesis has also demonstrated that the content of alumina determines significantly the erosion resistance of magnesia based castables.

If the developed MA spinel bonded magnesia based mixtures have acceptable physical and mechanical properties as well as very good erosion resistance to basic slags, the penetration resistance is still poor. Potential methods to improve the penetration resistance would be the addition of zirconia or zircon, or graphite.

Zirconia is believed to be able to decrease the penetration depth of magnesia based castables. The main mechanism is the capture of the CaO from slag by zirconia to form solid $CaZrO_3$, which will close the pores of the refractories to limit the slag penetration; meanwhile, the viscosity of slag would increase due to the reduction of CaO, therefore the penetration can be possibly minimized. Due to the expensive cost of zirconia, the replacement of zirconia by zircon can be considered, but the introduction of SiO_2 must be carefully studied.

Graphite is another potential additive for the magnesia based castables to suppress the slag penetration due to its non-wetted feature. The castable formation, mechanical properties and anti-oxidation characteristics would then need to be investigated.

The preformed spinel, used in this thesis, are those of Al_2O_3-rich or near stoichiometric spinel, so it is still necessary to estimate the effect of MgO-rich spinel on the

properties of castables.

The workability and rheology of castables can be improved by careful study of suitable deflocculants. The special retarders and deflocculants for the hydratable alumina and fine magnesia particles need further investigation.

Some mechanical and corrosion results should also be repeated in order to increase the experimental precision and reliability. Fine tuning of the composition, for example total alumina amount and ultrafine alumina amount in castables, should be taken into account in order to improve the properties.

REFERENCES

1. Li Zaigeng, He Jinzhou and Ye Guotian, "Phase Compositions and Setting Mechanisms of Low Cement, Ultra-Low Cement and Cement-Free Castables", Proceedings of Second International Symposium on Refractories, Beijing, China, Oct.30-Nov.2, 1992 pp540-549.
2. M.Rigaud, S.Palco and N.Wang, "Spinel Formation in the $MgO-Al_2O_3$ System Relevant to Basic Castables", UNITECR'95, Vol.1, pp387-394.
3. S.Asano, "Progress of Steel Making Technology and Refractories Situation in Japan", UNITECR'93, pp69-94.
4. M.Nakano, G.Yamaguchi and K.Saito, "On the Thickness Ratio of Two Spinel Layers Formed by Solid State Reaction", Yogyo-Kyokai-Shi, 79[4], 1971, pp119-123.
5. G.Yamaguchi et al., "Some Aspects of Solid State Reaction of Spinel Formation in the System $MgO-Al_2O_3$", Yogyo-Kyokai-Shi, 79[2], 1971, pp64-69.
6. Z.Nakagawa, N.Enomoto, I.S.Yi and K.Asano, "Effect of Corundum/Periclase Size on Expansion Behavior During Synthesis of Spinel", UNITECR'95, Vol.1, pp379-386.
7. B. Clavaud, J.P.Keihl and R.D.Schmidt-Whitley, "15 Years of Low Cement Castables in Steelmaking", First International Conference on Refractories, Nov.15-18, 1983, pp589-606.

8. B.Clavaud, J.P.Kiehl and J.P.Radal, "New Developments in Monolithic Refractories", Advances in Ceramics, Vol.13, Edited by R.E.Fisher, 1985, pp274- 283.

9. R.Rothrock III and L.Krietz, "New Developments in High-Strength, Abrasion-Resistant Castables", Advances in Refractories Technology, Edited by R.E.Fisher, 1989, pp272-293.

10. C.H.Liu, J.L.Mendoza and R.E.Moore, "Effect of Stress/Strain History on the Creep Behavior of Low-Cement Refractory Concretes", Advances in Refractories Technology, Edited by R.E.Fisher, 1989, pp325-342.

11. M.Kanda et al., "Deterioration with the Passage of Time in Low Cement Castable", Taikabutsu Overseas, Vol.13, No.2, pp15-20.

12. N.C.Fletcher, "The Development of Blast Furnace Trough Castables", UNITECR'89, pp719-730.

13. G.O.Hughes and P.L.Yoder, "The Effect of Groundmass Chemistry on the Bonding Matrix of Reduced-Lime Refractory Castables", UNITECR'91, pp254-259.

14. G.Maczura, V.Gnauck and P.T.Rothenbuehler, "Fine Aluminas for High Performance Refractories", The First International Conference on Refractories, Nov. 15-18, 1983, Japan, pp560-574.

15. S.Odanaka et al., "Effect of Alumina Fine Powder and Silica Flour Addition on Fluidity of Castable Refractories", Taikabutsu Overseas, Vol.10, No.1, pp35-37.

16. T.Yumoto et al., "Effect of Content of Alumina Cement, Silica Flour and Added Water on Strength of Castable", Taikabutsu Overseas, Vol.13, No.2, pp3-6.

17. A.Mathieu et al., "On the Use of 80% Al_2O_3 Cement as Mother Mix for Refractory

Products", UNITECR'91, pp202-210.

18. H.Sainte-Claire Deville, Ann. Phys. Chim., 46[3] 196, 1856.

19. David R.Lankard, "Evolution of Monolithic Refractory Technology in the United States", NEW DEVELOPMENTS IN MONOLITHIC REFRACTORIES Edited by R.E.Fisher, 1985, pp46-66.

20. Akira Nishikawa, "Technology of Monolithic Refractories", 1384, pp7-10.

21. H.Kato, H.Matsumura, M.Nishi and T.Masaoka, "Advances in Refractories Technology for Hot Metal Pretreatment", UNITECR'89, pp157-168.

22. T.Numata et al., "Development of Al_2O_3-MgO Castable Refractories", Tetsu-to-Hagane, 72, S110, 1986.

23. B.Nagai et al., "Development of High-Alumina Castable for Steel Ladles", Taikabutsu Overseas, Vol.10, No.1, pp23-28.

24. J.Mori et al., Structure Change of Alumina Castable by Adding Magnesia or Spinel", Taikabutsu, 47[1], 1995, pp20-24.

25. J.Karja and H.Nevala, "Experiences of Monolithic Ladle Linings in RAAHE Steel Works", UNITECR'93, pp1312-1319.

26. S.Banerjee, M.W.Anderson, J.P.Singh and R.Poeppel, "Reaction of Iron and Steel Slags with Refractory Materials", UNITECR'93, pp1481-1492.

27. S.Kamei, "Progress of Monolithic Refractories for Recent 10 Years in Japan", UNITECR 89, pp46-86.

28. T.Nishitani, S.Matsuo and T.Genba, "Application of the Alumina-Spinel Castable for BOF Ladle Lining", UNITECR 89, pp529-540.

29. H.Naaby, O.Abildgaard, G.Stallmann, C.Wohrmeyer and J.Meidell, "Refractory Wear Mechanisms and Influence on Metallurgy and Steel Quality as a Result of the Conversion to Endless Lining at Det Danske Stalvalsevaerk", Stahl und Eisen, Oct., 1994, pp198-204.

30. A.Yamamoto et al., "Development and Application of Unshaped Refractories in Stainless Steel Making", Stahl und Eisen, Oct., 1992, pp88-94.

31 T.Yamamura, Y.Hamazaki, T.Kaneshige, T.TToyoda, M.Nishi and H.Kato, "Alumina-Spinel Castable Refractories for Steel Teeming Ladle", Taikabutsu Overseas, Vol.12, No.1, pp21-27.

32. T.Kanatani, and Y.Imaiida, "Application of an Alumina-Spinel Castable to the Teeming Ladle for Stainless Steelmaking", UNITECR 93, pp1255-1266.

33. J.Mori, N.Watanabe, M.Yoshimura, Y.Oguchi, T.Kawakami and A.Matsuo, "Material Design of Monolithic Refractories for Steel Ladle", Ceram. Bull., Vol.69, No.7, 1990, pp1172-1176.

34. T.Yamamura, Y.Kubota, T.Kaneshige and M.Nanba, "Effect of Spinel Clinker Composition on Properties of Alumina-Spinel Castable", Taikabutsu Overseas, Vol.13, No.2, pp39-45.

35. Y.Sato, H.Joguchi and N.Hiroki, "Test Results of Alumina-Spinel Castable for Steel Ladle", Taikabutsu Overseas, Vol.12, No.1, pp10-14.

36. Hisaki Sumimura, Takashi Yamamura, Yukitoshi Kubota, Toshihiko Kaneshige, "Study on Slag Penetration of Alumina-Spinel Castable", UNITECR 1991, pp97-101.

37. R.Ebizawa, I.Ohishi, M.Kuwayama, A.Matsuo and E.Maeda, "Application of Basic

Refractories to Teeming Ladles", Proceedings of 2nd International Conference on Refractories, 1987 Japan, pp322-336.

38. Y.Watanabe, T.Ono, T.Yukinawa and S.Sakamoto, "Development and Application of Monolithic Refractory Containing Magnesia Clinker", Proceedings of 2nd International Conference on Refractories, 1987 Japan, pp494-506.

39. T.Yukinawa, "Development of Basic Dam Block for Tundishes", Taikabutsu Overseas, Vol.7, No.3, pp47-49.

40. W.H.Gitzen and L.D.Hart, "Explosive Spalling of Refractory Castables Bonded with Calcium Aluminate Cement", Ceramic Bulletin, Vol.40, No.8, 1961, pp503-507,510.

41. G.V.Givan, L.D.Hart, R.P.Heilich and G.Maczura, "Curing and Firing High Purity Calcium Aluminate-Bonded Tabular Alumina Castables", Ceramic Bulletin, Vol.54, No.8, 1975, pp710-713.

42. D.L.Hipps and J.J.Brown,Jr., "Internal Pressure Measurements for Control of Explosive Spalling in Refractory Castables", Ceramic Bulletin, Vol.63, No.7, 1984, pp905-910.

43. Kenji Oda, Hajime Itoh, Yakashige Matsumoto and Yasushi Ono, "Drying Characteristic of High-Dense Castable", Taikabutsu Overseas, Vol.13, No.2, pp21-28.

44. T. Yukizuna, "On the basic castable", Taikabutsu, 38[5], 1986, pp26-30.

45. F.Samukawa et al., "Slaking of Castables Containing Magnesia", Taikabutsu, 40[5], 1988, pp32-34.

46. T.Shindou and H.Nagata, "Relation between Crushing Size and Slaking Behaviour of Magnesia Clinker", Taikabutsu, 46[7], 1994, pp381-382.

47. "Castable Refractories with Metallic Aluminum for Rapid Drying", Taikabutsu, 46[11], 1994, pp594.

48. C.Chou, "Constituents and Characterization of Refractory Castables for Blast Furnace Troughs", Am.Ceram.Soc.Bull., 64[7], 1985, pp1003-1007.

49. T.Taniguchi and K.Watanabe, "Some results of testing on prepared unshaped refractories containing aluminium powder", Taikabutsu, Vol.29, No.11, 1977, pp591-595.

50. T.Taniguchi, M.Isikawa and H.Ohba, "Drying Character of Castable Refractories containing Al Powder", Taikabutsu, Vol.33, No.8, 1981, pp440-445.

51. T.R.Kleeb, J.R.Schartner, J.P.Sutton and R.M.Cullen, "Precision Manufactured Refractory Castables", UNITECR, 1993, pp572-582.

52. P.H.Havranek, "Recent Developments in Abrasion- and Explosion-Resistant Castables", Ceramic Bulletin, Vol.62, No.2, 1983, pp234-243.

53. "Slaking of magnesia clinkers", Taikabutsu 45[11], pp657; "Hydration of magnesia clinkers", Taikabutsu, 46[11], pp599; "MgO powder improved on the hydration resistance", Taikabutsu, 46[11], pp600; "Slaking of impurity-doped sintered magnesia", Taikabutsu, 46[11], pp601.

54. J.Mori, M.Yoshimura, Y.Oguchi, T.Kawakami and I.Ohishi, "Effect of Slag Composition on Wear of Alumina-Spinel Castable for Steel Ladle", Taikabutsu Overseas, 12[1], pp40-45.

55. B.Nagai, O.Matsumoto, T.Isobe and Y.Nishiumi, "Wear Mechanism of Castable for Steel Ladle by Slag", Taikabutsu Overseas, Vol.12, No.1, pp15-20.

56. I.Ohishi and R.Ebizawa, "Application of Alumina-Spinel Castable Refractories to Steel Ladle", UNITECR'91, pp105-107.

57. K.Adachi, M.Kuwayama, M.Yoshida and T.Yamamoto, "Progress in Ladle Refractories Technoques at at Kawasaki Steel, Mizushima Works", UNITECR'95, Vol.3, pp242-249.

58. Y.Ochiai, K.Matuso, R.Ohshima and A.Ohte, "Application of Monolithic Lining for the Steel Ladle at Kakogawa Works", UNITECR'95, Vol.3, pp203-210.

59. Hisaki Kato, M.Nishi, S.Uchida, U.Nagayama, H.Nakashima and H.Kyoden, "Application of Magnesia-Silica Castable Refractories to Slag Line of Steel Teeming Ladle", Transactions ISIJ, Vol.26, 1986, ppB-29.

60. M.Nishi, M.Kobayashi, A.Miyamoto, T.Anzai and K.Ichikawa, "Investigation on Basic Castable Refractories for Teeming Ladle", Taikabutsu, Vol.37, 1985, pp29-34.

61. H.Kyoden, Y.Hamazaki, R.Nakamura and T.Kaneshige, "Basic Castable", Shinagawa Technical Report, No.32, 1989, pp75-86.

62. S.Kataoka, "Refractories for Steelmaking in Japan", UNITECR'95, Vol.1, pp1-27.

63 A.Nagasoe, S-I.Tsurumoto and A.Kitamura, "Refractory Characteristics of Spinels with Various MgO Contents", Taikabutsu Overseas, Vol.11, No.3, pp20-28.

64 W.Jander, Z. anorg. allg. Chem. 163, 1927, pp1.

65 H.Dunwald and C.Wagner, Z. physik. Chem., Abt. B24, 1934, pp53.

66 B.Serin and R.T.Ellickson, J. chem. Physics 9, 1941, pp742.

67. A.M.Ginstling and B.I.Brounstein, J. appl. Chem. USSR (English Transl.), 23, 1950, pp1327.

68. K.Shinriki and T.Kubo, J. chem. Soc. Japan, ind. Chem. Sect., 57, 1954, pp619.

69. T.Sakaaino and T.Moriya, J. Ceram. Assoc. Japan, 62, 1954, pp243.

70. C.Kroger and G.Ziegler, Glastech. Ber., 26, 1953, pp346.

71. G.Valensi, Compt. Rend. 202, 1936, pp309.

72. R.E.Carter, J. chem. Physics, 34, 1961, 2010.

73. W.Komatsu, Reactivity of Solids, 1965, pp182.

74. R.E.Carter, "Mechanism of Solid-State Reaction Between Magnesium Oxide and Aluminum Oxide and Between Magnesium Oxide and Ferric Oxide", J.Am.Ceram.Soc., Vol.44, No.3, 1961, pp116-120.

75. S.F.Hulbert, D.A.Brosnan and R.H.Smoak, "Kinetics and Mechanism of the Reaction between MgO and Cr_2O_3". Reactivity of Solids, 1968, pp573-581.

76. F.S.Pettit, E.H.Randklev and J.Felten, "Formation of $NiAl_2O_4$ by Solid Reaction", J.Amer. Ceram. Soc., 49[4], 1966, pp199-203.

77. A.Yamakawa, M.Hashiba and Y.Nurishi, "Growth of Zinc Aluminate on the Sirfaces Normal to the Various Crystal Axes of an Alumina Single Crystal", J. Materials Science, 24, 1989, pp1491-1495.

78. H.Okada et al., "Effect of Physical Nature of Powders and Firing Atmosphere on $ZnAl_2O_4$ Formation", J. Am. Ceram. Soc., 68[2], 1985, pp58-63.

79. D.L.Ricoult and H.Schmalzied, "Internal Reaction in the (Mg, Me)O System", J. Materials Science, 22, 1987, pp2257-2266.

80. J.Beretka and T.Brown, "Effect of Particle Size on the Kinetics of the Reaction Between Magnesium and Aluminium Oxides", J. Am. Ceram. Soc., 66[5], pp383-388.

81. J.Beretka, "Kinetic Analysis of Solid-State Reactions Between Powdered Reactants", J. Am. Ceram. Soc., 67[9], 1984, pp615-620.

82. C.Wagner, Z. physik. Chem., Abt. B34, 1936, pp309.

83. H.Schmalzried, Z. physik. Chem., Neue Folge 33, 1962, pp111.

84. K.Hauffe and K.Pschera, Z. anorg. allg. Chem., 262, 1950, pp147.

85. J.J.Comer, N.C.Tombe and J.F.Fitzgerald, J. Amer. Ceram. Soc., 49, 1966, pp237.

86 Ernst Koch and Carl Wagner, "Formation of Ag_2HgI_4 from AgI and HgI by Reaction in the Solid State", Z.Physik.Chem., B34 [3/4] 317-21 (1936).

87 Mitsuko Onoda, Taikabutsu, 46[6], 1994, pp333-337.

88 Micheal B.Bever, "Encyclopedia of Materials Science and Engineering", Vol.6, R-S, pp4543-4545.

89 David W.Richerson, "Modern Ceramic Engineering", pp58-61.

90 Louis Navias, "Preparation and Properties of Spinel Made by Vapour Transport and Diffusion in the System $MgO-Al_2O_3$", J.Am.Ceram.Soc., Vol.44, No.9, 1961, pp434-446.

91 Joseph T.Bailey and Ralston Russell,Jr., "Sintered Spinel Ceramics", Ceramic Bulletin, Vol.47, No.11, 1968, pp1025-1029.

92 R.J.Bratton, "Coprecipitates Yielding $MgAl_2O_4$ Spinel Powders", Ceramic Bulletin, Vol.48, No.8, 1969, pp759-762.

93 Ronald C. Rossi and Richard M. Fulrath, "Epitaxial Growth of Spinel by Reaction in the Solid State", J.Am.Ceram.Soc., Vol.46, No.3, 1963, pp145-149.

94 A.M.Alper, R.N.Mcnally, P.H.Ribbe and R.C.Doman, "The System MgO-$MgAl_2O_4$", J.Am.Ceram.Soc., Vol.45, No.6, 1962, pp263-268.

95 E.F.Osborn, "Subsolidus Reactions in Oxide Systems in the Presence of Water at High Pressures", J.Am.Ceram.Soc., Vol.36, No.5, 1953, pp147-151.

96. H.Saalfeld and H.Jagodzinski, "The exsolution in Al_2O_3-supersaturated Mg-Al Spinel", Z.Kristallogr., 109, 1957, pp87-109.

97. H.Jagodzinski, "The Determination of Intermediate Structure Appearing During the Exsolution in Al_2O_3-supersaturated Mg-Al Spinel", Z.Kristallogr., 109, 1957, pp388-409.

98 G.Yamaguchi and T.Tokuda, "Some Aspects of Solid State Reactions Between Oxides", Bulletin of the Chemical Society of Japan, Vol.40, 1967, pp643-851.

99 Y.Chiang and W.D.Kingery, "Grain-Boundary Migration in Nonstoichiometric Solid Solutions of Magnesium Aluminate Spinel: I, Grain Growth Studies", J. Am. Ceram. Soc., Vol.72, No.2, 1989, pp271-77.

100 Alcoa Products Data: Sintered Spinel MR66, AR78, AR90.

101 C-E Minerals Products Data: Fused Spinel25, Spinel33.

102 A.N.Copp, "Annual Minerals Review: Magnesia/Magnesite", Am.Ceram. Soc. Bulletin, Vol.72, No.6, 1993, pp107-109.

103 Alcan Chemicals, "Product Data: Alumina C-70 series".

104 Alcan Chemicals, "Product Data: Alumina XA45 series".

105 Alcan Chemicals, "Product Data: Alumina Actibond 101".

106 Washington Mills, "Product Data: Brown, Fused Alumina".

107 T.Kanai et al., "Effect of Composition on Sintering and Bending Strength of Spinel Ceramices", Report RLEMTIT, No.13, 75-83(1987).

108 D.R.Dinger and J.E.Funk, "Particle Packing III -- Discrete versus Continuous Particles Sizes", Interceram, Vol.41, [5], 1992, pp332-334.

109 S.D.Majumdar et al., "Development of Cementless and Auto-Flow Aluminous Castable for Use in the Production of Cleaner Steel", Stahl und Eisen, Oct. 1994, pp 162-167.

110 Y.Hongo, Takabutsu Overseas, 9, 1989, No.1., pp35-36.

111 S.C.Maestrelli, L.Ferreira and J.B.Baldo, "The Effect of Cement Sunstitution for ρ-Alumina Partial Additions on the Thermo-Mechanical Properties of a Low Cement Refractory Concrete", UNITECR'95, Vol.1, pp337-342.

112 Akira Nishikawa, "Technology of Monolithic Refractories", 1984, pp221.

113 E.M.Levin, C.R.Robbins and H.F.McMurdie, "Phase Diagrams for Ceramists", 1964.

IMAGE EVALUATION
TEST TARGET (QA-3)

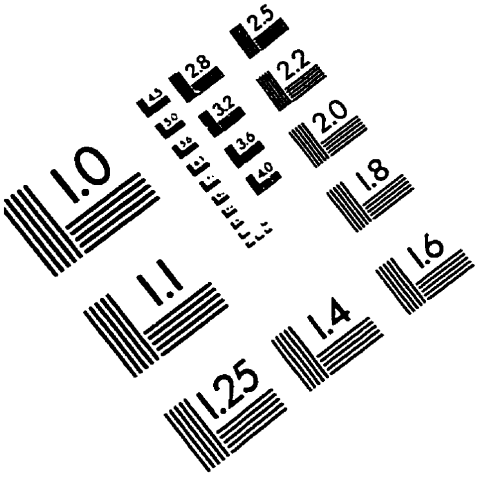

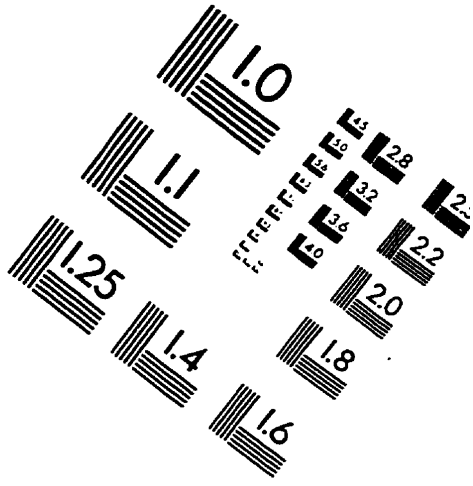

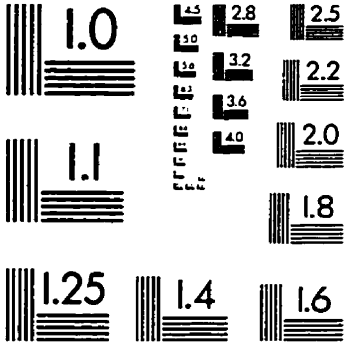

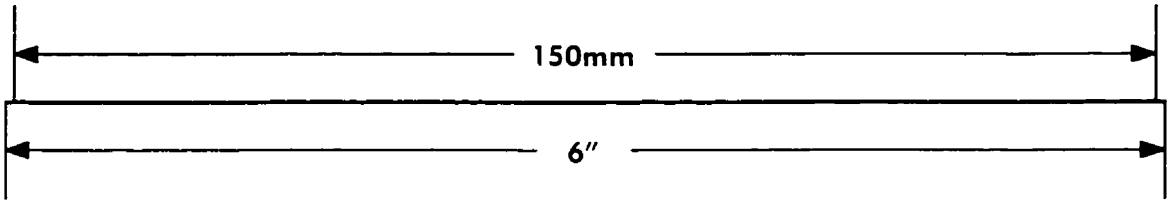

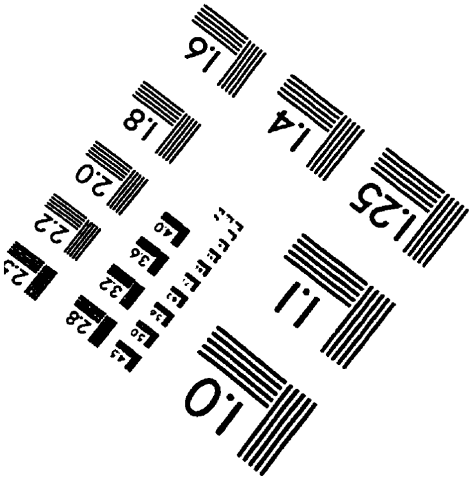

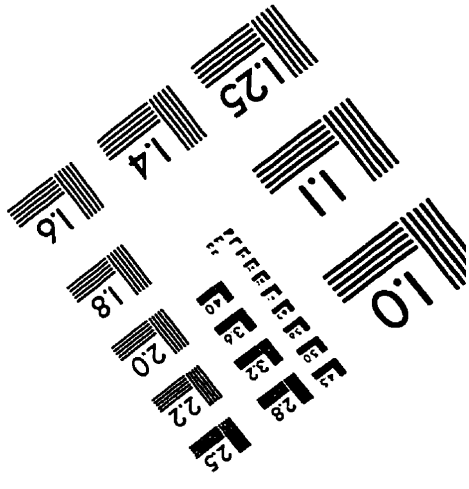

APPLIED IMAGE, Inc
1653 East Main Street
Rochester, NY 14609 USA
Phone: 716/482-0300
Fax: 716/288-5989